Advanced Fuel Research, Inc., 87 Church Street, East Hartford, CT 06108 USA

THE DUAL ROLE OF OXYGEN FUNCTIONS IN COAL PRETREATMENT AND LIQUEFACTION: CROSSLINKING AND CLEAVAGE REACTIONS

Final Report

#523085

For the Period

April 4, 1991 to September 30, 1993

MICHAEL A. SERIO
ERIK KROO
SYLVIE CHARPENAY
PETER R. SOLOMON

with contributions by:

RIPUDAMAN MALHOTRA*
DONALD MCMILLEN*

Work Performed Under Contract No. DE-AC22-91-PC91026

Michael Baird, Project Manager

by

ADVANCED FUEL RESEARCH, INC.

87 Church Street
East Hartford, CT 06108
(860) 528-9806

*SRI International, 333 Ravenswood Ave., Menlo Park, CA 94025

THE DUAL ROLE OF OXYGEN FUNCTIONS IN COAL PRETREATMENT AND LIQUEFACTION: CROSSLINKING AND CLEAVAGE REACTIONS

FINAL REPORT - CONTRACT NO. DE-AC22-91-PC91026

TABLE OF CONTENTS

DISCLAIMER

EXECUTIVE SUMMARY

A. Studies with Coals and Modified Coals

1. Demineralized and Ion-Exchanged Coals – During this project, work was done on preparing samples of modified coals and improving the FT-IR spectroscopy methods used to describe these coals. Samples of demineralized coals were prepared for both Zap and Wyodak coals. A portion of each sample was reacted with 1N barium solution, which has a pH value of around 8.2, in order to ion-exchange the carboxyl groups. A second set of samples was prepared by reaction with a solution of 0.8 N $BaCl_2$/0.2 N $Ba(OH)_2$, which has a pH of about 12.7. Both phenolic and carboxyl groups will be completely exchanged under the latter conditions. These samples were subjected to characterization by pyrolysis in a TG-FTIR apparatus and liquefaction in a donor solvent. The results show that, for both Wyodak and Zap, demineralization tends to increase the tar yield and decrease the yields of gas and char. For the Ba exchanged coals, there was a decrease of tar with the extent of ion-exchange with barium and a corresponding increase in the total amount of gas evolution. When the liquefaction results were examined, it was found that both the liquefaction and tar yields follow the order [demin.]>[demin. + Ba^{2+} (pH = 8)]>[demin. + Ba^{2+} (pH = 12.6)]. It was also found that for this set of samples, both the relative amounts of pyrolysis CO evolved before 750 ^{o}C and the total pyrolysis CO were indicators of the extent of retrogressive reactions in pyrolysis and liquefaction.

In order to examine the effects of cation type, preparation of ion-exchanged (including barium, calcium and potassium) demineralized Zap and Wyodak was also completed. Both vacuum dried and moist samples were prepared. The modified samples were subjected to functional group analysis as KBr pellets with FT-IR spectroscopy, and programmed pyrolysis analysis with TG-FTIR. Liquefaction experiments of these samples were also performed and products were analyzed. The data indicate that both the pyrolytic tar and liquefaction yields decrease with the extent of ion-exchange, i.e., in the order of (demineralized) > (ion-exchanged at pH 8) > (ion-exchanged at pH 12.5) for all three cations.

For the pyrolysis of vacuum dried samples, the tar yield was higher for the potassium-exchanged coals than the calcium and barium-exchanged samples, suggesting that bivalent cations tighten the coal structure by cross-linking coal fragments and make it more difficult for tar molecules to escape. The liquefaction results indicate that the potassium-exchanged samples have higher liquefaction yields (especially asphaltenes) than for the barium- and calcium-exchanged samples. This can probably be attributed to the same reason for the high pyrolytic tar yield, i.e., that bivalent cations can serve as a cross-linking agents to tighten the coal structure.

2. Moisturized Coals – A procedure for restoring the moisture level of modified coal samples was developed in the attempt to understand if moisture uptake for low rank coals is a reversible process and to see if moisture influences the role of the cations. These moisturized samples were subject to routine liquefaction experiments and pyrolysis analysis in the TG-FTIR. The saturation moisture content of the modified coal samples, for both Zap and Wyodak, increases with the extent of ion-

exchange, and varies in the range of 15-25 wt% (as-received basis). Moisturization reduces the tar yield in pyrolysis for the demineralized samples, increases the yield for pH 8 ion-exchanged samples, and has little effect on the yield for pH 12.6 ion-exchanged samples. Pyrolysis char yield, on the other hand, was reduced, for all the modified samples, by increased moisture content.

The results show that the moisture content can reach that of the raw samples by remoisturization for Zap, but not for Wyodak. Furthermore, the chemical structure of the coal samples seems to have been changed by remoisturization, since different CO_2 evolution behaviors were observed. In almost every case, the asphaltene yield was increased with moisturization except for the pH 8 Zap, in which case the asphaltene yield was slightly reduced. Interestingly enough, the oil yield was reduced for most of the modified samples with moisturization, except for the demineralized Zap and the pH 12.6 Wyodak. The indication from the above results is that moisturization favors the formation of the larger molecular weight asphaltenes in liquefaction, while the formation of the smaller molecular weight oils was less favored.

It is usually shown that the trends for improved liquefaction yields parallel those for improved tar yields in pyrolysis. However, it was found in this study that the influences of moisturization on the yields of pyrolytic tars and liquefaction toluene soluble yields are different in that moisturization does not appear to have a significant effect on tar yields. This indicates that moisture plays different roles for the formation of tars in pyrolysis and coal liquids in liquefaction. A possible explanation for the difference is that most of the moisture is depleted early in the pyrolysis process, whereas the moisture is retained in the reactor during liquefaction and can exist in a liquid phase.

It is known from the above results and the literature that the moisture is associated with cations in raw low rank coals. Consequently, an investigation was made to determine if the deleterious effects of cations could be mitigated by adding water to the donor solvent liquefaction system. Experiments were done with raw and demineralized Zap at three different temperature levels. At temperatures near or below the critical temperature of water (374° C), it appears that there is a profound beneficial effect of added water for the raw coal. Conversely, there is a significant deleterious effect of added water for the demineralized coals. The ability of water to interact with cations and affect the course of the thermal decomposition behavior is consistent with results that have been observed in hydrothermal treatment of coal, which mimics the geological aging process in many respects.

3. Methylated Coals - The methylation of a demineralized Zap Lignite sample was performed using a modification of the alkylation procedure previously employed at SRI International. The principal modifications were the addition of a second aliquot of base and alkylating agent to increase the extent of alkylation in a single stage reaction, and the extraction with methanol-water mixtures to more thoroughly remove tetrabutylammonium hydroxide and iodide from the product mixture. These modifications resulted in a methylated coal having very little nitrogen incorporation from the tetralkyl amine base, no incorporation of halogen, and a much more nearly correct ratio of incorporated carbon

and hydrogen than had been previously achieved with this coal.

4. Biological Pretreatment Samples - Upon the recommendation of Dr. Malvina Farcasiu, a sample of demineralized (DMN) Argonne Wyodak coal was prepared for the Michigan Biotechnology Institute (MBI). This was subjected to biological pretreatment for removal of carboxyl groups and sent back, along with samples of biopretreated raw coal and a control sample. The control sample was a raw Wyodak sample which had been added to the growth medium but which was not innoculated with bacteria. The five samples were subjected to FT-IR pellet analysis, TG-FTIR analysis, SEM/x-ray analysis, and liquefaction experiments in a donor solvent. In summary, the results from the various analyses indicate a modest benefit of the MBI biotreatment process for the raw coal and a negative result for the demineralized coal. In all cases, the best sample from a liquefaction standpoint was the normal demineralized coal. This is consistent with our other data from coal and model compound studies, which indicate that carboxyl groups are not bad actors as far as retrogressive reactions are concerned but rather the cations which are exchanged on these groups. Consequently, efforts on biological pretreatment should be redirected toward removal of cations rather than carboxyl groups.

5. FT-IR Analysis of Coals and Modified Coals – A Fourier transform infrared (FT-IR) spectroscopy method was developed to quantify the concentration of carboxyl groups in coals and modified coals. The results show the expected increases in COOH concentration when the coals are acid washed or demineralized and the expected decreases when the coal is calcium loaded. Work was also done to develop a curve resolving program to analyze the OH region of the FT-IR spectrum. If this data is considered (on a qualitative basis) along with the data supplied on carboxyl group changes, it can be seen that the changes in the free COOH and the o-dihydroxyl are usually in the same direction for each coal modification. This observation provides evidence that both of these groups can be ion-exchanged in the original coal, which probably is related to their propensity for undergoing retrogressive reactions.

The FT-IR spectra of coal contain a wealth of information that can be utilized in the development of quantitative analysis routines based on least squares curvefitting. In this work, the previously developed technique of Solomon et al. was modified by allowing the curvefitting algorithm to determine the positions of those bands prone to shifting. Reduced spectral ranges were used in order to accommodate the increased number of parameters to be determined. The initial parameters for the curvefitting algorithm (number of bands, band assignments) were set using data available in the literature. Because of the importance of the carboxylate groups in retrogressive reactions, the C=O stretching region was a particular focus. Raw and modified coal samples (acid washed, demineralized, and cation-exchanged) were analyzed in order to validate the proposed band assignments in the C=O stretching region. This parameter set differentiates free carbonyl (B2) and hydrogen-bonded carbonyl (B4) from carboxylic acid carbonyl (B3) and carboxylate (B7). One test of these assignments, which are based on literature data, is to plot B3 versus B7. This should be linear, assuming that the sum of the free carboxyl and carboxylate groups is constant and that the intensity of the overlapped aromatic

ring band in B7 is also constant. This relationship was found to hold for a set of raw, acid washed, and acid washed/cation-exchanged Zap coals.

B. Studies with Polymeric Model Systems and Model Compounds

1. Preparation and Characterization of C-C-O Polymers – The preparation of polymer mixtures dominated by hexa(phenylene) showed that characterization and functionalization of moderate molecular weight polyphenylenes proves to be very difficult, owing to the insolubility even of these low molecular weight oligomers. On the other hand, the preparation of moderate molecular weight C-C-O polymers (n = 10 to 30) has proven to be easier than anticipated, after difficulties with unwanted side reactions were suitably minimized with a phase-transfer catalyst approach. Although these polymers have a labile backbone and do not therefore provide a refractory framework with which to study unencumbered the reactions of carboxylic acid groups attached to the polymers, these materials will constitute the most coal-related polymer models that have been studied to date. They will, therefore, provide very appropriate surrogates for addressing the retrograde reactions of phenolic and carboxylic acid functions.

Subsequently, the preparation of moderate molecular weight C-C-O polymers (n = 10 to 30) was optimized. The synthesis of the 4-hydroxyphenethyl halide needed for the phase-transfer-catalyzed polymerization was shortened from three separated procedures to a sequence of three reactions carried out effectively in a single step. NMR, GPC, and pyrolysis-FIMS analyses of the polymer subsequently produced from this iodide showed it to have a weight-average molecular weight of somewhat over 4000 (n = ~35), to have the desired phenyl-O-C-C- structure and to be contaminated with ≤5% of related olefins and n-butyl amine. Pyrolysis-FIMS analyses supported the purity of the polymer and revealed that coordinated cleavage or unzipping appeared to be very facile at about 380°C. This coordinated cleavage did not result from any radical pathway that could be identified, but was strikingly reminiscent of the cleavage reported for lignins themselves (and not understood in those systems either).

2. Alternative Routes for Synthesis of -(C_6H_4-O-CH_2CH_2)$_n$- Polymers – As discussed above, we successfully developed a new route to these C-C-O polymers, and we believe they re-emerge as the better vehicle for addressing, in a polymeric context, the question of the effect of decarboxylation and other factors on crosslinking in low-rank coals. It was believed, in fact, that we had come to a satisfactory optimization of this new synthetic route with a single-reaction vessel preparation which would go all the way from the starting 4-hydroxyphenethyl alcohol to the 4-hydroxyphenethyl iodide by using three equivalents of trimethylsilyl iodide. However, this conclusion was premature: it was found that the final step - polymerization of the iodide - proceeds with poor yield because base-catalyzed elimination of HI is the major pathway. Consequently, a change was made in this synthesis, switching to the use of trimethylsilyl bromide.

3. Larger Scale Preparation of the -(C_6H_4-O-CH_2CH_2)$_n$- Polymers – The first attempted larger scale synthesis of the basic β-ether- bridged polymer involved the use of trimethylsilyl iodide, as indicated above. Starting with 5 grams of the 4-hydroxyphenethyl alcohol, we obtained the -(C_6H_4-O-CH_2CH_2)$_n$- polymer in good purity (by solution-phase ^{13}C- and proton- NMR), but in a yield of only ~16%. This gave us only about 700 mg of purified material, not enough even to perform one liquefaction experiment at the 1-gram scale that was being used at Advanced Fuel Research, Inc. (AFR). Since increasing the scale even to 10 grams would not give enough for more than 1 liquefaction experiment, and increasing the scale further can introduce other problems that would then have to be worked out, it was decided to try another variation of the same basic approach.

Because the polymerization of an earlier step-wise preparation of 4-hydroxy-phenethyl*bromide* had been quite efficient (though the bromide itself had been rather difficult to obtain), a final variation was tried in which the trimethylsilyl iodide was replaced by trimethylsilyl bromide. Starting with 5.0 grams of the 4-hydroxyphenethyl alcohol, we obtained 3.1 grams of the solid polymer (90% yield). The yield was not only very good, but this preparation appeared to be substantially higher in molecular weight than our previous preparations. It was completely insoluble in methylene chloride, THF, DMSO, and DMF. The structure and purity of this and the earlier soluble preparations of this polymer was examined based on GPC, NMR, and FIMS analyses. In brief, this higher molecular weight, insoluble polymer preparation passed all the structure and purity tests to which it was subjected.

4. Preparation of the -[C_6H_3(o-Me)-O-CH_2CH_2]$_n$- Polymer – The -O-C-C- linked polymer with a methoxy located ortho- to the bridge oxygen contains what is probably the most common lignin linkage type. Furthermore, it is undoubtedly a more reactive structure (presumably both with respect to cleavage and to crosslinking) than is -(C_6H_4-O-CH_2CH_2)$_n$- itself. Therefore, it was believed that the methoxy-substituted polymer was the model system that would reveal the most about the chemistry of low-rank coals. We chose to synthesize -(C_6H_4-O-CH_2CH_2)$_n$- first, anticipating both that the chemical behavior of the more complex polymer would be less informative if it was observed in isolation, and that we would learn useful lessons in the synthesis of the simpler polymer.

This work has involved: (1) completion of the synthesis of the -C-C-O- linked, methoxy substituted lignin-network polymer, —[C_6H_3(o-OMe)-O-CH_2CH_2]$_n$— polymer; (2) Analysis of the polymer via depolymerization under pyrolysis-FIMS (Py-FIMS) conditions; and (3) testing of several routes to selective cleavage of the O-Methyl bond so that the relative crosslinking tendencies of the methylated and unmethylated versions of the polymer could be determined.

5. Decarboxylation Studies with Model Compounds – The work on decarboxylation and coupling reactions for activated acids from this contract and from the literature was summarized. The following conclusions were reached: 1) simple benzoic acids (i.e., unsubstituted by anything except carbon) do not rapidly decarboxylate below 400 ^oC, except in the presence of strong base and or electron transfer

agents, and 2) upon decarboxylation, they tend to form rather smaller amounts of coupling products than might have been expected, either with themselves or with aromatics that are part of the solvent system. This is true even when the system contains no H-donor component that might be expected to scavenge aryl radical intermediates before they could couple. It is also true even when aromatics such as pyrene or naphthol, which are very good radical acceptors, have been added to the system. These low levels of coupling raise an important question. Is coupling associated with decarboxylation as important a part of retrograde reactions in low-rank coals as it has been assumed to be? This question was addressed by additional experiments with model systems, including the use of electron-transfer agents, as discussed below.

Decarboxylation reactions of phenyl-substituted alkane carboxylic acids were examined using the model compound phenylacetic acid. Its behavior was examined under a variety of conditions to probe the effects of added radical scavenger, base, and the electron transfer agent Fe_3O_4. Both decarboxylation and coupling were faster than with benzoic acid. Consonant with the results with benzoic acids, added scavenger decreased the degree of coupling in the absence of Fe_3O_4. Surprisingly, however, the addition of scavenger in the presence of Fe_3O_4 led to a 4-5 fold increase in the formation of the coupling product 1,3-diphenylacetone. This product accounted for about 40% of the reacted acid when this combination of reagents was present. In addition, since the analogous product was not identified in the benzoic acid system, this product indicates that some of the major coupling pathways of phenylacetic acid, and perhaps all alkane carboxylic acids, are significantly different than those of benzoic acids.

The reaction of the activated acid o-Anisic acid (2-methoxybenzoic acid) in the presence of Fe_3O_4 was also examined. Xanthenes were formed in about 9% yield under some conditions. These products were demonstrated to stem from the reactions of cresol with either phenol or itself, rather than directly from o-Anisic acid (the phenols are decarboxylation products of o-Anisic acid). It is apparently the juxtaposition of the methyl and hydroxyl groups that leads to the retrograde reactivity. These results suggest that phenolic groups could play a major or even dominant role in the retrograde reactions that occur during coal liquefaction in the temperature regime associated with CO_2 loss. Since such structures may be present in the coal matrix even prior to decarboxylation, what remains unclear is exactly to what degree such reactions necessarily arise as a consequence of decarboxylation.

Additional experiments were performed which involved testing the effect of iron sulfide as another iron salt of potential importance in crosslinking during the heating of coals. The effect of water on the behavior of phenylacetic acid was also tested. Finally, we prepared, purified, and tested the behavior of the calcium salts of benzoic acid and anisic acid [$Ca^{+}C_6H_4(o\text{-}OCH_3)CO_2^{-}$]. In brief, the decomposition of the calcium salts does *not* substantially increase the tendency for crosslinking to occur in association with decarboxylation. This is surprising in light of the evidence for cation influence on retrogressive reactions in coals and modified coals. This result suggests that an important experiment would be to study carboxyl polymers with/without calcium salts. However, it is unlikely that

this can be done under the current program since these polymers are not readily available.

C. Publications Resulting from this Project

Three papers were prepared for the International Conference on Coal Science (Banff, Alberta, CANADA, September 12-17, 1993) based on the work done under this project. The first is titled "The Role of Cations in Retrogressive Reactions During Pyrolysis and Liquefaction," which summarized the work done on coals and modified coals. The second is titled "Application of a Spectral Deconvolution Technique to Coal FT-IR Spectra," which described the use of FT-IR methods for measurement of carboxyl and hydroxyl functions. The third paper is titled "Pyrolysis Pathways and Kinetics of Polymeric Models for Low-Rank Coals" which focused on the thermal decomposition chemistry of the β-ether-linked lignin model polymers. In addition, two papers were prepared for the American Chemical Society (ACS) Division of Fuel Chemistry Meetings: 1) “Decarboxylation and Coupling Reactions of Coal Structures” (Washington, DC, 1992); and 2) “The Effect of Moisture and Cations on Liquefaction of Low Rank Coals” (Denver, 1993).

I. INTRODUCTION

The overall objective of this project was to elucidate and model the dual role of oxygen functions in thermal pretreatment and liquefaction of low rank coals through the application of analytical techniques and theoretical models. The project was an integrated study of model polymers representative of coal structures, raw coals of primarily low rank, and selectively modified coals in order to provide specific information relevant to the reactions of real coals. The investigations included liquefaction experiments in microautoclave reactors, along with extensive analysis of intermediate solid, liquid and gaseous products. Attempts were made to incorporate the results of experiments on the different systems into a liquefaction model.

II. TASK I - WORK PLAN

In the early phase of the project, work was completed on the project Test Plan and on a subcontract agreement with SRI International for the model compound studies. A copy of the work plan was included as Appendix A of the First Quarterly Report.

A literature review of various demineralization methods was completed. Experimental techniques found in the literature for coal demineralization [1] and ion-exchange [2,3] use batch type reactors to carry out the given treatment of coal which necessitates filtering of the coal sample any time the solvent is changed. Based on this review, an apparatus for continuous-flow, controlled-atmosphere demineralization and controlled pH ion-exchange of coals and other related materials was designed and constructed. To avoid a possible oxidation of the coal sample, a closed system was used, where instead of stirring the batch reactor contents, a continuous flow of solvent passes through the sample. By utilizing valves, it was possible to change solvents without opening the reactor. The different solvents were held in separate reservoirs which were all equipped with sparge valve systems to deoxygenate the solvents before use (with N_2 or He as needed).

Since one of the demineralization steps used 50% HF, all of the valves and tubing in the liquid line were made of teflon. A peristaltic pump was used to set the proper flow rate (2-50 ml/min.). A diagram of the apparatus is given in Fig. II-1.

The contents of each reservoir were as follows:

1. 50% HF
2. 6M HCL
3. Deionized water
4. Metal on NH_4^+ salt to be ion exchanged.
5. Basic solution

Reservoir 4 was equipped with a magnetic stirrer to set the proper pH of the ion exchange solvent by addition of a base solution from reservoir 6. The pH could be changed continuously and measured via flow through cell 7. The sample holder was a telfon filtering cell (50 ml) which was immersed into a water bath thermostat. The system was used to prepare modified coals, including demineralized and ion-exchanged coals.

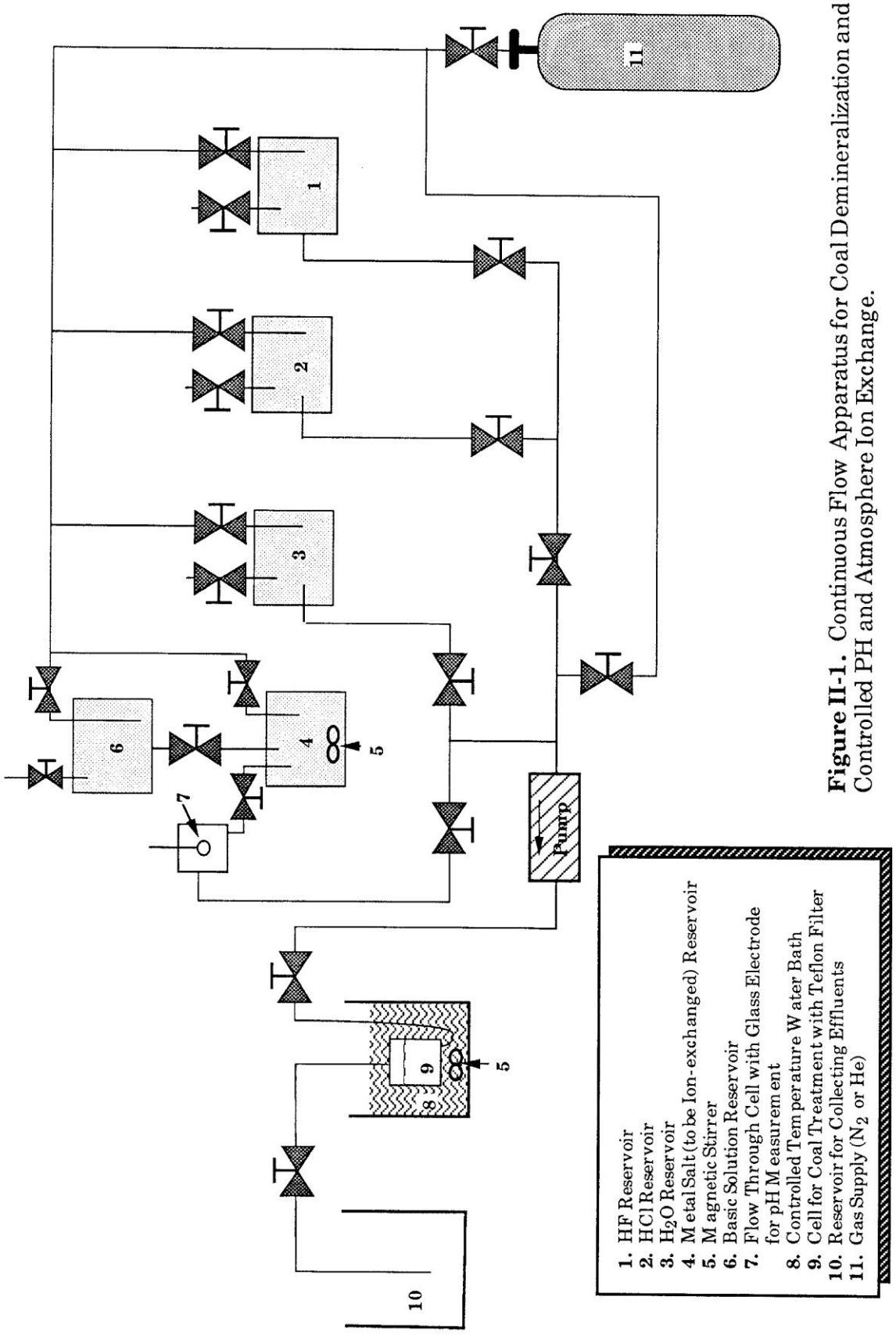

Figure II-1. Continuous Flow Apparatus for Coal Demineralization and Controlled PH and Atmosphere Ion Exchange.

III. TASK 2 - STUDIES WITH COALS AND MODIFIED COALS

During this project, work was done on preparing samples of modified coals and improving the FT-IR methods used to characterize these coals. This work is described below.

A. Preparation and Characterization of Demineralized and Ion-Exchanged Coal Samples

1. Demineralization Procedure

As discussed in the previous section, the procedure was similar to that described in the work of Bishop and Ward [1]. The coal samples used in this study were the Zap and Wyodak coals from the Argonne premium sample bank. The sample sizes were all -100 mesh. Before starting the acid treatment, the samples were thoroughly wetted by mixing with de-ionized water under a nitrogen environment. Demineralization involved washing the coal with a flow of 2M HCl for 45 minutes, 50% HF for 45 minutes, 2M HCl for 45 minutes, and de-ionized water for 120 minutes. The process was performed at 80 °C.

For the first several runs, the sample cell of the demineralization system was not equipped with a mixer, the sample treatment became diffusion limited and the results were not satisfactory. It was found that minerals were not totally removed, and that acids were still retained in the demineralized products since the water-washing was not completely effective. The sample cell was later equipped with a magnetic stirrer, and the demineralization results were much improved. After demineralization, the sample was dried by vacuum for at least 20 hours at room temperature. The vacuum dried sample was kept in a nitrogen box for analysis and liquefaction.

2. Ion-Exchange of Carboxyl Groups with Cations (Ba^{++})

The acidity constant (k_a) of carboxylic acids is around 10^{-5}, and that of phenols is around 10^{-10}. Theoretically, almost all carboxyl OH can be exchanged with cations at pH 8, whereas the phenolic-OH can remain in acid form, according to the following equation:

$$\frac{[A-]}{[HA]} = \frac{k_a}{[H^+]} \qquad (1)$$

where HA is either carboxyl or phenolic group in acid form. At pH 8, $[A^-]/[HA]$ would be a value of order 10^3 for carboxyl groups, and 10^{-2} for phenols. Schafer's experimental results also suggest that the carboxyl groups in coal can be completely exchanged with cations at pH around 8-8.5 [2]. 1N barium acetate solution, which has a pH value around 8.2, was used for ion-exchange with carboxyl groups.

Roughly 3 g of demineralized coal was mixed with 300 ml of 1N barium acetate in a cell under a nitrogen environment. After 5 minutes of mixing, the pH value of the mixture dropped to less than 7.5. The mixture was filtered through a Teflon membrane by increasing the nitrogen pressure, and the mixing cell was refilled with another 300 ml of barium acetate. The pH value of the solution dropped again after mixing. The filtration and refilling procedure was repeated, usually 15-20 times, until the pH value of the mixture in the cell reached 8.0 ± 0.1 and remained constant with mixing. The drop of the pH value was probably due to the release of H^+ from carboxylic acids in the coal.

The mixture was kept under continuous mixing conditions in a nitrogen environment for at least 20 hours before the acetate solution was purged out, and the cell was refilled with a final 300 ml charge of 1N barium acetate. After 10 minutes of mixing, the acetate solution was purged out, and the coal sample was washed with 150-200 ml of de-ionized water. The coal sample was then removed from the cell for vacuum drying, which lasted for at least 20 hours. The sample was kept in a nitrogen box after drying.

3. Ion-Exchange of Phenolic and Carboxyl Groups with Cations (Ba^{++})

According to equation 1, both phenolic and carboxyl groups can be totally exchanged with cations at pH around 12.5. Schafer [2] also reported that the exchange of -OH groups was complete at pH 12.6. In this study, a solution, recommended by Schafer, of 0.8 N $BaCl_2$ and 0.2 N $Ba(OH)_2$ having a pH of 12.7, was used for ion-exchange.

Approximately 3 g of a demineralized coal sample was stirred with 300 ml of the pH 12.7 solution in a nitrogen environment. After 5 minutes of mixing, the mixture was filtered through a membrane and the cell was refilled with another 300 ml of the pH 12.7 solution. The purging and refilling procedure was repeated 3 times, and the pH value of the final mixture was around 12.6. The mixture was continuously mixed under a nitrogen environment for at least 20 hours for exchange. After this long-time exchange period, the solution was purged out, and the cell was refilled with the pH 12.7 solution.

After 10 minutes of mixing, the solution was purged out, and the coal sample was washed with a solution of 0.1 N $BaCl_2$ and 0.03 N NaOH, which has a pH around 12.7, to avoid hydrolysis of the exchanged coal. The coal sample was then removed from the cell for vacuum drying. After drying, the sample was kept in a nitrogen box for further study.

It was noticed, in the process of ion-exchange that part of the coal structure was dissolved in the high pH value solution, since the filtrate had a yellowish color. This is most likely due to hydrolysis of the ester linkage in coal, i.e.,

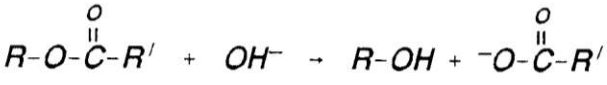

(2)

We estimated the amount of coal structures (so called humic acids) dissolved in the high pH value solutions during complete ion-exchange be about 6.6 wt% daf of the demineralized Zap and 17 wt% daf of the demineralized Wyodak.

The results of analysis of the raw, demineralized, and barium exchanged coal samples by programmed pyrolysis in the TG-FTIR are shown in Figures III-1 to III-4, and summarized in Table III-1. These results show that, for both Wyodak and Zap, demineralization tends to increase the tar yield, whereas both the gas and char yields were reduced. Table III-1 also shows a decrease of the tar yield with the extent of ion-exchange with barium, and a corresponding increase in the total amount of gas evolution.

The liquefaction results for different samples are shown in Table III-2. Comparing Table III-2 with Table IIII-1, it is found that both liquefaction and tar yields follow the order [demin.] > [demin. + Ba^{++} (pH · 8)] > [demin. + Ba^{++} (pH · 12.6)]. This result was expected, since having the carboxyl or phenolic groups in the salt form makes it easier to release CO_2 and CO, and therefore, to generate free radicals which would result in crosslinking of the coal structure.

For the Wyodak sample, both the tar and liquefaction yields are higher for the fresh sample than for the sample barium exchanged at pH 8. However, in the case of Zap, the fresh sample shows a higher yield of tars but lower yields in liquefaction than the sample exchanged with barium at pH 8. It can be seen in Tables III-1 and III-2 that the demineralized Wyodak containing H^+, which was due to incomplete washing after acid treatments, shows a low liquefaction yield, although the tar yield in pyrolysis is high. Since the retrograde reactions during coal pyrolysis or liquefaction appear to be in part due to the crosslinking between carboxyl and/or hydroxyl functions, it is possible that the H^+ retained in the demineralized coal catalyzes the retrograde reactions by the following mechanism:

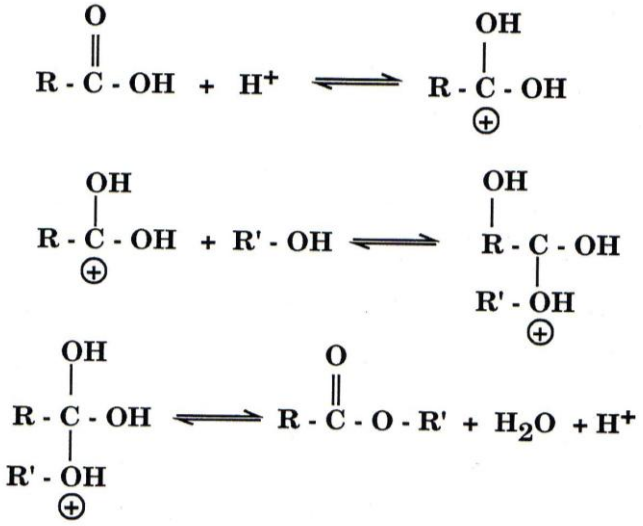

(3)

TABLE III-1 - Results of Pyrolysis Experiments with Coals and Modified Coals

	Proximate Analysis (wt.%), as rec.				Pyrolysis Products (wt.%, daf)					
Coal (Type/Preparation)	Ash	Moisture	Fixed C	Volatile	Char	Tars	CO_2	CO	H_2O	CH_4
Zap Lignite										
fresh	10.3	22.5	38.9	28.3	57.1	7.3	8.9	14.7	14.3	2.2
demin.	1.5	3.5	50.8	44.2	53.5	20.1	4.84	10.4	8.4	2.73
demin. + Ba^{++} (pH=8)	15.4	5.1	43.8	35.7	55.1	5.53	11.7	15.8	18.6	2.55
demin. + Ba^{++} (pH=12.6)	37.8	9.0	27.6	25.6	51.9	2.87	10.5	24.1	15.5	2.56
Wyodak										
fresh	13.8	22.5	36.8	26.9	57.8	15.7	7.15	15.7	13.3	3.3
demin. + H^+	6.0	4.0	4.6	4.4	51.1	25.4	4.0	11.2	7.0	3.1
demin.	0	2.2	49.2	48.6	50.3	29.7	2.45	9.58	4.69	2.82
demin. + Ba^{++} (ph=8)	14.9	4.4	43.5	37.2	53.9	13.6	8.80	13.6	12.4	2.85
demin. + Ba^{++} (ph=12.6)	36.2	6.0	29.7	28.1	51.4	12.8	6.42	19.6	10.6	2.92

TABLE III-2 - Product Yields from Liquefaction Experiments with Coals and Modified Coals in DHP

	Toluene Solubles		Toluene Insolubles	Gas						
Coal (Type/Preparation)	Total	Oils		Total	H_2O	CO_2	CO	CH_4	C_2H_6	C_2H_4
Zap Lignite										
fresh*	26	12	69	5.0	---	4.3	0.24	0.25	0.21	0.03
demin.	52	26	46	2.2	0.019	1.1	0.43	0.27	0.29	0.05
demin. + Ba^{++} (pH=8)	37	25	55	8.2	0.018	7.3	0.40	0.20	0.24	---
demin. + Ba^{++} (pH=12.6)	15	15	84	1.0	---	0.3	0.27	0.023	0.41	---
Wyodak										
fresh*	39	13	56	5.2	0.021	4.1	0.34	0.31	0.36	0.08
demin. + H^+	36	14	64	0.36	0.017	---	0.19	0.041	0.11	0.01
demin.	54	22	43	2.9	0.013	2.2	0.31	0.11	0.24	0.04
demin. + Ba^{++} (ph=8)	37	25	62	0.70	0.015	---	0.43	0.076	0.19	---
demin. + Ba^{++} (ph=12.6)	7	5	89	3.9	0.090	3.4	0.23	0.023	0.12	0.04

* Data from Serio et al. [4].

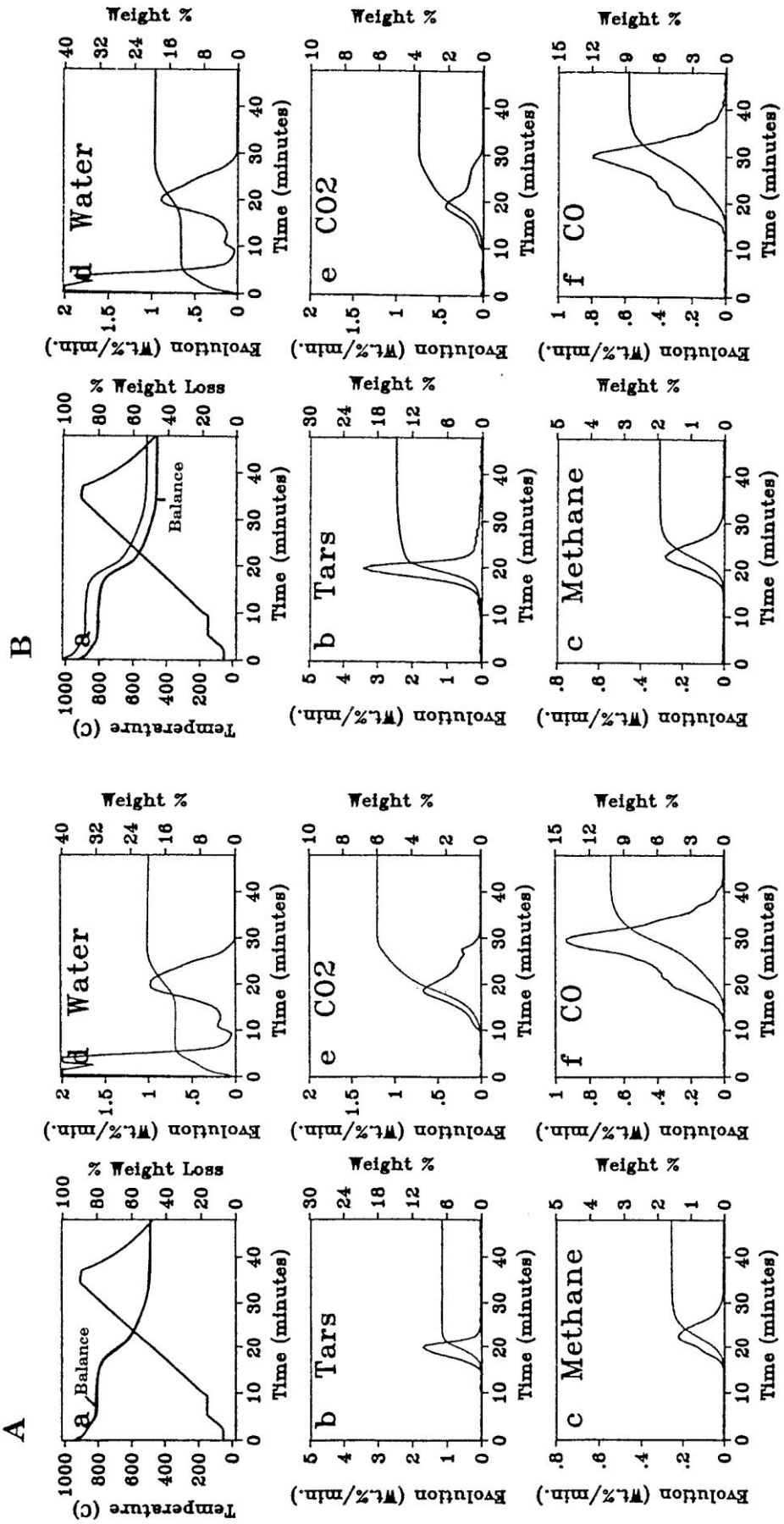

Figure III-1. TG-FTIR Analysis of Raw Coals. a) Zap; b) Wyodak.

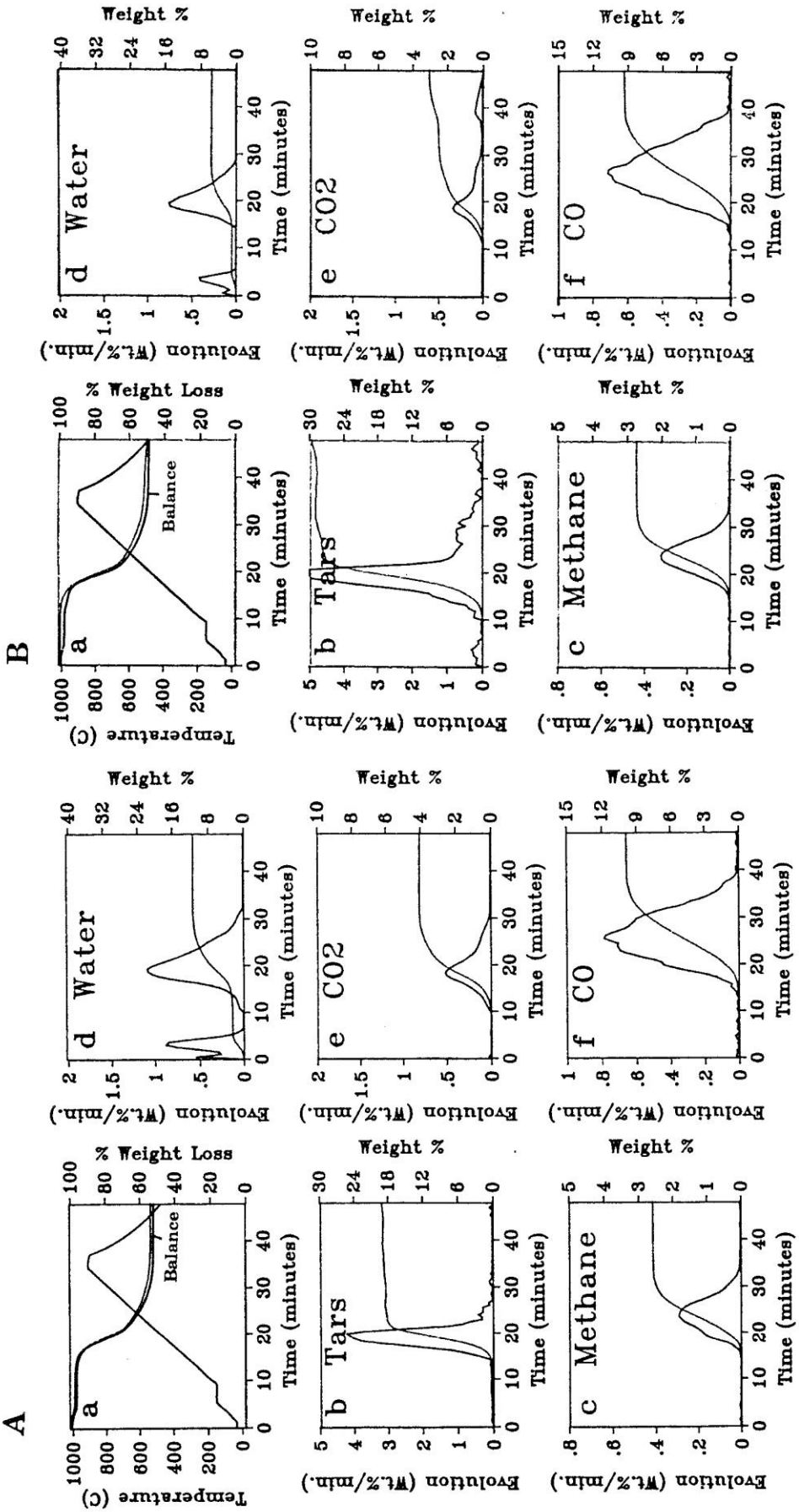

Figure III-2. TG-FTIR Analysis of Demineralized Coals. a) Zap; b) Wyodak.

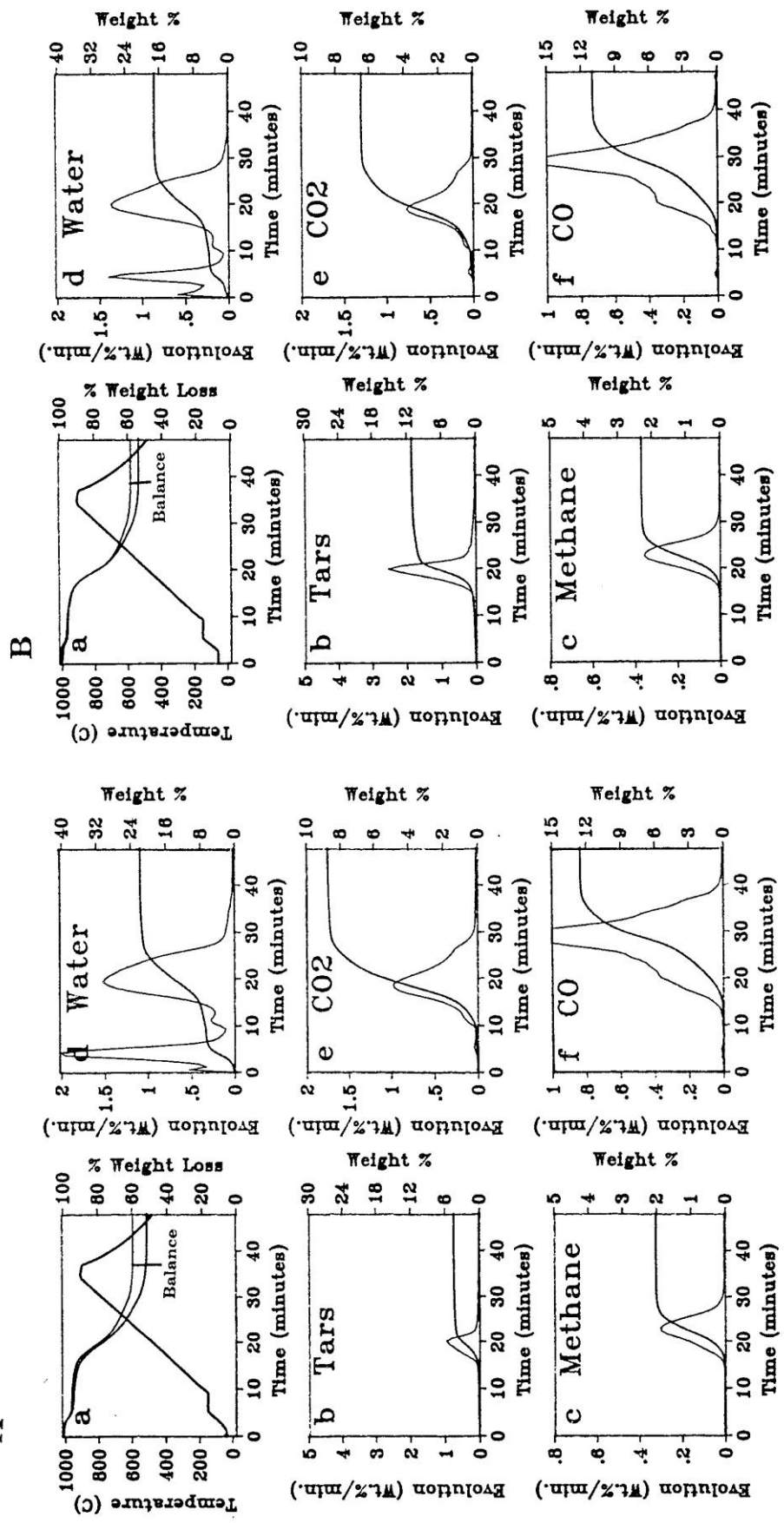

Figure III-3. TG-FTIR Analysis of Coals which have had Carboxyl Groups Exchanged with Barium. a) Zap; b) Wyodak.

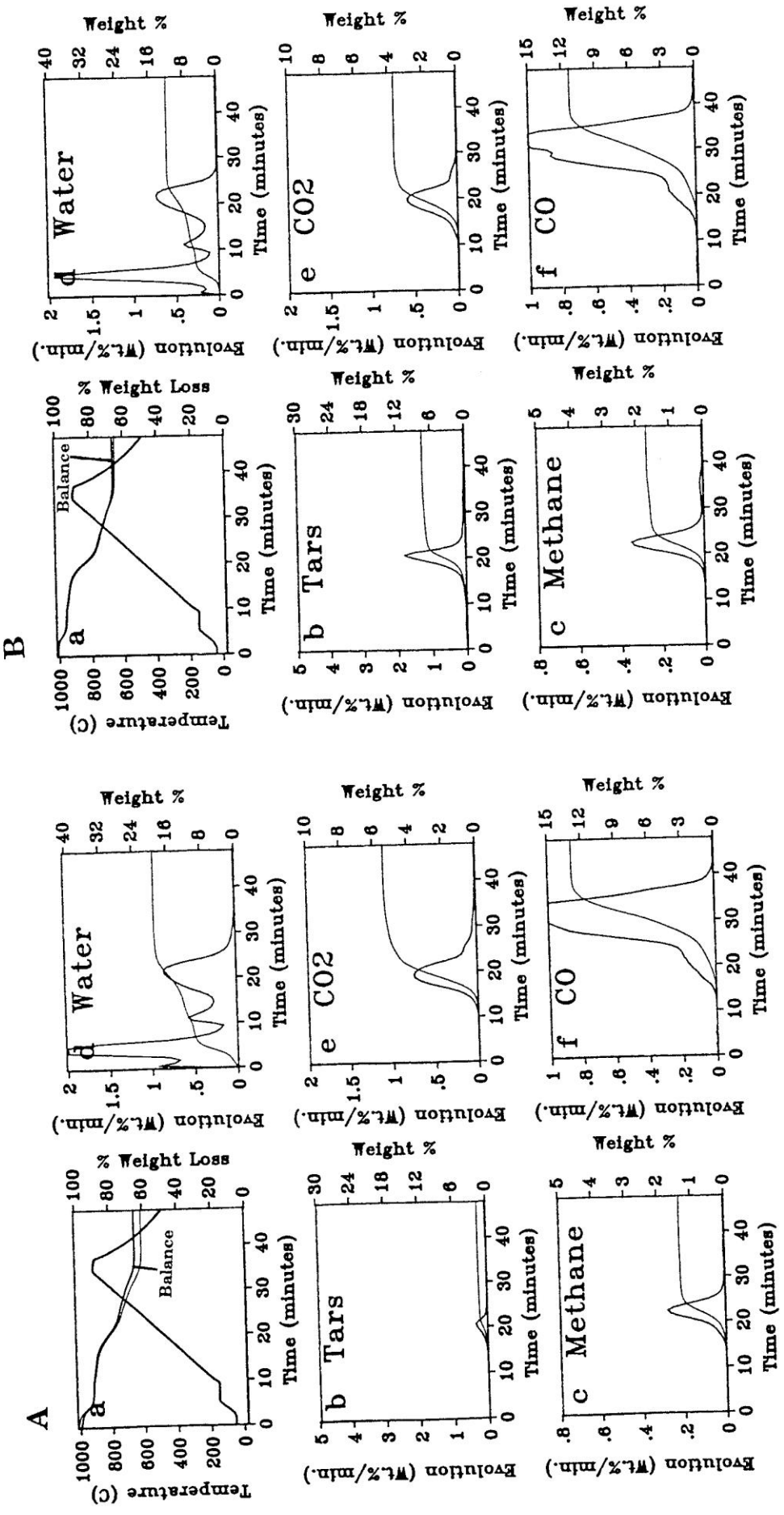

Figure III-4. TG-FTIR Analysis of Coals which have had Carboxyl and Phenolic Groups Exchanged with Barium. a) Zap; b) Wyodak.

The catalytic effect of H^+ was found to be more prominent in the liquid phase, since the liquefaction yield was depressed for the acid-contaminated sample, whereas the tar yield in pyrolysis was still high. This result indicates that excess acid should be avoided in order to obtain high liquefaction yields.

It is of interest to note that barium exchange at pH 8 does not reduce the oil yield in liquefaction for demineralized samples for both Zap and Wyodak. Since only carboxyl groups were exchanged at pH 8, it is suggested that oil molecules, which have smaller molecular weights than asphaltenes, contain more phenolic OH groups than carboxyl groups. Table III-2 also shows that barium exchange at pH 12.6, where both carboxyl and phenolic OH were exchanged into salt forms, significantly reduced both oil and asphaltene yields in liquefaction.

It is also of interest to note that the gas yields of liquefaction and pyrolysis do not always follow the same trend. Table III-1 shows that, in pyrolysis, the total yield of oxygen-containing gases (i.e., CO_2, CO, and H_2O) always increases with decreasing tar yield. Table III-2 shows the expected increase of the liquefaction yields with tar yield. However, the gas yields in liquefaction show an irregular variation. For example, the CO_2 yield is high for the partially barium exchanged Zap lignite, and is significantly reduced for the completely barium exchanged sample. The Wyodak subbituminous coal shows the opposite trend. For the ion-exchanged Zap lignite, the decrease of the CO_2 yield in liquefaction can be explained by the loss of some organic components, which contain CO_2-forming functions, during barium exchange at high pH. However, the behavior shown for the Wyodak coal is not able to be explained at this time.

Several aspects of the data revealed in Figs. III-1 to III-4 merit further comment. For samples which contain acidic functions in the salt form, including fresh and barium exchanged samples, there is always a water evolution peak present at around 200 ^oC. This 200 ^oC peak is obscure for demineralized samples. It is very likely that this peak is due to the evolution of moisture which was ionically bonded on the salt structure. For vacuum dried samples, it can be seen that the moisture content always increases with the amount of barium in the samples. This indicates that the acidic functions in the salt forms attract polar water molecules. These attracted water molecules cannot be removed by vacuum drying, but only by raising the temperature of the sample.

For CO evolution in pyrolysis, the demineralized samples show the major evolution at temperatures between 400 and 800 ^oC. CO evolution also occurs in a similar temperature range for fresh and ion-exchanged samples. However, the evolution is depressed at temperatures lower than about 750 ^oC, but elevated above this temperature by comparing with that of the demineralized samples. It was also noted that the fraction of CO evolving before 750 ^oC increases with increasing tar yield, as shown in Fig. III-5. This observation is significant. The higher CO evolution at temperatures lower than 750 ^oC for

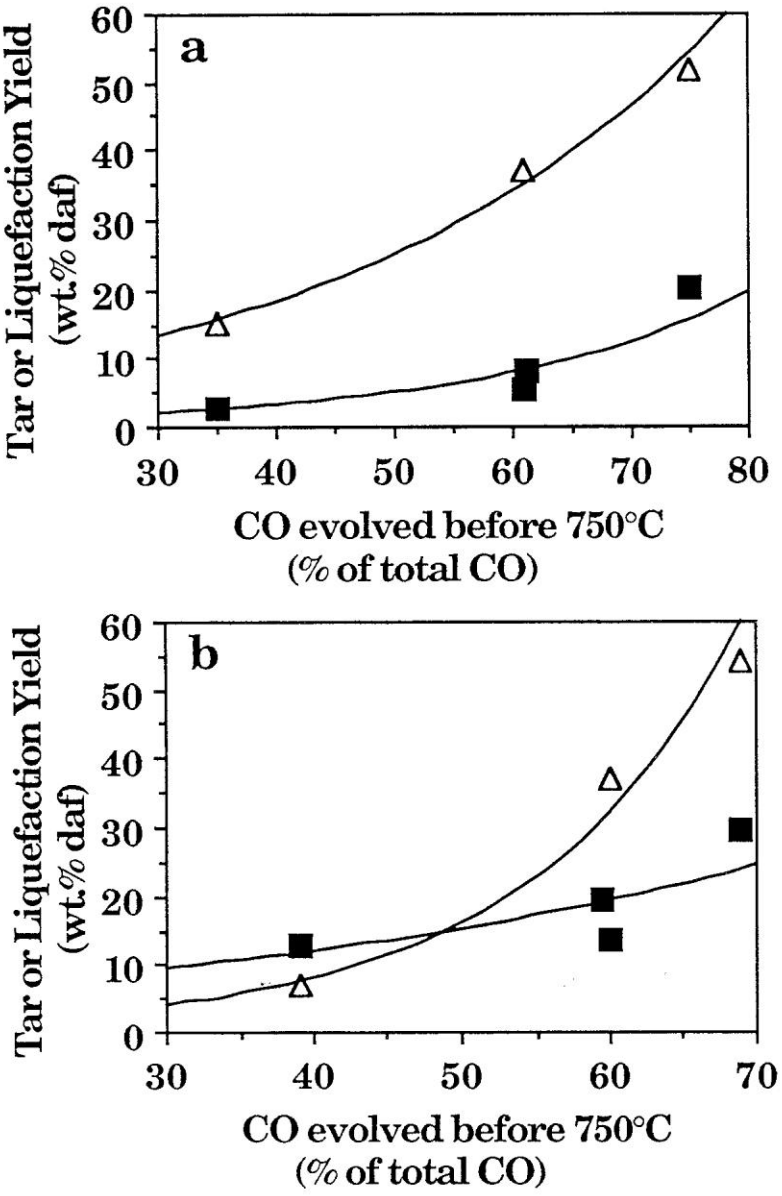

Figure III-5. Correlation of Pyrolysis Tar Yield (■) and Toluene Solubles from Liquefaction (△) with Pyrolysis CO Evolution Before 750°C. a) Zap; b) Wyodak.

demineralized samples is probably due to more oxygen functions evolving as CO without crosslinking.

For ion-exchanged samples, the depressed CO evolution at lower temperatures is probably caused by oxygen retention through crosslinking between oxygen functions, and the CO evolved at 750 °C or above, is likely from the decomposition of the crosslinking reaction products, which include ether, carbonyl and ester linkages, in the condensed char structure. The correlation of the total CO evolution in coal pyrolysis with pyrolytic tar and liquefaction yields was studied, as shown in Fig. III-6. The data show that both tar and liquefaction yields increase with decreasing total (pyrolysis) CO yield. Therefore, both the relative amount of CO evolved before 750 °C and the total CO evolution are indicators of the extent of crosslinking.

The CO_2 evolution curve does not show any shape variation due to the change of cation content. However, the yield is basically a decreasing function of tar yield. This has been explained by the mechanism that elimination of CO_2 would create aryl radicals to enhance crosslinking.

Figures III-1 to III-4 also show that CO_2, H_2O, and low temperature CO evolve in a similar temperature range. This might imply that these products are derived from a consecutive mechanism. Stoichiometrically, the following mechanism is a possible one:

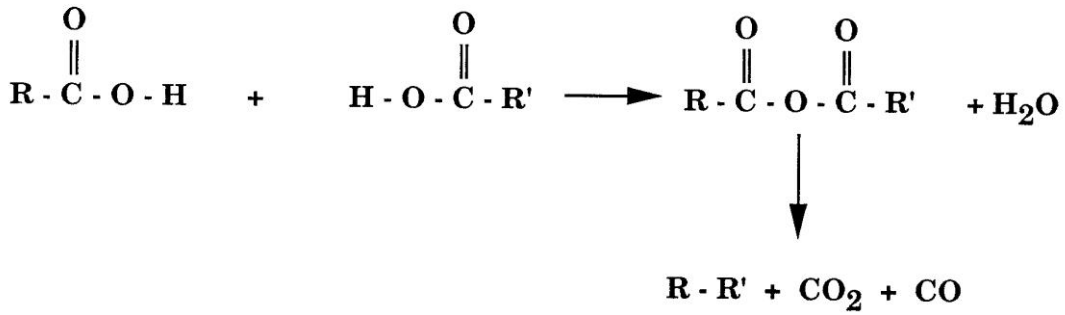

(4)

The CH_4 yield remains nearly constant for the different samples, and the shapes of the evolution curves are similar. Its value is 2.51 ± 0.2 wt.% daf for Zap lignite, and 3.0 ± 0.3 wt.% daf for Wyodak.

In theory, all of the carboxyl groups of demineralized samples can be exchanged with barium at pH 8. Consequently, it follows that one could determine the concentration of carboxyl groups in coal by knowing the amount of barium ion exchanged at pH 8. The chemical composition of ash formed by combustion of the barium exchanged sample is predominantly BaO. Therefore, from the ash content of the samples ion-exchanged at pH 8, one can estimate the concentration of carboxyl groups in the coal.

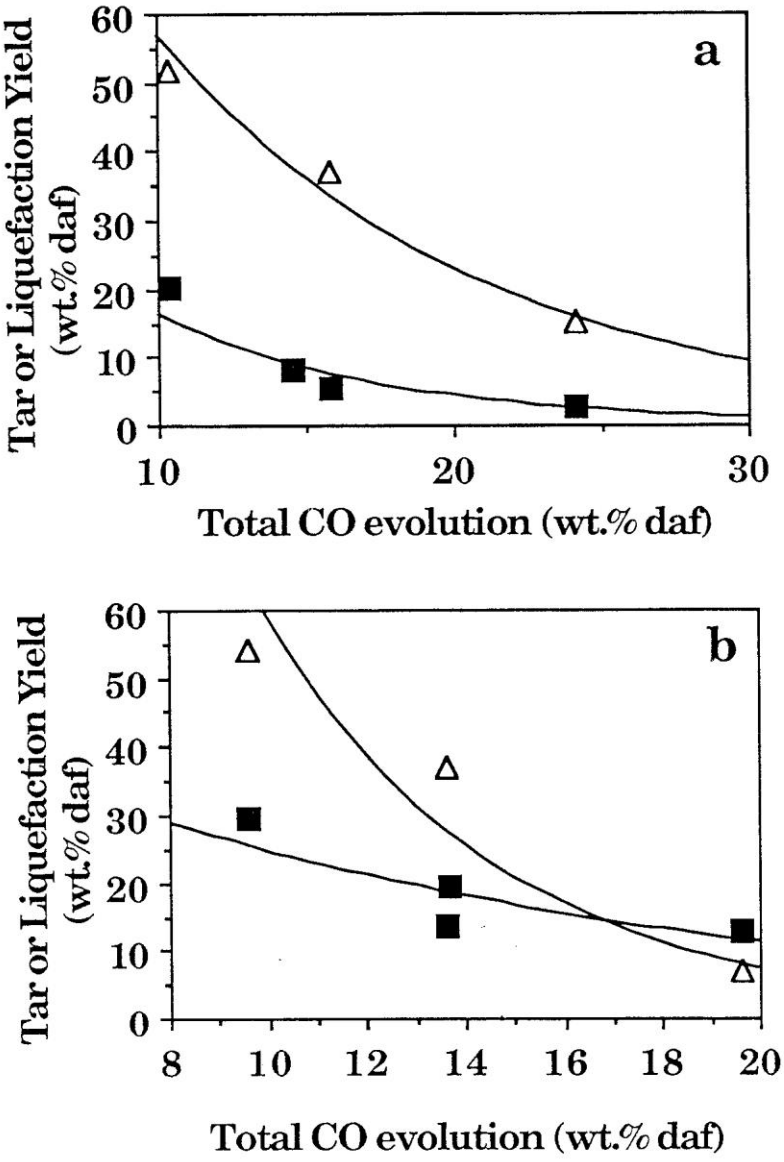

Figure III-6. Correlation of Pyrolysis Tar Yield (■) and Toluene Solubles from Liquefaction (△) with Total Pyrolysis CO Evolution. a) Zap; b) Wyodak.

Similarly, the total concentration of carboxyl and phenolic groups can be determined by the ash content of the sample ion-exchanged at pH 12.6. The concentration of phenolic groups can be obtained from the difference of the above two measurements. The concentrations of carboxyl and phenolic groups determined in this manner for Zap and Wyodak are shown in Table III-3. The results shown in Table III-3 are similar to those determined by Schafer [2,5] for Australian low-rank coals, using barium titration methods. It can be questioned as to whether all of these groups can be exchanged because of steric problems and if the cations could interact with additional sites in the coal. Additional insight can be gained from quantitative measurements from FT-IR methods for comparison (see Section E below).

TABLE III-3 - The Carboxyl and Phenolic Contents of Zap and Wyodak (meg g^{-1} dry and ash free basis)

	Carboxyl Group	Phenolic Group	Total Acidity
Zap Lignite	2.52	6.74	9.26
Wyodak Subbit	2.40	5.76	8.16

4. Coals Exchanged with Barium, Calcium and Potassium

In order to examine the effects of cation type, preparation of ion-exchanged (including barium, calcium and potassium) demineralized Zap and Wyodak was also completed. Both vacuum dried and moist samples were prepared, using procedures described previously. As usual, the modified samples were subjected to functional group analysis as KBr pellets with FT-IR, and programmed pyrolysis analysis with TG-FTIR. Liquefaction experiments of these samples were also performed and products were analyzed. The pyrolysis and liquefaction results are summarized in Tables III-4 to III-7.

The data in Tables III-4 to III-7 show that both the pyrolytic tar and liquefaction yields decrease with the extent of ion-exchange, i.e., in the order of (demineralized) > (ion-exchanged at pH 8) > (ion-exchanged at pH 12.5). However, it is realized that this is not a fair comparison for the samples exchanged at pH 12.5, since considerable amounts of humic acids were observed to dissolve in the high pH value solutions. The dissolution of coals in the aqueous alkaline solutions may be due to the breaking of ester bonds in coal, i.e., RCOOR' + OH- $\rightarrow$ RCOO- + R'OH. This coal dissolution mechanism was also proposed by other workers [6]. The solubility of coal in alkaline solutions varies with the cations contained in the solution. The color difference of the calcium and potassium solutions after ion-exchange at high pH is striking, in that the potassium solution has a much darker color, indicating much more coal dissolved in the monovalent cation (K+ here) solution than the bivalent cation (Ca++ here) solution. A photograph of the two solutions is shown in Fig. III-7. A possible reason is the fact that Ca++ ions can act as cross-links between two acid groups of different coal fragments [6], whereas K+ can only interact with one acidic site. The results also show that the barium solution extracted more coal

TABLE lll-4
Pyrolysis Results of Vac. Dry Modified Coal Samples

Coal (Type/ Preparation)	Proximate Analysis (wt.%), as rec.				Pyrolysis Products (wt.%, clan					
	Ash	Moisture	Fixed C	Volatile	Char	Tars	CO,	CO	H20	CH,
Zap Lignite, Vac. Dry										
demin.	2	4	51	44	**54**	20	4.8	10.4	8.4	2.7
demin. + K' (p118)	7	6	50	37	57	11	8.6	9.9	16.0	1.9
demin. + Ca' ' (pH8)	7	5	51	37	58	9.5	8.6	13.5	10.3	2.4
demin. + B a " (pH8)	15	5	44	36	55	5.5	11.7	15.8	18.6	2.6
demin. + K' (pH12.5)	16	6	45	34	57	4.9	9.9	12.4	13.5	1.6
demin. + C a ' ' (pH12.5)	25	7	34	33	51	3.8	8.2	22.6	12.6	2.0
demin. + Ba** (pH12.5)	38	9	28	26	52	2.9	10.5	24.1	15.5	2.6
Wyodak, Vac. Dry										
demin.	0	2	49	49	50	30	2.5	9.6	4.7	2.8
demin. + K' (pH8)	4	4	52	40	57	16	8.3	9.0	13.1	2.1
demin. + C a ' ' (p1-18)	6	4	49	41	55	**14**	6.1	11.6	9.8	2.7
demin. + **Be '** (pH8)	15	4	**44**	37	54	**14**	8.8	13.6	12.4	2.9
demin. + Ba' ' (0112.6)	36	6	30	28	51	13	6.4	19.6	10.6	2.9

TABLE III-5
Pyrolysis Results of Moisturized Modified Coal Samples

Coal (Type/Preparation)	Proximate Analysis (wt.%), as rec.				Pyrolysis Products (wt.%, dat)					
	Ash	Moisture	Fixed C	Volatile	Char	Tars	CO2	CO	H,0	CH,
Zap, Moisturized										
demin.	2	15	41	42	50	16	6.5	16.8	11.1	2.8
demin. + K+ (pH8)	7	20	41	31	57	12	8.2	11.6	7.9	1.6
demin. + Ca+ + (pH8)	6	21	40	33	55	11	7.0	16.0	4.9	2.3
demin. + Ba+ + (pH8)	13	24	33	30	53	9	10.0	15.6	13.7	2.0
demin. + K+ (pH12.5)	10	29	32	29	53	5	14.7	13.0	8.1	1.4
demin. + Ca+ + (pH12.5)	19	22	27	31	47	6	12.0	27.1	4,1	1.9
demin. + Ba+ + (p1112.5)	31	24	18	27	40	5	14.6	27.3	14,2	2.2
Wyodak, Moisturized										
demin.	0	15	41	45	48	25	5.3	11.1	12.4	2.9
demin. + K+ (p1-18)	14	17	33	36	48	15	10.4	12.6	12.5	2.2
demin. + Ca+ + (pH8)	4	17	42	37	53	15	7.7	13.7	8.3	2.7
demin. + Ba+ + (p1-18)	13	20	35	32	52	17	6.4	14.5	11.7	2.4
demin. + Ba+ + (p1-112.6)	28	25	19	28	40	11	12.8	27.2	8.0	2.5

TABLE III-6
Liquefaction Results of **Vac Dry Modified Coal Samples**

	Toluene Solubles			Toluene Insolubles	Gas						
Coal (Type/Preparation)	Total	Oils	Asphaltene		Total	H2	CO,	CO	CH4	C2H6	C2/14
Zap Vac Dry											
demin.	52	26	26	46	2.2	0.02	1.1	0.43	0.27	0.29	0.05
demin. + K'(pH8)	30	11	19	62	8.4	---	7.7	0.27	0.17	0.20	0.02
demin. + C a - (p1-18)	25	13	12	72	3.4		2.7	0.30	0.22	0.14	-
demin. + Be.' ' (pH8)	37	25	12	55	8.2	0.02	7.3	0.40	0.20	0.24	---
demin. + K' (pH12.5)	17	5	12	77	5.8	0.05	5.0	0.24	0.27	0.28	
demin. + C a " (pH12.5)	(--)	(---)	3		0.9		0.7	0.04	0.08	0.07	---
demin. + B a " (pH12.5)	15	15	0.5	84	1.0		0.3	0.27	0.02	0.41	
Wyodak Vac Dry											
demin.	54	22	32	43	2.9	0.01	2.2	0.31	0.11	0.24	0.04
demin. + K^+ (pH8)	46	26	20	46	8.5	0.04	7.6	0.34	0.21	0.27	0.01
demin. + Ca' + (pH8)	14	4	10	82	4.1		3.8	0.19	0.04	0.06	-
demin. + B a - (pH8)	37	25	12	62	0.7	0.02		0.43	0.08	0.19	---
demin. + Ba" + (pH12.5)	7	5	2	89	3.9	0.09	3.4	0.23	0.02	0.12	0.04

TABLE III-7
Liquefaction Results of Moisturized Modified Coal Samples*

	Toluene Solubles			Toluene Insolubles	Gas						
Coal (Type/Preparation)	Total	Oils	Asphaltene		Total	H_2	CO_2	CO	CH_4	C_2H_6	C_2H_4
Zap, moisturized											
demin.	56±5	28±2	28±7	40±5	4.3	---	3.9	0.18	0.01	0.10	---
demin. + K^+ (pH8)	25	20	5	66	9.5	---	8.9	0.40	0.04	0.14	---
demin. + Ca^{++} (pH8)	29	18	11	66	4.5	---	4.1	0.20	0.12	0.08	---
demin. + Ba^{++} (pH8)	17	8	9	74	8.5	---	7.4	0.88	0.15	0.08	0.01
demin. + K^+ (pH12.5)	28	10	18	57	15.3	---	14.9	0.13	0.13	0.12	0.02
demin. + Ca^{++} (pH12.5)	10	9	2	87	2.2	---	1.9	0.24	0.01	0.05	---
demin. + Ba^{++} (pH12.5)	13	3	10	76	10.7	---	10.1	0.45	0.10	0.10	---
Wyodak, moisturized											
demin.	57	11	46	38	4.7	0.05	4.0	0.32	0.11	0.14	---
demin. + K^+ (pH8)	55	29	26	32	12.8	0.01	12.0	0.33	0.17	0.23	0.02
demin. + Ca^{++} (pH8)	32	13	19	63	4.7	---	4.3	0.22	0.06	0.08	0.01
demin. + Ba^{++} (pH8)	25	7	18	67	8.7	---	6.8	1.93	0.11	0.06	---
demin. + Ba^{++} (pH12.5)	26	15	12	67	7.0	0.01	6.7	0.27	0.01	0.01	0.02

* Conditions: 440 ^oC, 30 min., dihydrophenanthrene solvent (0.5 g coal; 3 g solvent)

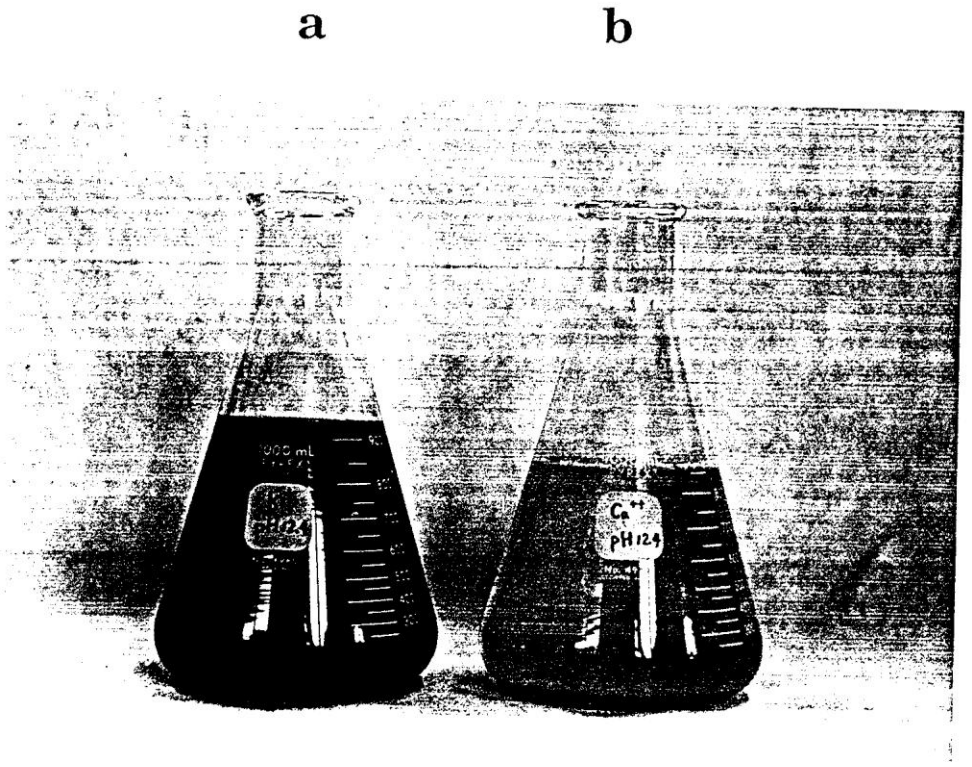

Figure III-7. The Solutions after Ion-Exchange with Demineralized Zap Lignite. a) Potassium Chloride at pH 12.4; b) Calcium Acetate at pH 12.4

than the calcium solution. It is likely that coal solubility in aqueous alkaline solutions increases with the size of the cations of the same valence. If this is true, the dissolution of coal in sodium solution would be expected to be less than that in the potassium solution. Our results indicate that this is the case, but this requires further study. In summary, at similar pH values (~12.5), the amounts of Zap lignite extracted by 1 liter of the cation solutions in 20 hours increases in the order of $Ca^{++} < Ba^{+} < K^{+}$.

It can be seen in Table III-4, for the pyrolysis of vacuum dried samples, that the tar yield was higher for the potassium-exchanged coals than the calcium and barium-exchanged samples, suggesting that bivalent cations tighten the coal structure by cross-linking coal fragments and make it difficult for larger tar molecules to escape [7]. Also shown in Table III-4, the CO yield in pyrolysis for different ion-exchanged samples generally shows a trend opposite to that of the tar yield. The possible reasons for this have been discussed above. The CH_4 yield also showed a trend opposite to that of the tar yield for the ion-exchanged samples. This has been generally reported in coal pyrolysis studies. By reincorporation into the solid matrix by more stable bonds, the tar precursors can yield volatiles only by cracking off of small side groups, hence the increased CH_4 yields with decreasing tar yields.

The liquefaction results in Table III-6 indicate that the potassium-exchanged samples have higher liquefaction yields (especially asphaltenes) than for the barium- and calcium-exchanged samples. This can probably be attributed to the same reason for the high pyrolytic tar yield, that bivalent cations can serve as a cross-linking agents to tighten the coal structure. Also, the gas evolution, especially CO_2, was highest for the potassium-exchanged samples during liquefaction. The reason for this is not clear, but it may be due to catalytic activity of the potassium. In previous work, higher pyrolysis CO_2 yields have generally been associated with lower liquefaction yields [4].

In considering the size effect of the cations on the pyrolytic tar and liquefaction yields, one should compare the data for the barium- and calcium-exchanged samples. It is interesting that the size of the cations has an opposite effect on the tar and liquefaction yields. In pyrolysis, the tar yield for the barium-exchanged samples is lower than that of the calcium-exchanged samples. This could be due to the larger size of barium, which hinders escape of tars in the coal particles. However, according to Table III-4, the char yield was not higher for the barium-exchanged samples, while the yields of oxygen-containing gases and CH_4 were higher. This suggests more severe cracking off of oxygen functions in the tars from the barium-exchanged samples due to a longer residence time in the coal particle. In liquefaction, the yield was higher for the barium-exchanged samples. The reason for this is not clear, but it may be related to the fact that more coal was dissolved in the barium-containing alkaline solution than the calcium one.

B. Preparation and Characterization of Moisturized Coal Samples

Remoisturization of vacuum dried Zap and Wyodak was done in the attempt to understand if moisture uptake for low rank coals is a reversible process and to see if moisture influences the role of the cations. A procedure for restoring the moisture level of modified coal samples was developed. The moisturized samples were prepared by enclosing the vac-dry modified samples in a box with a nitrogen purge of 100% humidity. The sample exposure to moisture was performed for several days (~6 days) until no further moisture uptake was observed. These moisturized samples were subject to routine liquefaction experiments and pyrolysis analysis in the TG-FTIR.

The TG-FTIR pyrolysis data for the moisturized coal samples are summarized in Table III-5. The saturation moisture content of the modified coal samples, for both Zap and Wyodak, increases with the extent of ion-exchange, and varies in the range of 15-25 wt% (as-received basis). The pyrolysis results indicate that the coal structure varies with the moisture content. Moisturization reduces the tar yield in pyrolysis for the demineralized samples, increases the yield for pH 8 ion-exchanged samples, and has little effect on the yield for pH 12.6 ion-exchanged samples. Pyrolysis char yield, on the other hand, was reduced, for all the modified samples, by increased moisture content.

The gas evolution during pyrolysis was also influenced by the moisture content. For example, a significant amount of CO was evolved at temperatures around 850 ^{o}C for the moisturized samples, but this was not observed for the vac-dry samples. It is also of interest to note, only in the case of the demineralized samples, that there was much more CO product in the TG-FTIR char combustion cycle for the moisturized than the vac-dry. This implies that the form of the mineral matter, which acts as a combustion catalyst, is different. The effect of the moisture content on the mineral matter could also be important in the liquefaction behavior.

The results in Table III-5 indicate that the moisture content can reach that of the raw samples by remoisturization for Zap, but not for Wyodak. Furthermore, the chemical structure of the coal samples seems to have been changed by remoisturization, since different CO_2 evolution behaviors were observed. A comparison of the CO_2 evolution behavior for raw and remoisturized coal samples is given in Fig. III-8.

In almost every case, the asphaltene yield was increased with moisturization except for the pH 8 Zap, in which case the asphaltene yield was slightly reduced, as shown by comparison of Tables III-6 and III-7. Interestingly enough, the oil yield was reduced for most of the modified samples with moisturization, except for the demineralized Zap and the pH 12.6 Wyodak. The indication from the above results is that moisturization favors the formation of the larger molecular weight asphaltenes in liquefaction, while the formation of the smaller molecular weight oils was less favored.

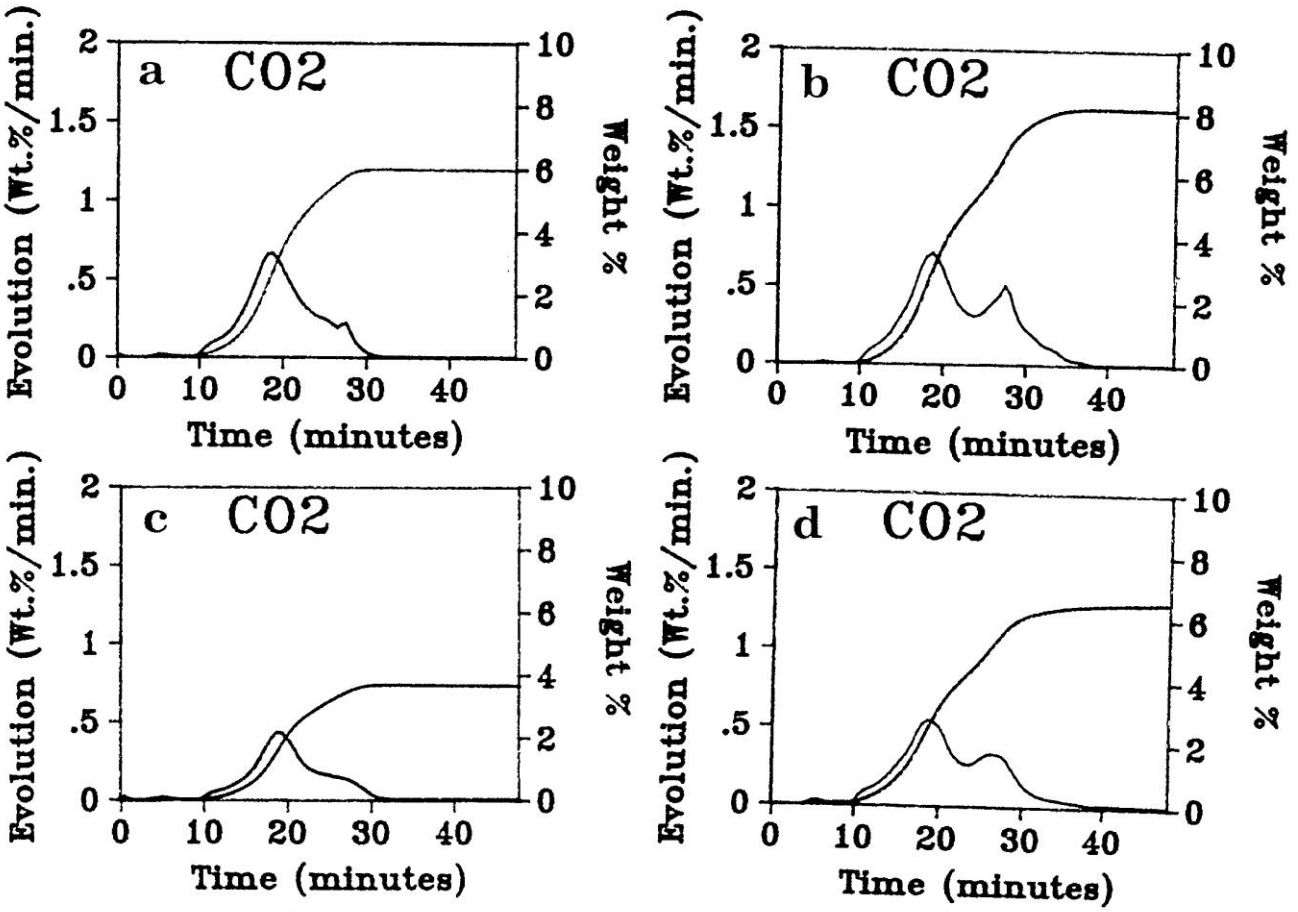

Figure III-8. CO_2 Evolution During Coal Pyrolysis. a) Raw Zap; b) Remoisturized Zap; c) Raw Wyodak; d) Remoisturized Wyodak.

It is usually shown that the trends for improved liquefaction yields parallel those for improved tar yields in pyrolysis. However, it was found in this study that the influences of moisturization on the yields of pyrolytic tars and liquefaction toluene soluble yields are different in that moisturization does not appear to have a significant effect on tar yields. This indicates that moisture plays different roles for the formation of tars in pyrolysis and coal liquids in liquefaction. A possible explanation for the difference is that most of the moisture is depleted early in the pyrolysis process, whereas the moisture is retained in the reactor during liquefaction and can exist in a liquid phase. This aspect requires further investigation.

The results in Table III-6 and III-7 also indicate that the moist samples have a higher gas yield in liquefaction than the vacuum dried samples. The increase in gas yield is mainly from CO_2 and CO (especially CO_2), whereas the yields of hydrocarbon gases decrease with moisturization. One possible explanation for this result is that moisture may react with side chain structures in coal, which are the sources for the formation of oils and hydrocarbon gases during liquefaction, to form oxygen functions. The subsequent reaction of these oxygen functions produces more CO_2, CO and asphaltenes in the liquefaction of moist coals.

The detailed results for the pyrolysis and liquefaction experiments are given in Tables III-5 and III-7 and were discussed above. In general, pyrolysis tar yields and the toluene solubles yields from liquefaction for the remoisturized samples were similar to those for the vacuum dried samples. It appeared that the liquefaction results were more sensitive to the presence of moisture, although the increases in asphaltene yields were generally balanced by decreases in oil yields. As discussed above, a possible explanation for the difference is that most of the moisture is depleted early in the pyrolysis process, whereas the moisture is retained in the reactor during liquefaction and can exist in a liquid phase under the right conditions.

It is known from the above results and the literature [5] that the moisture is associated with cations in raw coals. Consequently, an investigation was made to determine if the deleterious effects of cations could be mitigated by adding water to the donor solvent liquefaction system. Results from experiments with raw and demineralized Zap at three different temperature levels are given in Table III-8. At temperatures near or below the critical temperature of water (374° C), it appears that there is a profound beneficial effect of added water for the raw coal (note the significant reduction in CO_2 evolution). Conversely, there is a significant deleterious effect of added water for the demineralized coals. The ability of water to interact with cations and affect the course of the thermal decomposition behavior is consistent with results that have been observed in hydrothermal treatment of coal, which mimics the geological aging process in many respects.

TABLE III-8 - Effect of Added Water on Liquefaction of Raw and Demineralized Argonne Zap Coal

Temp. Level (°C)	Water Addition	Toluene Solubles wt.%, daf		CO_2 Yields wt.%, daf	
		Raw	Demin.	Raw	Demin.
350	yes	13	0	0.0	1.1
	no	1	27	5.4	2.4
375	yes	23	19	2.4	1.5
	no	11	40	5.2	2.2
400	yes	31	24	5.2	0.8
	no	30	58	4.1	4.2

C. Preparation and Characterization of Methylated Coal Samples

As part of the study of the effects of coal modification, the preparation of alkylated coals was carried out at SRI International. A 15 gram sample of de-mineralized Argonne Zap Lignite was prepared at AFR and sent to SRI. The methylation of this coal in a single batch was begun using a slight modification of the procedure employed in the earlier phase of this project. A portion of the "fully" methylated coal will be subjected to either ether cleavage or ester hydrolysis to generate a sample in which only one type of acidic oxygen is methylated (see below). The major purpose of this combination of demineralization and complete and partial methylation is, of course, to determine the effect of methylation per-se, and to see if it accomplishes substantially different things than the demineralization.

The major modifications in the alkylation procedure were the addition of second aliquots of tetrabutylammonium hydroxide and methyl iodide and soxhlet extraction with a water-methanol mixture during the work-up of the methylated coal. These changes were made after consulting with Dr. Leon Stock of the University of Chicago and Dr. A. C. Buchanan of Oak Ridge National Laboratory. In brief, the rationale was that methanolic water both improves the wetting of the coal and has higher solubility for tetrabutylammonium iodide. This rationale seems to have merit, since the nominal uptake of nitrogen (0.09/100C) was only one fifth of that observed in our previous large scale methylation of Zap lignite. We began the methylation procedure with 13.17 grams of demineralized dried coal, and recovered 13.2 grams of the methylated product. Samples of the alkylated and unalkylated coal were sent for elemental analysis. The results of the elemental analyses are shown in Table III-9.

As Table III-9 indicates, the change in nitrogen is small, and the change in total halide is insignificant. The empirical formula for the unmethylated (but demineralized) Zap is $C_{100}H_{85.6}N_{1.17}O_{26.4}$ and that for the methylated product (assuming that oxygen stayed constant during methylation and workup) is $C_{116.8}H_{109.9}N_{1.26}O_{26.4.}$ Since the empirical formula is only a set of ratios it is necessary to assume an absolute change (or lack of one) for some element in order to stipulate the absolute change in carbon and hydrogen. The assumption that oxygen does not change gives an empirical formula that corresponds to a $\triangle$C of 16.8 and a $\triangle$H of 24.3, or a shortage of 9.3 hydrogens. These values change slightly if it is assumed that the nominal increase of 0.09 in nitrogen is real and that part of the observed increases in carbon and hydrogen are due to incorporation of the tetrabutyl ammonium group. If, on the other hand, we assume that sulfur is the most likely to have neither decreased nor increased during the methylation procedures and therefore hold it constant during the calculation of the empirical formula, we arrive at a formula (Table III-9) that corresponds to a $\triangle$C of 7.0, a $\triangle$H of 15.08, and a $\triangle$N of 0.01. The carbon and hydrogen proportions are now exactly correct, though the apparent degree of methylation is less. In any case, the uptake of nitrogen and apparent shortage of incorporated hydrogens during this methylation are much less than they were in the previous large scale methylation of Zap. In that earlier alkylation, the observed increase in hydrogen was only 43% of that expected based on the nominal increase in carbon. With this demineralized coal and new alkylation procedure, the increase in

hydrogen was 69% of that expected based on the increase in carbon, even for the "worst" case, where oxygen is held constant and the carbon and hydrogen are adjusted assuming the nominal increase in nitrogen comes from incorporation of tetrabutylammonium ion. Thus, depending on the bases chosen for comparing the elemental compositions, we conclude that from 7 to 15 carbons were introduced, the increase in hydrogen was from 70 to 100% of that expected based on the carbon increase, and that there was ≤0.09 N/100 C introduced.

TABLE III-9 - Elemental Analysis and Empirical Formulas for Demineralized Zap Lignite Before and After Methylation

ELEMENT	NON-METHYLATED	METHYLATED
C	71.19	71.14
H	5.08	5.60
O	25.02	21.55
N	0.97	0.90
S	0.81	0.76
Total halide	200	210
Ash	0.16	0.56
Empirical Formula	$C_{100}H_{85.6}N_{1.17}S_{0.426}O_{26.4}$	$C_{116.8}H_{94.06}N_{1.08}S_{0.398}O_{0.426}$
Emp. For. (Constant Oxygen)		$C_{116.8}H_{109.9}N_{1.26}S_{0.465}O_{26.4}$
Emp. For. (Const. O,N)		$C_{115.3}H_{106.6}N_{(1.17)}O_{26.4}$
Emp. For. (Const. S)		$C_{107.0}H_{100.7}N_{1.16}O_{24.19}$

D. Preparation and Characterization of Biologically Pretreated Coal Samples

Upon the recommendation of Dr. Malvina Farcasiu, a sample of demineralized (DMN) Argonne Wyodak coal was prepared for the Michigan Biotechnology Institute (MBI). This was subjected to biological pretreatment for removal of carboxyl groups [8] and sent back to us along with samples of biopretreated raw coal and a control sample. The control sample was a raw Wyodak sample which had been added to the growth medium but which was not innoculated with bacteria. At AFR, the five samples were subjected to FT-IR pellet analysis, TG-FTIR analysis, SEM/x-ray analysis, and liquefaction experiments in a donor solvent.

The results for the curve resolving of the carbonyl region of the FT-IR spectra are shown in Table III-10. The results from the liquefaction experiments are shown in Table III-11 (see below).

Table III-10 shows the data for the carboxylic acid carbonyl and the sum of the free and hydrogen bonded or conjugated carbonyls. The COOH concentration measurements were somewhat variable

when duplicate pellets were measured, but indicate a slight decrease in the carboxyl concentration as a result of biotreatment of the raw coal. A surprising result was the apparent increase in the COOH concentration for the DMN, biotreated sample when compared to the normal DMN sample. Unfortunately, there was no control done for the DMN sample so it cannot be established if this was due to the addition of the acidic growth medium. However, this is a likely explanation. The changes in the sum of the free and H-bonded carbonyls for the control sample suggests that significant changes have taken place as a result of the processing, which is done prior to the biological activity. This is a major difficultly in interpreting these results.

TABLE III-10 - FT-IR Analysis of Carbonyl Region for Normal and Biotreated Samples

Coal	Peak heights (arbitrary units)	
	COOH	C = O*
Raw	0.06	0.08
DMN	0.09	0.11
Raw, control	0.05	0.25
Raw, biotreated	0.04	0.21
Raw, biotreated	0.04	0.25
DMN, biotreated	0.15	0.14
DMN, biotreated	0.19	0.18

* Sum of free and H-bonded forms

TABLE III-11 - Liquefaction Yields (DAF%) for Normal and Biotreated Samples

Coal	Tol. sol.	Oils	Asph.	CO_2	CO	CH_4
*Raw	34	19	15	0.8	0.1	0.03
*DMN	54	22	32	2.2	0.3	0.1
*DMN + H^+	36	14	22	0.0	0.2	0.04
Raw, Control	38	24	14	3.9	0.3	0.05
Raw, biotreated	41	26	15	0.6	0.3	0.11
DMN, biotreated	42	25	17	0.5	0.3	0.12

* Liquefaction done in dihydrophenanthrene

The liquefaction experiments were carried out at 400° C for 30 min. with 6:1 tetralin: coal. Table III-11 shows the results of these experiments on the MBI samples along with values for the raw Argonne Wyodak coal. The biotreatment of the raw coal leads to only modest increases in the liquefaction yields. The biotreatment of the demineralized coal actually resulted in yields lower than expected from the normal demineralized coal. However, we have found that residual acid (from incomplete washing) can significantly reduce the solubles yields, as indicated in Table III-11. Consequently, the benefit of the biotreatment may have been offset by the addition of the acidic nutrient media to the coal.

In the case of the biotreated raw coal, there was a modest reduction in the CO_2 yield in liquefaction due to biotreatment which is consistent with the modest reduction in carboxyl groups. However, there was a very large increase for the raw control sample which was not reflected in a large increase in carboxyl group content (see Table III-10). In addition, the results for the DMN samples are hard to reconcile since the trends for CO_2 yields and carboxyl content are in opposite directions. We have found that the CO_2 yield in liquefaction is very sensitive to the liquefaction conditions and can also be influenced by secondary reactions. Another factor, in this case, is the unknown effect of the addition of the nutrient media.

The results for the TG-FTIR analysis and SEM/x-ray analysis are given in Tables III-12 and III-13, respectively. The results for the tar yields from programmed pyrolysis in the TG-FTIR are largely consistent with the results from the liquefaction experiments, i.e., there appeared to be a modest benefit to biotreating the raw coal and a significant detriment to biotreating the demineralized coal. Again, the lack of a control for the demineralized sample makes the interpretation of the latter results more difficult. It was noted by the investigators at MBI that maintaining an optimum pH for the demineralized samples was more difficult.

There was a decrease in CO_2 yield from TG-FTIR analysis for the biotreated samples, but not as large as the decrease in the CO_2 yield for the normal demineralized samples (see Tables III-1 and III- 4). These changes do not correlate with the change in the free carboxyl content reported in Table III-10. This is not surprising in light of the fact that it is the cation-exchanged (carboxylate) form which is more likely to produce CO_2 upon pyrolysis. It is also true that model polymers which have no carboxyl group content will produce CO_2 upon pyrolysis, possibly due to secondary reactions of CO and H_2O.

The results for the SEM/x-ray analysis of the normal and biotreated samples are given in Table III-13. Since this system is in need of recalibration, these numbers should not be considered absolute.

TABLE III-12 - Summary of TG-FTIR Results on Normal and Biotreated Wyodak Samples

Sample Identification

SPECIES	RAW	RAW, CONTROL	RAW, BIOTREATED (#5)	RAW, BIOTREATED (#13)	DMN	DMN BIOTREATED (DRI)	DMN BIOTREATED (DLI)
% Char, DAF	54	54	52	53	50	53	54
% Ash, AR	7	7	8	10	0	5	2
% M, AR	25	10	6	8	2	3	4
Tars, DAF	15	18	21	21	30	20	21
CH_4, DAF	2.2	2.3	2.1	1.8	2.8	2.4	2.2
H_2O, DAF	12	10	11	11	5	14	11
CO_2, DAF	5.4	4.7	4.6	4.4	2.4	4.4	4.0
CO, DAF	13.4	10.7	10.1	8.2	9.6	7.4	7.0
ΣO, DAF*	21	18	19	18	12	19	17

* Sum of oxygen in H_2O, CO, and CO_2

TABLE III-13 - Summary of Sem/X-Ray Analysis Results on Normal and Biotreated Wyodak Samples

Sample Identification

SPECIES (DRY WT. %)	RAW	RAW, CONTROL	RAW, BIOTREATED (#5)	RAW, BIOTREATED (#13)	DMN	DMN BIOTREATED (DRI)	DMN BIOTREATED (DLI)
% Ash	6.44	5.76	6.98	6.65	0.30	1.96	1.99
% Na	0.00	0.00	0.00	0.19	0.00	0.05	0.06
% Mg	0.23	0.00	0.00	0.00	0.03	0.09	0.10
% K	0.01	0.03	0.32	0.59	0.00	0.22	0.25
% Ca	1.09	1.17	1.10	0.74	0.04	0.18	0.18
% S (o)	0.36	0.47	0.54	0.48	0.35	0.47	0.53
% S (m)	0.19	0.18	0.17	0.11	0.13	0.17	0.16

The numbers for total ash content show the same general trends as the TG-FTIR values in Table III-12. The values for the calcium content, most of which is exchanged on carboxyl groups, do not appear to be affected much by biotreatment. As expected, these values are much lower for the demineralized samples. The values of organic or mineral sulfur are small to begin with and did not appear to be affected much by biotreatment.

In summary, the results from the various analyses indicate a modest benefit to the MBI biotreatment process for the raw coal and a negative result for the demineralized coal. In all cases, the best sample from a liquefaction standpoint was the normal demineralized coal. This is consistent with our other data from coal and model compound studies which suggest that carboxyl groups are not bad actors as far as retrogressive reactions are concerned but rather the cations which are exchanged on these groups. Consequently, efforts on biological pretreatment should be redirected toward removal of cations rather than carboxyl groups.

E. FT-IR Spectroscopy Methods for Carboxyl and Phenolic Group Determinations

An FT-IR spectroscopy method was developed to quantify the concentration of carboxyl groups in coals and modified coals which is based on the work of Starinsic et al. [9]. Some preliminary data are shown in Table III-14. These are not yet quantitative, since we have used a literature value of the extinction coefficient which will be different for our instrument. However, the relative changes with the various coal modifications can be compared. The results show the expected increases in COOH concentration when the coals are acid washed or demineralized and the expected decreases when the coal is calcium loaded.

TABLE III-14 - Preliminary Data on Determination of Carboxyl Functionalities Using FT-IR Method

Coal Type	Treatment	Wavenumber (cm^{-1})	DAF % COO(H) X k_n*
Zap	---	1702	6.47
	HCl wash	1702	7.00
	Ca^{2+} load	1704	2.02
Demin. Zap	---	1695	10.99
	Ca^{2+} load	1710	2.93
	Ca^{2+} load HCl wash	1702	8.97
Wyodak		1701	4.90
Demin. Wyodak		1702	7.26

NOTES:
k_n = normalization factor
* amounts based on peak height

Work was also done on the development of a curve resolving program to analyze the OH region of the FT-IR spectrum. Problems with curve resolving routines are associated with the initial choice of parameters for input to the program. It is essential to have a prior knowledge of the number of bands in the region that is to be resolved as well as good initial estimates of the peak position of each band and its width and half height. One way to help with the choice of the initial inputs to the program is to examine the second derivative of the original coal spectra. However, the problem with this approach is that small peaks may be obscured by the noise level, thus underestimating the number of peaks.

A second approach is to examine the solid state spectra of every possible component separately to determine the number of peaks and peak positions as inputs to the program. This would not necessarily provide the right peak positions for an actual coal sample, but would provide a good idea of the number of distinct peaks.

Our approach to assessing the performance of a particular set of input parameters was to do curve resolving with coals and modified coals where there was good literature evidence of changing functional group concentrations due to the modification. This approach was followed by Starinsic et al. [9], who determined the change of the carboxyl group content due to demineralization and ion exchange.

While it seems to be difficult to resolve all of the various constituents in the carboxyl (1700 cm^{-1}) region, an examination of model compound hydroxides shows a simpler picture:

- All hydroxides have a broad band around 3500 cm^{-1}, except for the ortho-dihydroxides which have one or two additional peaks in the 3500-3600 cm^{-1}. This feature allows us to see them separately by including two bands in this region.

- What interferes with this simple picture are the ortho-aliphatic monophenols and, to a lesser extent, condensed ring functionalities where the OH band is shifted towards higher wavenumbers. This kind of shift occurs also if the OH hydrogen becomes less hydrogen bonded.

- There appears to be two or three bands in the 3600-3700 cm^{-1} region originating from the mineral content of the coal. These can either be subtracted using proper mineral spectra or added to the curve resolving scheme.

Based on these considerations, the synthetically constructed set of bands would consist of three mineral (3690, 3650, 3620), four OH (3550 for the dihydroxy, 3500, 3450 for the shifted and 3400 for the OH) bands and three additional bands between 3200 and 3000 cm^{-1}.

The observations from the preliminary work on curve resolving the OH region can be summarized as follows:

- The peak around 3450 cm^{-1} is due to strongly absorbed H_2O molecules which are removed upon drying the acid treated coal but not the Ca^{2+} treated or original (untreated) coal.

- The peak around 3400 cm^{-1} is the (mono)-phenolic peak. It increases after acid washing and cannot be back exchanged by Ca^{2+} below pH 8.

- The peaks around 3510 cm^{-1} and 3550 cm^{-1} are from ortho-dihydroxy groups and/or chemically bound water which are not removed by drying and show a maximum, along with the monophenols (or meta-para-diphenols), with hydrothermal pretreatment time.

Some of the preliminary results for curve resolving the OH region are shown in Table III-15. If this data is considered (on a qualitative basis) along with the data supplied in Table III-14 on carboxyl group changes, it can be seen that the changes in the free COOH and the o-dihydroxyl are usually in the same direction for each coal modification. One of the key findings of this work is that while carboxyl groups ion-exchange at pH=8.1 and phenolic groups ion-exchange at pH>>8.2, ortho dihydroxy functionalities ion-exchange at pH=7 and thus behave like carboxyls. This unusual behavior is the result of intramolecular hydrogen bonding between the two neighboring oxygens to increase the resonance stability of the ortho-hydroxy-phenoxy radical or ion. Based on our work under a separate contract, which concerned water pretreatment of coal [10], we believe that the ortho-dihydroxy functions play a special role in promoting retrogressive reactions. Consequently, these functions were further studied as model compounds under the current program (see below).

TABLE III-15 - Preliminary Results of Curve Resolving The OH Region Using FT-IR Methods For Coals and Modified Coals

Coal Type	Treatment	DAF % Arbitrary Units*	
		Phenolic - OH	Dihydroxy - OH
Zap	---	0.16	0.04
	HCl wash	0.22	0.13
	Ca^{2+} load HCl wash	0.20	0.27
	Hydroth. pretr. 350 °C, 20'	0.18-0.22	0.07-0.20
Demin. Zap	---	0.17	0.14
	Ca^{2+} load	0.21	0.09
	Ca^{2+} load HCl wash	0.20	0.15
Wyodak	---	0.15	0.03
	Hydroth. pretr. 350 °C, 20'	0.25-0.27	0.03-0.11
Demin. Wyodak	---	0.20	0.21
Zap	---	0.16	0.04
Wyodak	---	0.15	0.03
Ill. #6	---	0.13	0.11
Pitt.	---	0.08	0

* Based on peak height

Fourier transform infrared (FT-IR) spectra of coal contain a wealth of information that can be utilized in the development of quantitative analysis routines based on least squares curvefitting. However, since the exact composition of the coal is not known, the selection of parameters, such as the number, position, and width of the bands, is not straightforward. The application of Fourier self-deconvolution, maximum likelihood restoration, and the calculation of derivative spectra has been shown capable of narrowing bandwidths in order to facilitate the selection of these parameters [11,12]. However, these techniques provide poor results for spectra with highly overlapped bands, baseline errors or high noise levels [11,12] Although coal spectra typically exhibit these shortcomings, some of these approaches have been utilized [9,13]. As an alternative to the approach mentioned above, Solomon et al. [14,15] defined a set of 24 Gaussian bands with fixed positions and widths that could reproduce coal spectra within the experimental error. Although good correlations were observed for coal samples of different

rank, the use of fixed band positions prevents the observation of band shifts induced by changing inter- and intramolecular interactions in the coal structure.

In this work, we have modified the technique of Solomon et al. [14,15] by allowing the curvefitting algorithm to determine the positions of those bands prone to shifting. Reduced spectral ranges were used in order to accommodate the increased number of parameters to be determined. The initial parameters for the curvefitting algorithm (number of bands, band assignments) were set using data available in the literature. The key to this approach is that known modifications were made to the hydroxyl and carboxyl functional groups within the coal structure in order to test the curvefitting results. Because of the importance of the carboxylate groups in retrogressive reactions, recent efforts have focused on the C=O stretching region. Raw and modified coal samples (acid washed, demineralized, and cation exchanged) were analyzed in order to validate the proposed band assignments in the C=O stretching region given in Table III-16. This parameter set differentiates free carbonyl (B2) and hydrogen-bonded carbonyl (B4) from carboxylic acid carbonyl (B3) and carboxylate (B7). One test of these assignments, which are based on literature data, is to plot B3 versus B7. This should be linear, assuming that the sum of the free carboxyl and carboxylate groups is constant and that the intensity of the overlapped aromatic ring band in B7 is also constant. This relationship was found to hold for a set of raw, acid washed, and acid washed/cation-exchanged Zap coals, as shown in Figure III-9.

TABLE III-16 - Band Positions and Assignments Used For Input Parameters For The C=O Stretching Region (*indicates fixed band position)

band #	Position	Assignment
B1	*1772	
B2	*1738	C=O
B3	1708	COOH
B4	1690	C=O..H
B5	1650	broad water band
B6	1600	arom.str. 1
B7	*1575	COO-, arom.str. 2
B8	1508	
B9	1454	

Acid washing the raw Zap samples results in an increase in the COOH/COO-band intensity ratio. Cation exchanging the acid washed samples returns the COOH/COO-ratio to approximately the same value observed for the raw coal. This is demonstrated more quantitatively in Figure III-9. Coal samples with a relatively wide range of COOH/COO-ratios were prepared by cation exchanging

demineralized coal samples using different cations under varying conditions [16] (see Figure III-10). Clearly, a linear relationship between the intensities of the carboxylic acid band and the carboxylate band is demonstrated.

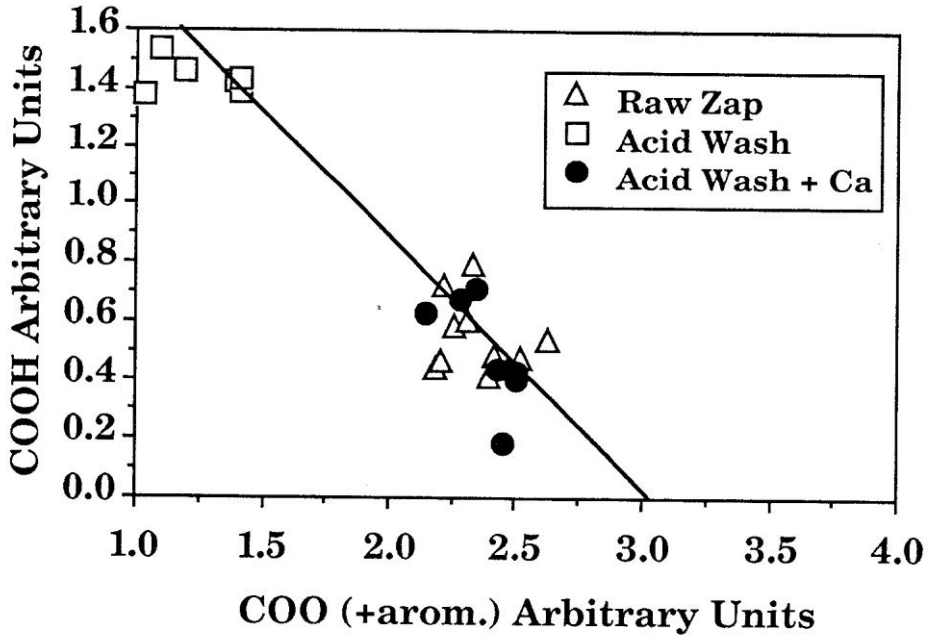

Figure III-9. Relationship of Carboxylic Acid and Carboxylate Band Intensities for Raw, Acid Washed, and Acid Washed-Cation Exchanged Zap Coals.

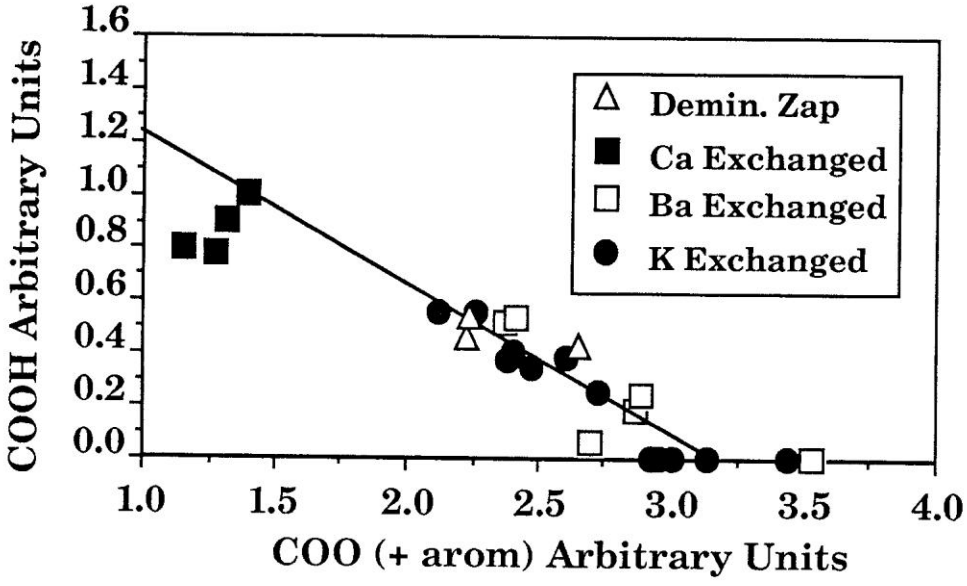

Figure III-10. Relationship of Carboxylic Acid and Carboxylate Band Intensities for Demineralized and Demineralized-Cation Exchanged Zap Coals.

IV. TASK 3 - STUDIES WITH POLYMERIC MODEL SYSTEMS AND MODEL COMPOUNDS

A. Introduction and Objectives

It has become increasingly clear in recent years not only that retrograde reactions substantially hinder the liquefaction of low-rank coals, but also that oxygen functional groups in the coal structure are major actors in these retrograde reactions. The evidence connecting oxygen groups to the formation of new, strong bonds, though convincing, is largely phenomenological in nature rather than mechanistic. Thus we know that crosslinking is correlated with the evolution of CO_2 and H_2O and therefore that carboxyl and/or phenolic groups are involved, but we do not know exactly how or why. In order to best mitigate the retrograde reactions it is necessary to better understand their mechanisms i.e., to know what factors promote and inhibit these reactions.

Task 3 complements the other tasks in this project in that it seeks to help understand why certain pretreatments tested with real coals are found to mitigate retrograde reactions and thus help lead to improved or different pretreatments. The approach to achieving this goal was to prepare and study the behavior of polymeric coal models under liquefaction conditions. This approach provided us not only with starting materials and products that were better known than is possible with real coals, but also with structures and reaction conditions that are more relevant to the liquefaction of real coals than are the typical "model compound" studies. Polymeric models should be more relevant to coals, particularly with respect to mass-transport factors. The difficulty is not to make them too relevant: If the polymers are too much like real coals, both they and their products will be unanalyzable. Therefore, judicious choices are necessary as to what oxygen-containing structures are key to retrograde reactions in low-rank coals.

The first objective of Task 3 was to prepare polymer models having phenolic, carboxylic, and/or aryl ether groups considered to be important in low rank coals. There are two aspects to the choice of appropriate polymers: the choice of the polymeric backbone and the choice of the functional groups. One approach is to focus on the chemistry of the chosen functional groups in a polymeric matrix by selecting a polymer backbone that is itself not subject to cleavage under the reaction conditions. The other approach is to choose a backbone that is presumed to be coal-relevant and seek to understand its behavior first without, and then with, appended, relevant oxygen functional groups. We have followed both of these approaches, using in the first case a refractory backbone of biaryl linkages (i.e., poly(phenylenes)), and in the second case a backbone having the major linkage type known to exist in lignins and presumed to be at least partially retained in low-rank coals. The bulk of our effort - and progress – was made in the second approach, including background studies on the behavior of carboxylic acids under coal liquefaction conditions. In this report, we describe each of these aspects in turn.

B. Studies with Polymeric Model Systems

1. Synthesis of Polymers with a Polyphenylene Backbone

The desire to emulate coal by studying the behavior of an insoluble polymeric model must of course be tempered by the fact that insoluble polymers are extremely difficult to characterize. Accordingly, the philosophy we adopted was to generate a low-molecular weight oligomer of poly(phenylene) that would be be soluble enough to permit characterization and functionalization and yet be high enough in molecular weight such that reactions at one unit of the polymer would generate species in close proximity to other units, rather than being totally isolated by intervening solvent, as is often the case in the reactions of monomeric model systems. At the time of writing the proposal, poly(phenylene) was commercially available as a potential starting point for functionalization, but by the beginning of the project, this was no longer the case, and a special synthesis became necessary. Following this approach, we settled on a synthesis targeted at octa(phenylene), or C_6H_5-$(C_6H_4)_n$-C_6H_5 , where n = 6.

We followed the procedure of Bamfield and Quam [17] which involves heating a paste of bromoarenes, water, sodium formate and Pd/C. We used a 1:1 molar mixture of 4,4'-dibromobiphenyl and 4-bromobiphenyl to maximize the chances for octa(phenylene) (n= 6).

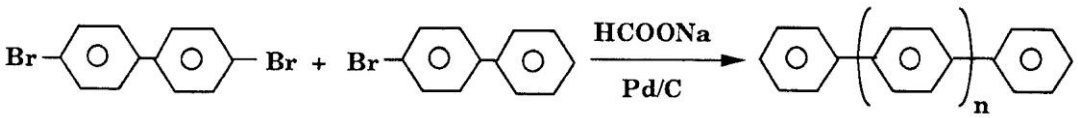

(5)

The reaction products turned out to be very insoluble and difficult to purify. Tetra(phenylene) is reported to be insoluble in ether [18], and the higher oligomers can only be less soluble. Presumably it is molecular stiffness and the π-π cloud interactions that makes these materials so insoluble at such low molecular weights. In fact, mass spectral analysis of the crude mixture using desorption chemical ionization showed not only a fair amount of hexa(phenylene) (n = 4, m/z = 438), but also additional peaks at m/z 270 and 284 (whose source we are not certain of). The insolubility of these products made them difficult to work with, and if the unfunctionalized polymer is so insoluble, it was doubtful if we would be able to prepare well-characterized polymers in anything approaching the 10,000 Da range that was originally selected for emulation of the crosslinked coal molecule. Other polymeric substrates, were considered that might serve as the backbone, but there are no structural types other than poly(phenylenes) that provide a polymer backbone that is truly refractory under liquefaction conditions. It is interesting to note that 1,3,5-triphenyl benzene, having the same molecular weight as the sparingly soluble linear tetraphenylene, is reported to be soluble in ether [19], and it is possible that some approach could be devised based on this non-linear poly-aryl. However, concurrent work demonstrated that one of the alternative approaches using more inherently coal-related (and more reactive) C-C-O linked polymers was simpler and more promising than we had thought, as discussed above.

2. Synthesis of C-C-O Polymers

Preparation and Characterization of C-C-O Polymers

The C-C-O "β-ether" linkage between adjacent aromatic rings is the most abundant linkage in lignins, from both angiosperm and gymnosperm sources. In the absence of evidence to the contrary, we have assumed that some significant fraction of these linkages survive into the low-rank coals. If these linkages are important in lignites and subbituminous coals, they provide a very interesting situation. The β-ether linkage is known to be quite labile, via a free radical chain reaction, under coal liquefaction conditions [20]. In its simplest form, in phenylphenethyl ether (C_6H_5-O-CH_2-CH_2-C_6H_5), the β-ether linkage has a half life at 400 °C of 120 minutes, forming styrene and phenol [21]. Thus, one might speculate that if lignite were composed substantially of such linkages, it would simply fall to pieces under liquefaction conditions- *unless* retrograde reactions were very facile. Indeed, in previous work [4], we found that two different polymers presumably consisting largely of the β-ether linkage showed both facile cleavage and extensive crosslinking. However, this observation was clouded by the fact that side reactions could not readily be eliminated in the polymer synthesis (using mercuric trifluoracetate of 4-allylphenol and eugenol (2-methoxy-4-allylphenol)), and we were never able to obtain polymers that gave the correct elemental analysis. For this reason, more extensive study and interpretation of those polymer preparations was judged to be premature.

In the current work, a new route to these C-C-O polymers was successfully tested, and we believe they re-emerge as the better route to address, in a polymeric context, the question of the effect of decarboxylation and other factors on crosslinking in low-rank coals.

The potential alternative direct synthesis of C-C-O bridged polymers that was explored involves reaction of 4-hydroxyphenethyl bromide (or its analogs) in base, a reaction that in principle looks very simple. In practice, it is difficult to prevent the formation of unwanted products via a rapid intramolecular displacement that gives an intermediate spiroketone. However, we have been able to find phase transfer catalysis conditions where the activity of OH- is sufficient to initiate polymerization by opening the intermediate spiro compound, but the base concentration is insufficient to interfere with successful propagation to form moderate molecular weight C-C-O polymer.

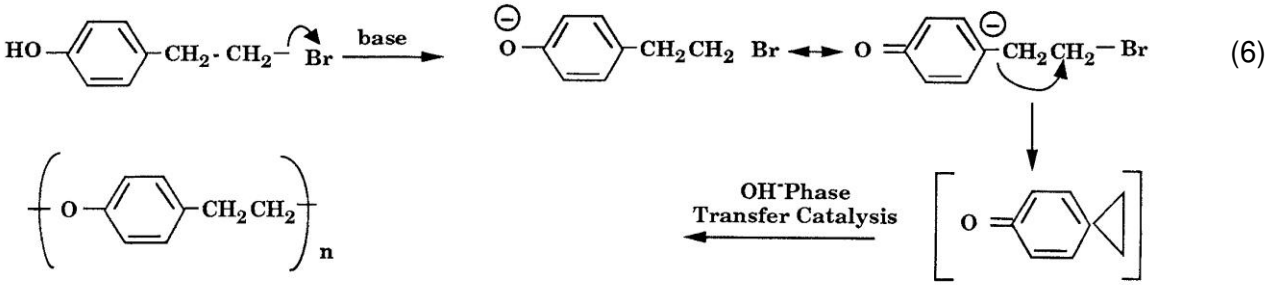

(6)

NMR analysis indicates this product to have the carbon-Br bond in the starting material replaced by a carbon-oxygen bond, i.e., to consist of the desired C-C-O polymer. The molecular weight distribution was determined by gel-permeation chromatography (GPC) using THF as the solvent. Two different polymer fractions were analyzed: one was completely soluble, in THF and the other was only about 70% soluble. The molecular weight distribution of the latter, of course, applies only to the soluble portion. The weight average molecular weights were about 1150 and 2100, respectively, corresponding to about 10 and 17 monomer units in the average molecules. About 25% of the second sample (THF-soluble portion) had a molecular weight above 3000 Da. It was anticipated that minor modifications of the synthesis procedure would increase the molecular weight substantially; in any case, solubility fractionation of the mixture would allow us to separate, characterize, functionalize, and use a higher molecular weight portion, such as that soluble in warm dimethylformamide.

The next step was to make larger quantities of the -Ph-O-CH_2CH_2- polymer for pyrolysis and liquefaction tests. Also, since 3-methoxy-4-hydroxyphenethyl alcohol (homovanillyl alcohol) is commercially available, we also proceeded with the synthesis of the 3-methoxy analog of the above polymer. Except for the missing methyl side chain, this polymer (-(m-OMe)C_6H_3-O-CH_2CH_2-) is identical to the polymer that could not be obtained in high purity via direct polymerization of eugenol during the previous contract [4]. With these two polymers in hand, we would then be in a very good position to see whether the unusual cleavage and crosslinking behavior of the -C-C-O- linkage in lignins is mirrored by the behavior of the same linkage in alcohol-free polymers. It should also be possible to modify these polymers to examine the impact of decarboxylation in a context that is arguably more coal-relevant than any previously used in polymeric coal model studies.

The synthesis route was futher optimized collapsing three separate steps into a single, one-reaction-vessel process. The three-step generation of 4-hydroxyphenethyl bromide (or its analogs) that was described above was replaced by the reaction of 4-hydroxyphenethyl alcohol in three equivalents of trimethylsilyliodide. As shown below, these reactants first generate trimethylsilylethers from the both the phenolic- and aliphatic-OH. The extra equivalent of trimethylsilyliodide then generates the alkyl iodide from the alkyl ether, leaving the aryl ether (which is not subject to nucleophilic displacement) intact. In the workup, the latter ether is cleaved with mild acid, and the net result is the generation of 4-hydroxyphenethyl iodide in a single reaction vessel in high yield. The 4-hydroxyphenethyl iodide was isolated and the phase-transfer catalysis approach discussed above was used to produce the C-C-O bridged polymer.

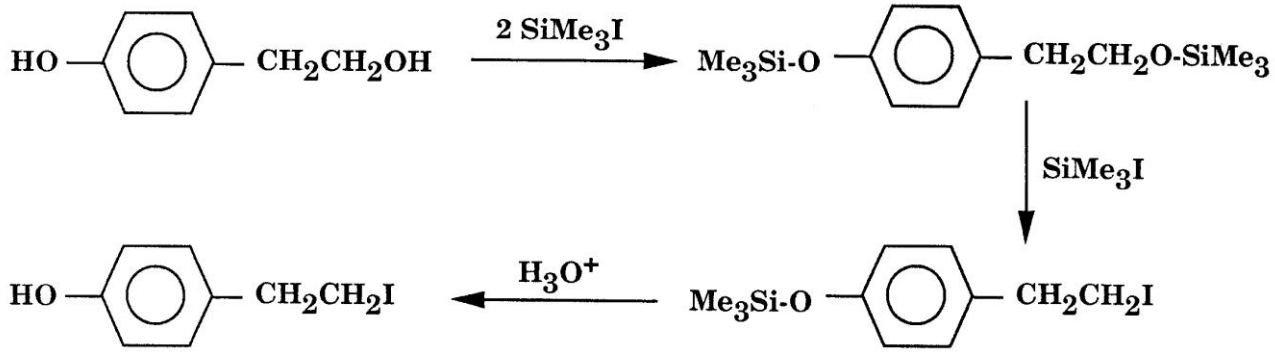

Scheme 1. One-Step Synthesis of 4-hydroxyphenethyl iodide.

Alternative Routes for Synthesis of -(Ar-OCH$_2$CH$_2$)$_n$- Polymers

In the current work, we have successfully developed a new route to these C-C-O polymers, and we believe they re-emerge as the better vehicle for addressing, in a polymeric context, the question of the effect of decarboxylation and other factors on crosslinking in low-rank coals. It was believed that we had come to a satisfactory optimization of this new synthetic route with a single-reaction vessel preparation which would go all the way from the starting 4-hydroxyphenethyl alcohol to the 4-hydroxyphenethyl iodide by using three equivalents of trimethylsilyl iodide. However, this conclusion was premature: it was found that the final step - polymerization of the iodide - proceeds with poor yield because base-catalyzed elimination of HI is the major pathway. Consequently, a change was made in this synthesis, switching to the use of trimethylsilyl bromide. This reaction sequence is outlined in Scheme 2.

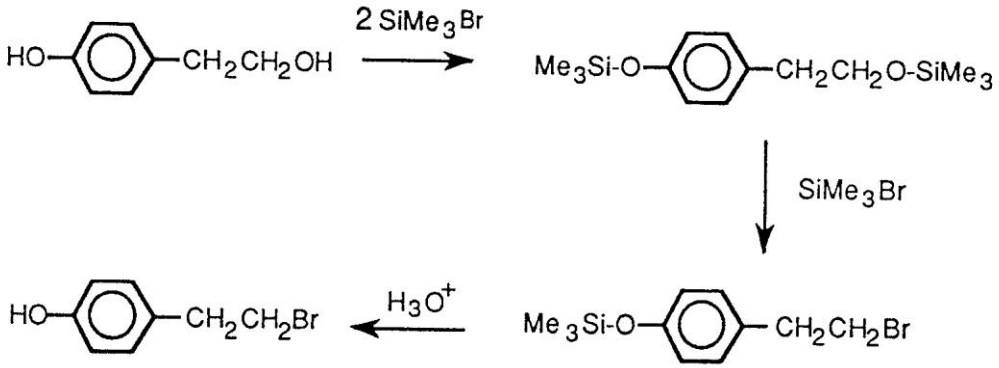

Scheme 2. Shortened synthesis of 4-hydroxyphenethyl bromide with trimethylsilyl bromide.

The 4-hydroxyphenethyl bromide was isolated and the phase-transfer catalysis approach described in Equation 6 was used to produce the C-C-O bridged polymer.

Larger Scale Preparation of the -(C$_6$H$_4$-O-CH$_2$CH$_2$)$_n$ Polymer

The first attempted larger scale synthesis of the basic β-ether- bridged polymer involved the use of

trimethylsilyl iodide, as discussed above. Starting with 5 grams of the 4-hydroxyphenethyl alcohol, we obtained the -(C_6H_4-O-CH_2CH_2)$_{n-}$ polymer in good purity (by solution-phase ^{13}C- and proton- NMR), but in a yield of only ~16%. This gave us only about 700 mg of purified material, not enough even to perform one liquefaction experiment at the 1-gram scale that was being used at Advanced Fuel Research, Inc. (AFR). Since increasing the scale even to 10 grams would not give enough for more than 1 liquefaction experiment, and increasing the scale further can introduce other problems that would then have to be worked out, we decided to try another variation of the same basic approach.

Because the polymerization of an earlier step-wise preparation of 4-hydroxy-phenethyl*bromide* had been quite efficient (though the bromide itself had been rather difficult to obtain), a final variation was triedin which the trimethylsilyl iodide was replaced by trimethylsilyl bromide, as shown in Scheme 2. Starting with 5.0 grams of the 4-hydroxyphenethyl alcohol, we obtained 3.1 grams of the solid polymer (90% yield). The yield was not only very good, but this preparation appeared to be substantially higher in molecular weight than our previous preparations. It was completely insoluble in methylene chloride, THF, DMSO, and DMF. The structure and purity of this and the earlier soluble preparations of this polymer are discussed below in the section entitled "GPC, NMR, and FT-IR Analyses of the Polymer Preparations." In brief, this higher molecular weight, insoluble polymer preparation passed all the structure and purity tests to which it was subjected.

Although the use of an insoluble polymer presents a difficulty in that the starting molecular weight distribution cannot be characterized, it does provide a polymeric material whose behavior should be more relevant to the originally insoluble portion of low-rank coals than would be for our earlier lower molecular weight soluble polymer preparations.

Preparation of the -[C_6H_3(o-Me)-O-CH_2CH_2]$_n$- Polymer

The -O-C-C- linked polymer with a methoxy located ortho- to the bridge oxygen contains what is probably the most common lignin linkage type. Furthermore, it is undoubtedly a more reactive structure (presumably both with respect to cleavage and to crosslinking) than is -(C_6H_4-O-CH_2CH_2)$_n$- itself. Therefore, it was believed that the methoxy-substituted polymer was the model system that would reveal the most about the chemistry of low-rank coals. We chose to synthesize -(C_6H_4-O-CH_2CH_2)$_n$- first anticipating both that the chemical behavior of the more complex polymer would be less informative if it was observed in isolation, and that we would learn useful lessons in the synthesis of the simpler polymer.

For this slightly more complex polymer, we could not combine the three ether-formation, halide formation, ether cleavage steps, because the pre-existing -OMe group would itself have been cleaved. Instead, each of the steps was carried out individually, as shown below in Scheme 3.

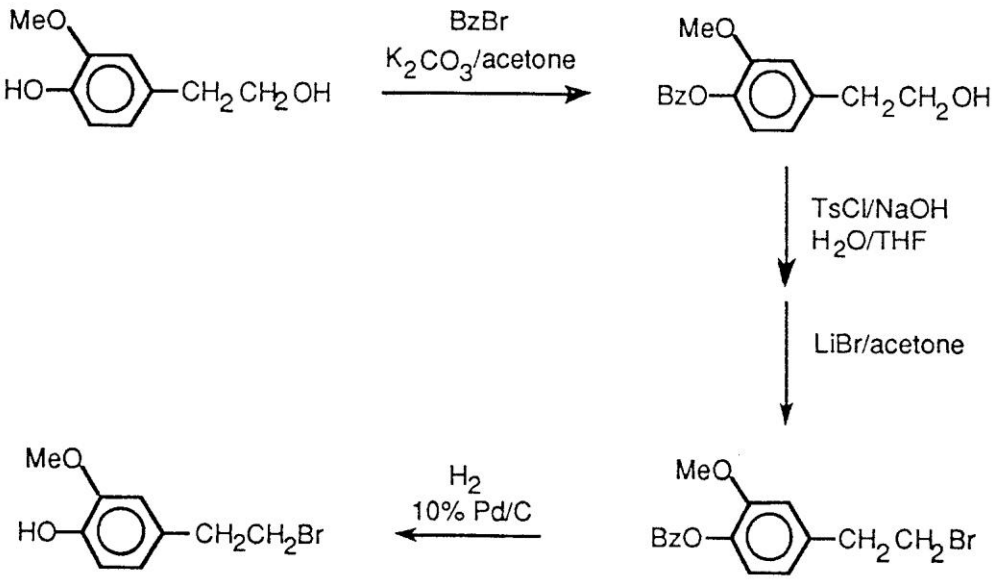

Scheme 3 Synthetic route to the -[C_6H_3(o-Me)-O-CH_2CH_2]$_n$- precursor.

We were, however, able to obtain the products of each of the individual steps in Scheme 3 in high yield. After each of the first three steps, the product was isolated and characterized by solution-phase NMR. This technique provided a convenient monitor of the extent to which the desired transformation(s) were achieved. The chemical shifts of the methylene protons on the bridge carbon connected to oxygen (the "β-ether" carbon) provide the most direct assessment of the extent of transformation. The chemical shifts allow one to readily distinguish between -CH_2OH, -CH_2OTs, and -CH_2Br, and -CH_2-OPh-.at 3.85, 4.3, 3.4, and 4.15 ppm relative to TMS, respectively. By this criterion, the products of the first three steps all were of satisfactory purity.

The 4-hydroxyphenethyl bromide product of the catalytic hydrogenolysis in Step 4 was purified by column chromatography, since thin-layer chromatography showed it to have two components. Even if it didn't have two components, the difficulty of purifying the insoluble polymer to be made in the next step dictates that we begin the polymerization with an intermediate of suitable purity.

GPC, NMR, and FT-IR Analyses of the Polymer Preparations

For all of the earlier -($C_6H_4OCH_2CH_2$)n- preparations that have been at least partly soluble in THF, solution-phase NMR has been the analytical tool of choice for structural determination. It is also a good measure of impurity above about the 3% level (for impurities that contain C and H). Clear distinctions can be made between the proton- and carbon- types in the starting materials and various products, including the most probable side products, such as olefins. NMR results for the soluble polymer preparations supported the expected polymer structure and a level of impurity (apart from traces of tributylamine) of less than about 5%. GPC indicated weight average molecular weights (for

those portions soluble in THF) ranging from about 2000 to 4000.

Since no solution-phase NMR is possible for the insoluble product, we obtained in our final larger-scale synthesis of -($C_6H_4OCH_2CH_2$)n-, a comparison of the IR absorption spectrum with those of previously confirmed, lower molecular weight, soluble polymer preparations, which offered the simplest basis for structural confirmation. Notwithstanding any differences in molecular weight, the IR spectra should be essentially identical, *if* the current preparation indeed has the anticipated structure. In fact, the FTIR spectrum of this batch was essentially identical with that of the previous batch (except for the intensity of one absorption at ~1460cm^{-1}), for which solution-phase NMR was confirmatory both for structure and purity.

Pyrolysis-FIMS of the -C-C-O- Polymers

Introduction – The similarity in IR spectra was sufficient to warrant the next step - analysis by pyrolysis-Field Ionization Mass Spectrometry (FIMS) to observe the thermal fragmentation behavior and perhaps obtain some information on the molecular weight distribution. This py-FIMS analysis was performed and the spectrum of the insoluble polymer is shown in Figure IV-1. For comparison, that of one of the earlier, soluble polymer preparations is shown in Figure IV-2. The FIMS-"volatile" fractions were 79 and 89%, respectively. The FIMS spectra are clearly quite similar, both being dominated by oligomeric fragments at 120, 240, 360, 480, 600, and 720 mass units (representing -($C_6H_4OCH_2CH_2$)$_n$- with one double bond somewhere in the molecule, most often presumably in the terminal alkyl group). The intensity-temperature profiles for these masses clearly indicate no significant fraction of any of these peaks is present as such in the original polymer: they are all generated by thermal decomposition in the temperature-programmed FI source.

The relative intensities of the main peaks in the two spectra are quite similar. The most apparent difference is that the insoluble polymer spectrum (Figure IV-1) is considerably "cleaner", having much lower intensities of the various peaks in between the main fragments. For example, the satellites that vary from the main peaks by +n(12), +n(14), and -2 have only 1/3 to 1/2 the relative intensity in Figure IV-1 that they have in Figure IV-2. Also the peak at m/z 185, due to unremoved tri-n-buytl amine is only about 1/10 of that in the earlier preparation (Figure IV-2). The lower level of miscellaneous impurities is also reflected in the vacuum evaporation curves, where less than about 2% of the detected volatiles from the recent preparation appear by 250°C , as compared to about 6-7% with the older polymer. In Figure IV-1, there are two unidentified peaks at m/z 161 and 271 accounting together for about 2% of the total ion intensity. Bromine appears to be completely absent, as indicated

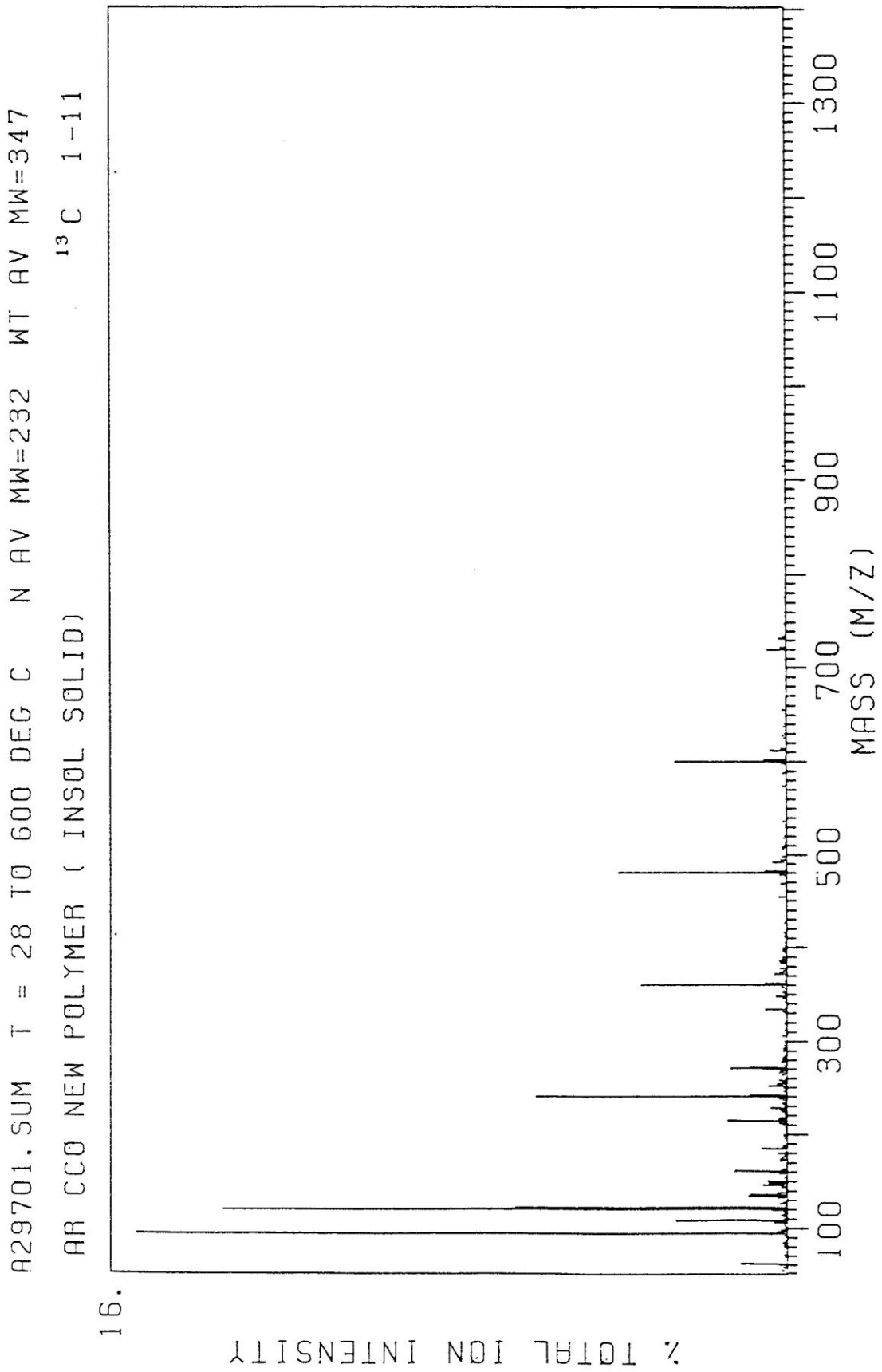

Figure IV-1. Pyrolysis-FI mass spectrum of Insoluble – $(PhOCH_2CH_2)n$– polymer preparation.

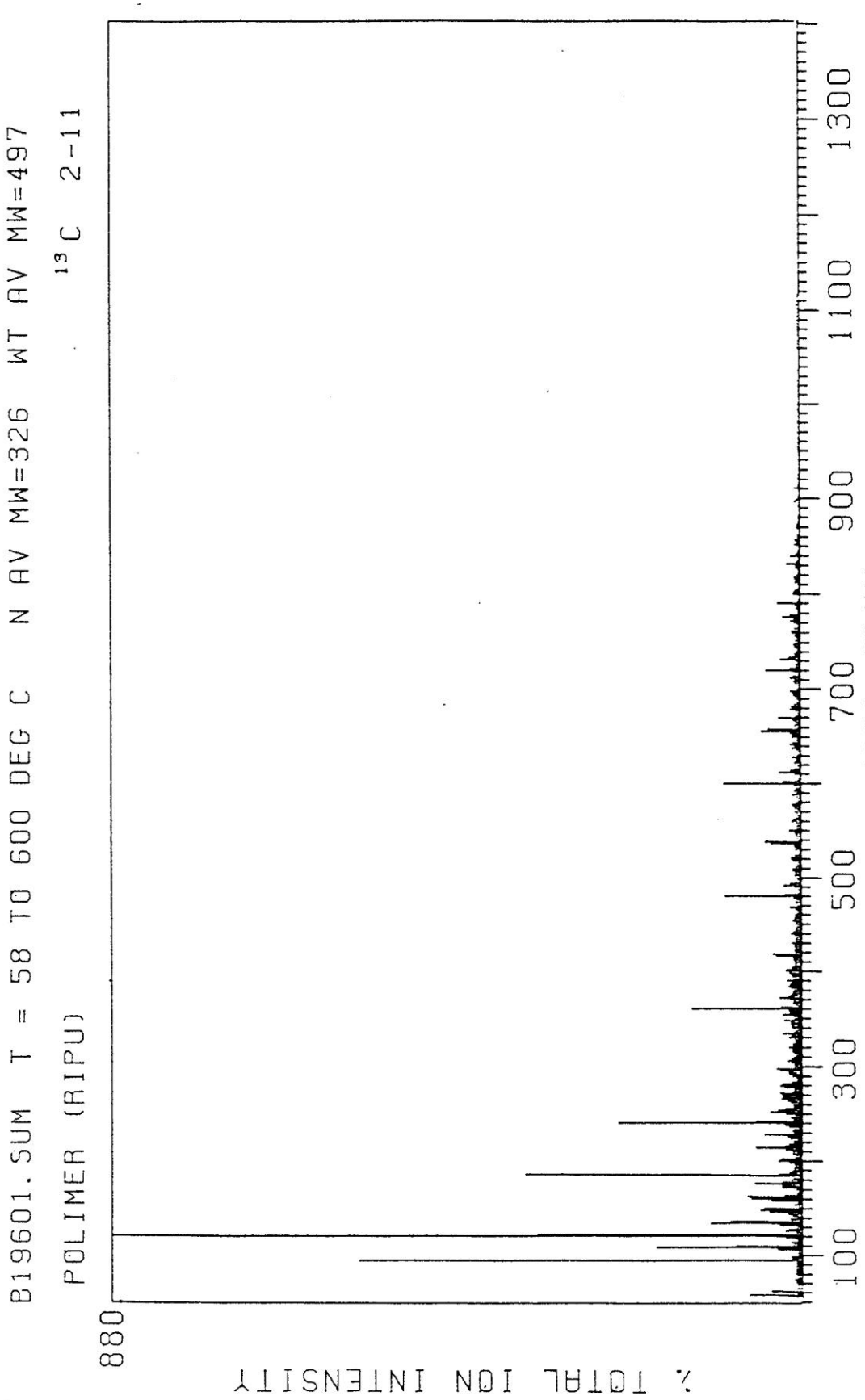

Figure IV-2. Pyrolysis-FI mass spectrum of THF-soluble – ($PhOCH_2CH_2$) n– (polymer preparation.

by the absence of any twin peaks attributable to structures containing the equal-abundance isomers of bromine. It thus appears from the IR and FIMS spectra that, on the basis of purity and confirmed structure, this polymer will be suitable for meaningful liquefaction and other conversion studies.

The Py-FIMS analyses already allow us to draw some interesting, if still tentative, conclusions about thermal behavior of these materials. It should be noted that the satellites at +12, +14, and -2 are not impurities as such. They, like the main peaks, are not present in the original polymer, but are produced in the thermal decomposition process that sets in about 350°C. For some reason there are more transalkylation and other interconversion reactions taking place with the more impure polymer, thus amplifying further its appearance of impurity. While these subtle differences may ultimately tell us more about the chemistry of fragmentation and crosslinking of these polymers, the spectra are much more similar than they are different. The basic conclusion is that, notwithstanding significant differences in residual tributylamine and differences in molecular weight, the two polymers show the same pyrolytic behavior.

However, the large FIMS-volatile fractions in both of these cases (79% and 89% for Figures IV-1 and IV-2, respectively), together with the similar distribution of oligomeric fragments, suggests that liquefaction yields of the polymer itself will be very high. The monomeric fragment as m/z 120 is the most abundant fragment not only in the sum spectra, but also in the individual spectra recorded as the probe temperature is rising. Below 250°C, there is virtually no intensity at m/z 120, 240, etc. Any organic structure of mass 120 (or even 240) will vaporize long before 250°C. At about 300°C, the onset of thermal decomposition is reached and all of these fragments appear. Even at the onset of decomposition, the intensity of the monomeric fragment is at least twice the intensity of any of the other fragments. This means that either there is coordinated bond cleavage (i.e., unzipping), or that the polymer is so heavily crosslinked (or becomes so during heating) that only very small pieces, mainly monomer, are released during pyrolysis. The results described here strongly suggest that the former conclusion is correct: bond scission is coordinated rather than random. If crosslinking *were* competitive with what clearly is facile bond scission, then the volatile fractions would not be so high, and the higher molecular weight polymer preparation would presumably be subject to much more crosslinking than its lower molecular weight cousin.

The apparent absence of competitive crosslinking for the -$(C_6H_4$-O-$CH_2CH_2)_n$- polymer is in marked contrast to the polyeugenol (nominal structure -$[C_6H_3$(o-Me)-O-$CH(CH_3)CH_2]_n$-) that we prepared and studied briefly in the previous contract [4]. With that polymeric model of low-rank coal, we saw facile thermal generation of monomeric and other small fragments, but rapid crosslinking, as evidenced by low yields not only in pyrolysis but also from liquefaction in a very good hydrogen-donor solvent. Since there were side reactions we were unable to eliminate in the polyeugenol preparation, as reflected in unsatisfactory analytical results, we cannot now say whether the incorporation of the o-OMe group or an originally crosslinked structure was the cause of the low yields. Thus it is important to compare the

conversion behavior of the -(C_6H_4-O-CH_2CH_2)$_n$- polymer discussed here and of a well characterized sample of -[C_6H_3(o-Me)-O-CH_2CH_2]$_n$-.

General Features and Mechanistic Expectations – The pyrolysis-FI mass spectrum for the three-day preparation of —[C_6H_3(o-OMe)CH_2CH_2-O-]$_n$— , shown in Figure IV-3, is similar in general terms to those for the —[PhCH_2CH_2-O]$_n$— polymer preparations shown in Figures IV-1 and IV-2 (reproduced here as Figure IV-4). However, there are interesting differences that indicate variations in pyrolytic behavior. All the spectra show a series of oligomers (more precisely, a series of oligomers with a double bond in one of the ethylene groups, presumably preferentially the terminal -CH_2=CH_2 grouping) that would be expected from simple non-reductive cleavage. In all cases, a dominance of monomer over dimer, trimer, etc., *from the onset of decomposition through its completion* indicates that the linkages are being cleaved in a coordinated or unzipping manner. We can qualitatively rationalize this unzipping by postulating that the radical-chain H-abstraction —β-scission processes that account for the decomposition of monomeric -C-C-O- linked structures would here lead to the chain transfer H-abstraction reactions occurring preferentially on the end unit. This sequence is illustrated in Scheme 4.

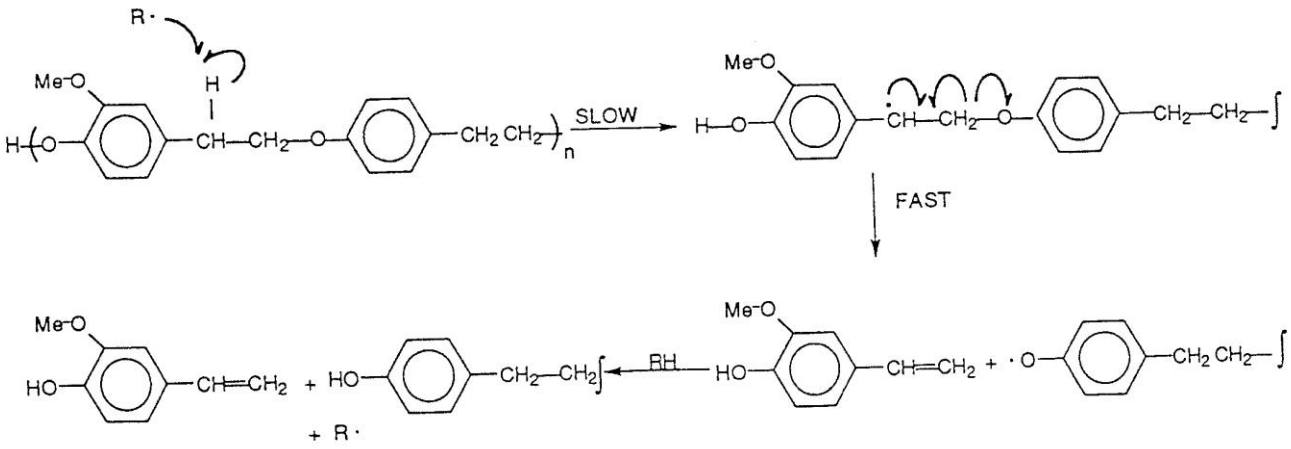

Scheme 4. Possible radical-chain unzipping sequence for –C-C-O- polymers.

Autoacceleratory Character of the Decomposition – In view of the probable coiled configurations of these linear polymers, and thus the likely proximity of many interior chain positions, rationalization of the pronounced unzipping tendency simply in terms of a radical chain mechanism does not appear really satisfactory. In any case, central bond cleavage is clearly a chain or an autocatalytic process, such that once cleavage begins at about 300°C, it proceeds progressively more rapidly, leading to essentially complete volatilization by 350°C. This behavior is illustrated by the vacuum "evaporation" curves shown in Figures IV-5 and IV-6, depicting the temperature dependence of volatiles formation observed during acquisition of the spectra in Figures IV-3 and IV-4, respectively. While both curves are very steep after the threshold is passed at about 300°C, the curve in Figure IV-5 for the—[C_6H_3(o-

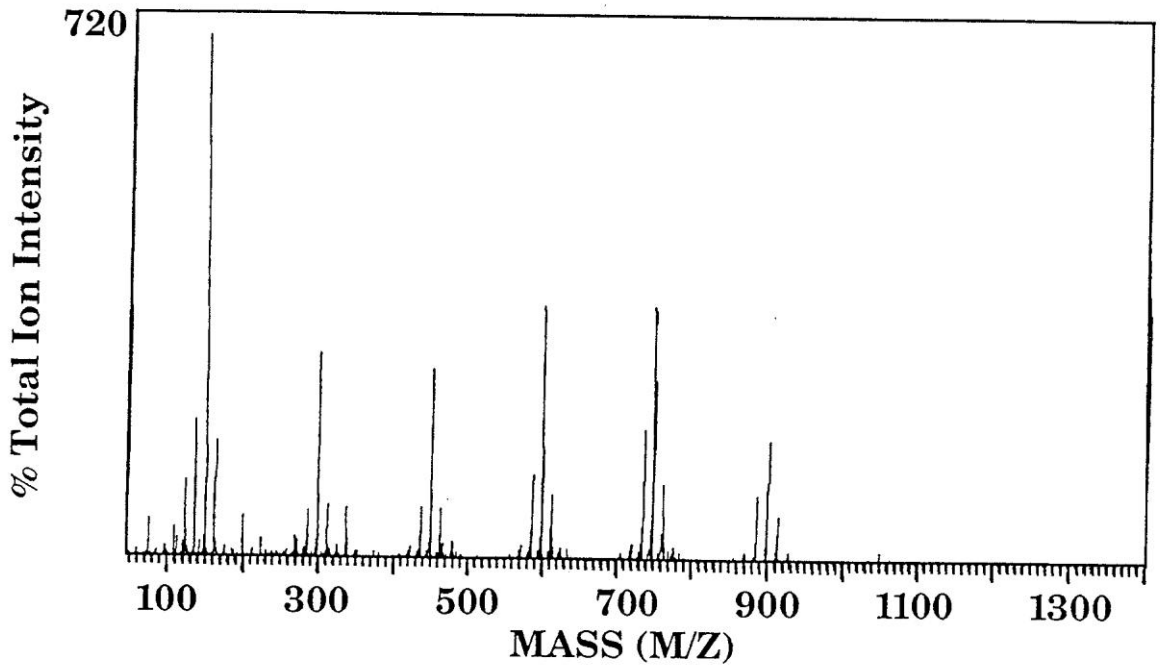

Figure IV-3. Pyrolysis-FI Mass Spectrum for –[C_6H_3(o-OMe)CH_2CH_2-O-]n-Polymer.

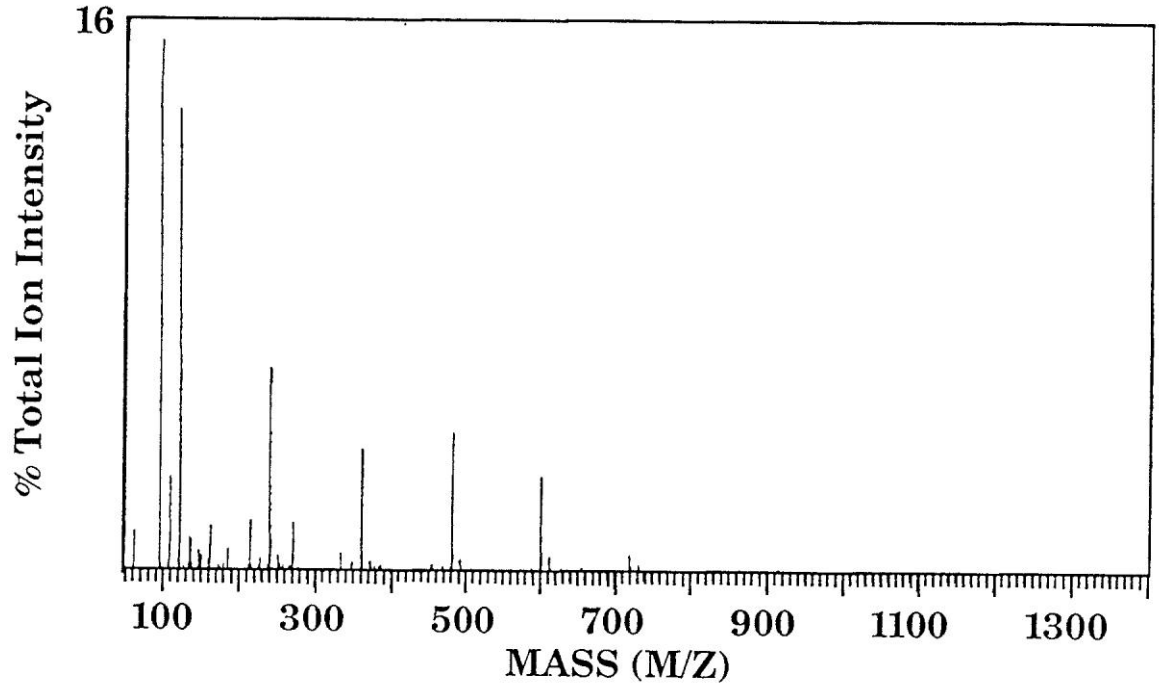

Figure IV-4. Pyrolysis-FI Mass Spectrum for –[PhCH_2CH_2-O-]n-Polymer.

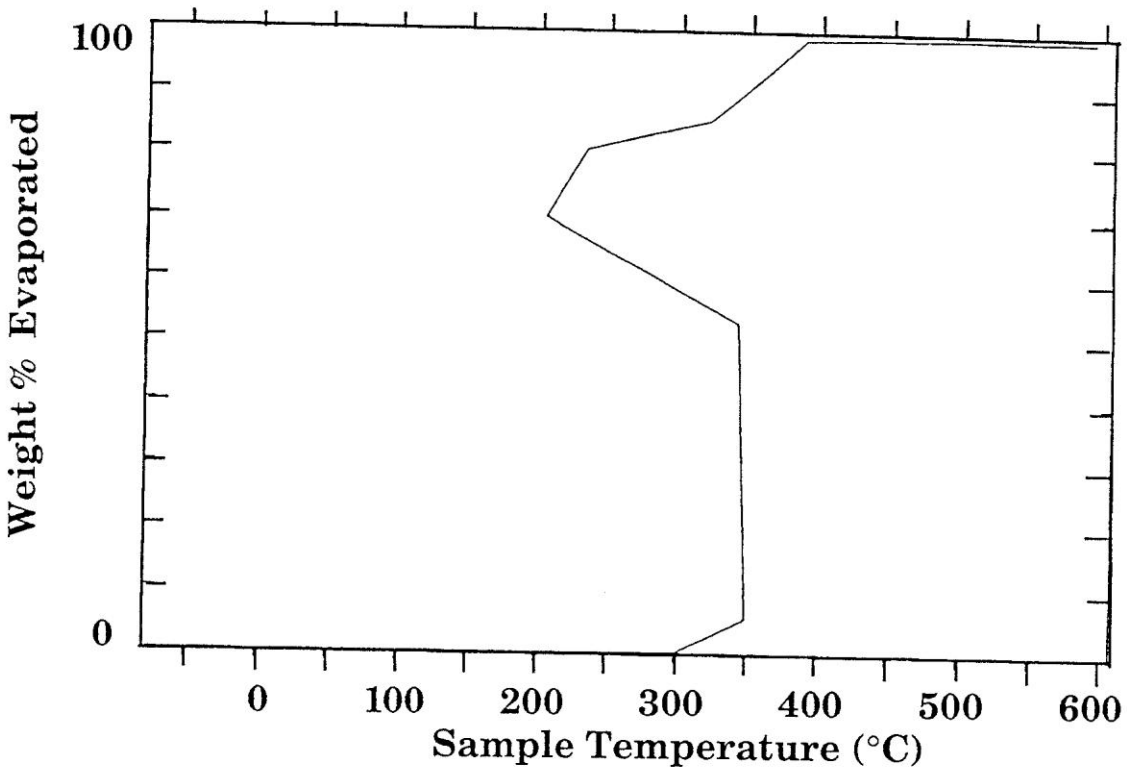

Figure IV-5. Vacuum Evaporation Curve for –[C_6H_3(o-OMe)CH_2CH_2-O-]n-Polymer.

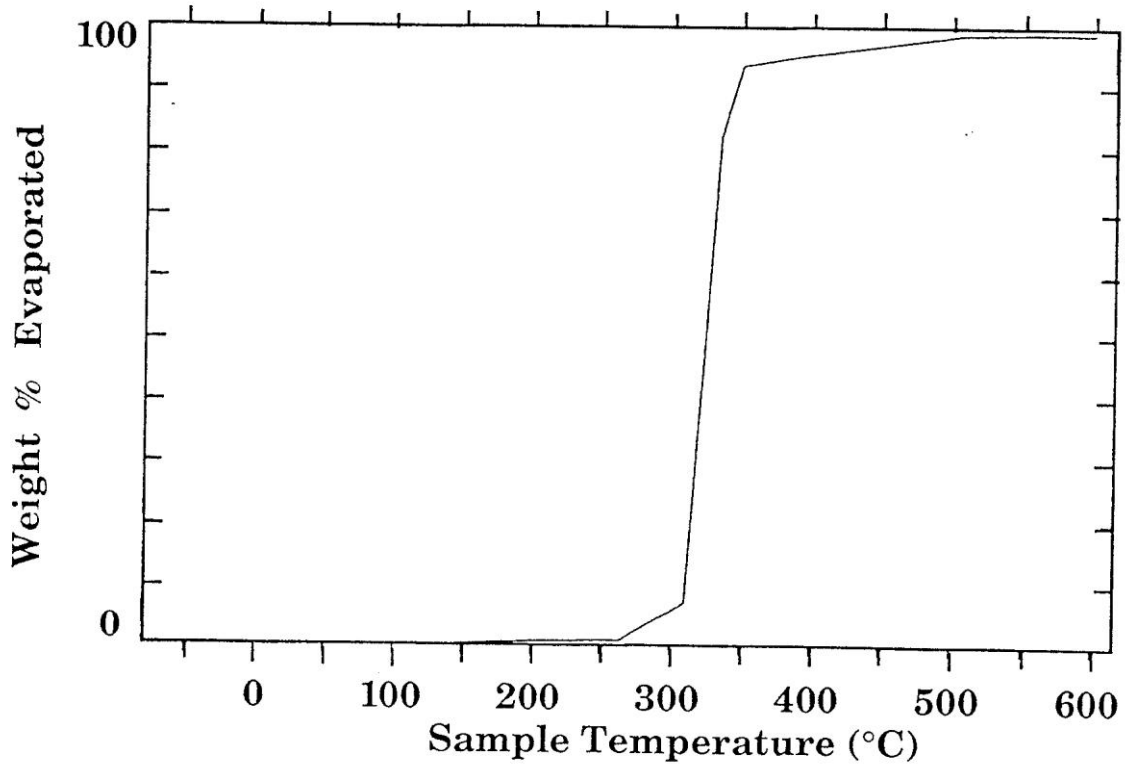

Figure IV-6. Vacuum Evaporation Curve for –{$PhCH_2CH_2$-O-]n-Polymer.

OMe)CH_2CH_2-O-]$_n$— polymer is drastically "overhung." In other words, the ion current rose so quickly once the decomposition threshold was passed (at ~ 300°C) that the probe temperature had to be decreased substantially to keep from exceeding the ion counting capability of the instrument. We note that the threshold itself actually does *not* occur at a significantly lower temperature than for the —[$PhCH_2CH_2$-O-]$_n$ polymer: in both cases the threshold appears between 300 and 350°C. However, once decomposition begins, it proceeds much more rapidly with the methoxy-substituted polymer. That is, there is a much more pronounced autocatalytic behavior with that material.

Our current thinking is that this striking autocatalysis may be indicating a new reaction pathway. The reasoning is as follows, proceeding in two steps from phenylphenethyl ether ($PhCH_2CH_2$-O-Ph, "PPE"), the simplest "dimer" unit one can consider a prototype for these β-ether lignin-like polymers. This prototype has been studied by several groups in recent years, notably Klein and Virk [22], Britt and Buchanan, [23] and Gilbert and Gajewksi [21]. This work has been authoritatively reviewed by Poutsma [20]. The changes in bond strength one expects in going from PPE to the simple -C-C-O- polymer and then to the methoxy-substituted -C-C-O- polymer are shown in Table IV-1, together with the half-lives for decomposition. The bond strength estimates are made, in large part, on the basis of recent kinetic studies published by Stein for pyrolysis of anisole derivatives [24].

TABLE IV-1 - Bond Strengths and Decomposition Rates for -C-C-O- Linked Aromatic Ring Systems

STRUCTURE	BDE [a] CH_2—O	BDE [a] ArC(H)—H	$t_{½}$ Obs (min)	
	kcal/mol	kcal/mol	300°C	350°C
$PhCH_2CH_2OPh$	60	85	4 X 10^4	2500
—[$OPhCH_2CH_2OPhCH_2CH_2$]$_n$—	59.6	~83	5 [b] (325°C)	
—[C_6H_3(o-OMe)CH_2CH_2-O-]$_n$—	55.7	~83	$_{<1}$ [b] (325°C)	

a. Estimates based upon data and derived values in references 24 and 25. Because the differences are small, values have *not* been rounded to nearest kcal; even though *absolute* accuracy for any given estimate is probably only 1-2 kcal/mol, the relative accuracy should be substantially better.

b. Values taken from vacuum vaporization curves, based on fraction vaporized during the 300° to 350°C interval.

As reviewed by Poutsma, [20] the data for PPE indicate an H-abstraction —β-scission radical-chain decomposition that is initiated by CH_2-O bond homolysis, and in which the H-abstraction chain-transfer step is the slower of the two propagation steps, as shown above in Scheme 4. Comparing first the behavior of the simple —[$PhCH_2CH_2$-O-]$_n$— polymer with PPE, we see that at 300°C, where 2.3RT = 2.62 (in kcal/mol units), and therefore where every ~2.6 kcal/mol decrease in activation energy results in a factor of 10 in rate increase, there would be less than a two-fold increase in initiation rate and no

more than a six-fold increase in propagation resulting from the 2 kcal/mol decrease in the enthalpic requirement of the H-abstraction step. Together these factors, assuming similar termination rates, would lead one to expect an about an order of an order of magnitude increase in overall rate. However, the observed rate went up by more than a factor of 500.

Moving to the —[C_6H_3(o-OMe)CH_2CH_2-O-]$_n$— polymer, we see that a ~4 kcal/mol decrease in CH_2-O bond strength should increase the rate of initiation by a factor of about ten as compared to the —[$PhCH_2CH_2$-O-]$_n$— polymer, but that there should be little further effect on the H-abstraction propagation step, because the added methoxy group is meta- to the -CH_2- group. (The CH_2-O β-scission will be accelerated by ortho-methoxy substitution, but in the decomposition of β-phenethyl ether itself, the β-scission has been shown [20] to be, by a substantial margin, to *not* be the rate-limiting propagation step. Therefore, a decrease in CH_2-O bond strength should have little impact on the overall propagation rate.) Faster initiation without faster propagation should tend to lower the onset temperature but decrease the steepness of the vaporization curve in Figure IV-5. Since this clearly is not what happened with the methoxy polymer as compared with the simple —[$PhCH_2CH_2$-O-]$_n$— polymer, it appears that a new mechanism may be intervening as this system is made polymeric and progressively more lignin-like.

This conclusion, of course, is at this stage highly speculative; however, it is consistent with the fact that the bond cleavage lifetimes observed for both polymers are substantially shorter than those reported for β-phenylphenethyl ether (Ph-O-CH_2CH_2Ph). To summarize, the terminal hydroxy group, as it apparently does with lignins, seems to activate the adjacent -C-C-O- linkage to an extent not readily explained by the radical-chain chemistry considered sufficient for the simple ether itself. Furthermore, the addition of a methoxy group ortho- to the O-Ar attachment additionally enhances the reaction rate in a way that is not readily explained by the expected radical-chain chemistry.

Generation of Satellite Peaks from Loss and Addition of Methyl Groups – Another prominent difference between the Py-FIMS of the unsubstituted and methoxy-substituted -C-C-O- polymers lies in the different levels of satellites they generate at ±n(14) mass units from each of the main oligomer peaks. This difference can easily be seen by comparison of the spectrum in Figure IV-3 for —[C_6H_3(o-OMe)CH_2CH_2-O-]$_n$— with that in Figure IV-4 for the— [$PhCH_2CH_2$-O-]$_n$ polymer. Qualitatively it is not surprising that the satellite peaks at -14 and -28 are more prominent with the methoxy-substituted polymer, given that the ArO— Me bond is moderately weak, but the size of these satellites is a quantitative surprise. The -14 satellites could be formed by simple homolysis of one of the ArO-Me bonds in the methoxy polymer, but since literature data suggest O-Me bond in the OH-terminated aromatic ring (est. BDE = ~60 kcal/mol) should exhibit a homolysis half-life of about 20,000 minutes at 300°C and 400 minutes at 350°C, the roughly 12 minutes required to go from 300 to 350°C and generate the volatiles would appear to be insufficient to allow roughly one out of every five monomer units to have lost a methyl group. Therefore, we tentatively conclude that the loss of methyl groups is

somehow coupled to cleavage of the central linkage.

The rather small variation in intensity of the satellite peaks relative to their respective "parent" oligomer peaks shown in Figure IV-3 is something we do expect to see. Since in all interior units of any oligomer, the O-Me bond strength is about 3 kcal/mol higher (with 300- and 400°C- half-lives of 300,000 and 4,000 minutes, respectively) , we do expect, in oligomer units below n = ~10, to have most of the O-Me cleavage occur on the terminal ring system. In accord with this expectation, the intensity of satellites at - 14 Daltons in Figure IV-3 increases from roughly 20% of the oligomer parent in the monomer to only about 40% of the parent in the hexamer.

The additional implication of observing rather little methyl loss except from the terminal unit is that notwithstanding its moderately weak bond, most of the O-Me arylalkyl ether bonds can, *under appropriate conversion condtions*, perhaps remain intact long enough to provide crosslink protection for the dihydroxy aromatic units. This presumably explains why there was 100% vaporization during Py-FIMS of the — $[C_6H_3(o\text{-}OMe)CH_2CH_2\text{-}O\text{-}]_n$— polymer, but the presumption needs to be tested (see below).

Extent of Cleavage by Hydrodealkylation – One other very noticeable difference between the — $[PhCH_2CH_2\text{-}O]_n$— and— $[C_6H3(o\text{-}OMe)CH_2CH_2\text{-}O\text{-}]_n$— polymers is the much larger intensity of the peak corresponding to dealkylated monomer (i.e, to phenol in the former case, and methoxy phenol, or guaiacol, in the latter case) in the polymer *not* having the methoxy substitution. Thus the m/z 94 peak in Figure IV-4 is much larger than the m/z 124 peak in Figure IV-3. As we have previously noted, formation of phenol (or guaiacol) requires not only cleavage of the C-O linkages on either side of a given aromatic ring (a non-hydrogenative, or non-reductive, cleavage), but also a hydrodealkylation or hydrogenolysis to remove the two-carbon chain, as shown below.

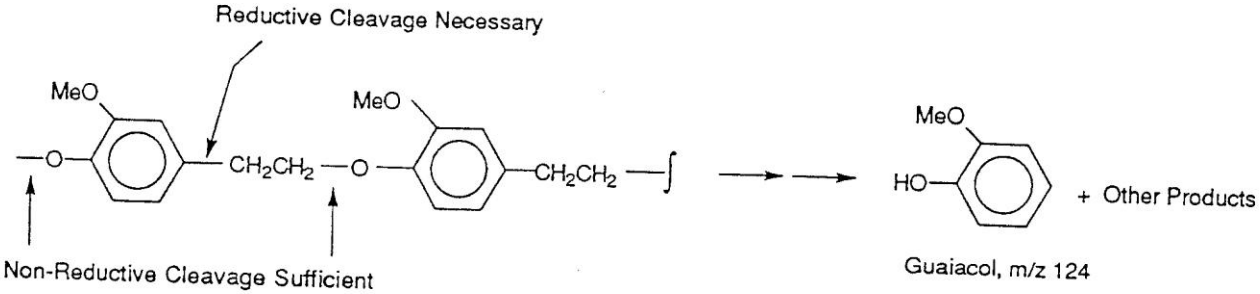

Scheme 5. Required bond cleavages to form dealkylated monomer.

The ultimate origin of the hydrogen necessary to form the dealkylated or otherwise reduced oligomers is not evident in the FI mass spectrum of Figure IV-4. That is, the sum of hydrodealkylated and reduced oligomers, at least up to n = 3, is about ten times the sum of oxidized oligomers. Presumably the necessary additional hydrogen has come from the 20% of the — $[PhCH_2CH_2O]_n$— that failed to volatilize under the pyrolysis-FIMS conditions. Such disproportionation phenomena are quite common

in pyrolytic processes, such as the hydrotreating of petroleum- or coal-derived resids, although the detailed mechanisms are generally unclear [25].

In the case of the — $[C_6H_3(o\text{-}OMe)CH_2CH_2\text{-}O\text{-}]_n$— polymer, there is much less hydrodealkylation. As can be seen in Figure IV-3, the ratio of guaiacol to $HOC_6H_3(o\text{-}OMe)\text{-}Ch{=}CH_2$ is only about one-tenth of (0.14 vs 1.2) the ratio of phenol to HOPh-Ch=CH_2 from — $[PhCH_2CH_2\text{-}O]_n$— (Figure IV-4). We do not yet know whether this is because the methoxy substitution actually slows hydrogenolysis, or simply because it speeds up the competing cleavage of the O-C bonds in the main linkages. It is noteworthy that the — $[C_6H_3(o\text{-}OMe)CH_2CH_2\text{-}O]_n$— polymer whose Py-FIMS spectrum is shown in Figure IV-3, was 100% (i.e., 97±3%) volatile. That is, there was very little hydrogen-poor char whose formation would have freed up the hydrogen necessary for widespread hydrogenolysis. This leads one to ask, once again, [25] the question, "To what extent (i.e., with what inevitability) is hydrogenolysis, which one wants, driven by crosslinking, which one does not want (at least in the coal liquefaction, heavy-oil processing contexts)?" In any case, a similar observation, namely that free phenolic groups on polymer models results in both more crosslinking *and* in more indiscriminate bond scission than results from their methylated analogs, can be drawn from pyrolysis-FIMS data for other polymer types published several years ago by Solomon and coworkers [26].

Implications of -C-C-O- Polymer Decomposition Behavior –To summarize the thermal decomposition behavior, both the $[PhCH_2CH_2\text{-}O]_n$— polymer and its methoxylated analog, —$[C_6H_3(o\text{-}OMe)CH_2CH_2\text{-}O\text{-}]_n$—, undergo rapid coordinated linkage cleavage, or unzipping, in the 300 to 350°C temperature region, yielding 80% or more volatile material under the temperature-programmed vacuum pyrolysis conditions of FIMS analysis. This general behavior was expected, inasmuch as the simplest element of these polymers, phenylphenethyl ether undergoes fairly rapid central bond cleavage in a radical-chain H-abstraction—β-scission process. However, the facility and pronounced autocatalytic depolymerization of the two new polymers was quantitatively unexpected. By the same token, the crosslinking, or retrograde reaction, has been rather less than we expected (and less than we observed last year with a more impure and potentially pre-crosslinked sample of the —$[C_6H_3(o\text{-}OMe)CH_2CH_2\text{-}O\text{-}]_n$— polymer). The surprising facility of depolymerization of the remnants of lignin most likely to be found in low-rank coals provides some tentative conclusions and raises further questions relevant to the liquefaction of low-rank coals. First, if crosslinking (in low-rank coals) is to be competitive with this type of depolymerization, the crosslinking must be exceedingly facile. Second, it follows then that *none* of the rather limited crosslinking behavior we observed in our studies with various aromatic and aliphatic (and at least arguably coal-related) carboxylic acids was facile enough to support the long-standing speculation that decarboxylation instigated crosslinking is the major cause of retrograde reactions during preheating and/or liquefaction. Third, these results throw attention regarding the issue of retrograde reactions back to phenolic -OH as the major site/source of crosslinking and further emphasize the importance of comparing the conversion behavior of the —$[C_6H_3(o\text{-}OMe)CH_2CH_2\text{-}O\text{-}]_n$— polymer with the unmethylated analog —$[C_6H_3(o\text{-}OH)CH_2CH_2\text{-}O\text{-}]_n$—. Fourth, the unexpected facility

and autocatalytic nature of the —[C_6H_3(o-OMe)CH_2CH_2-O-]$_n$— depolymerization, which cannot readily be explained by simple free radical pathways, raises the question of whether electron-transfer may be important in the decomposition of these model coal polymers, and if so, whether explicit attempts to exploit such chemistry might be practical.

Demethylation of the —[C_6H_3(o-Me)-O-CH_2CH_2]$_n$— Polymer – The complete lack of crosslinking observed under Py-FIMS conditions for this polymer, if anything, increases the relevance comparing its behavior with that of the analog containing free -OH rather than -OMe groups. Four different reactions for effecting the selective cleavage of the ArO-Me bond in the presence of the ArO-CH_2 bond were studied. The first reaction is the method of Harrison, [27] which involves heating of the polymer with LiI in collidine at 185°C for about 10 h. During the reaction the sample darkened considerably, although after aqueous work up, the solid isolated was only light brown, and was partially soluble in $CDCl_3$. The ^{1}H NMR of the $CDCl_3$ solution was essentially identical to that of the starting material, except that the peak due to the methoxy group now had the same area as that due to the O-CH_2 peak. Also, there was a small broad peak at 5.5 ppm, most likely due to free phenolic. These data are consistent with cleavage of about a third of the methyls in the starting polymer.

The second reaction was a variation on the first one. It involved heating the polymer with NaCN in DMSO at 185°C [28]. Unfortunately, the product from this reaction was only slightly soluble in DMSO. The soluble portion was found to be the unconverted starting material. The rest of the product was dark and intractable. We also tried the method of McKervey [29] using lithium aluminum hydride in benzene. However, this procedure was not successful with our polymer.

Finally, we attempted the reaction with iodotrimethylisilane. This reagent is potent enough to cleave the ArO-CH_2 linkages as well, and we hoped that be carefully controlling the conditions, we might achieve the desired selectivity. Tests in small scale experiments in NMR tube showed that the cleavage of O-CH_3 was about three times faster than that of the O-CH_2 linkage.

C. Studies with Model Compounds

1. The Behavior of Carboxyl Functions in a Coal Liquefaction Environment

Introduction

The dilemma posed by the desire to have a characterizable polymeric backbone constructed of units that have low solubility at even rather low molecular weights has forced us to reconsider our approach. We essentially face the problem that the multiple objectives of insolubility (behavior like coal) and substrate and product characterizability tend to be mutually exclusive. Accordingly, it became clear that additional understanding of the thermal behavior of the carboxylic and phenolic functions in coal-

related monomeric systems was necessary in order to make truly appropriate choices for polymer and carboxyl function type before additional extensive synthesis effort is made. These studies will also be needed to establish the baseline for considering the effect of polymeric environment. Carboxyl functions have been implicated in the crosslinking of coals during at relatively low temperatures [30,31], and Solomon and coworkers [32] have been able to model the pyrolytic loss of solvent swelling by including one additional crosslink in the network for every CO_2 evolved. Moreover, pretreatments that have been found to be effective in promoting liquefaction have also shown a corresponding decrease in the early CO_2 evolution [33]. These results strongly suggest that carboxyl functions are involved in the low-temperature crosslinking of coals. However, the chemical reactions linking decarboxylation with coupling have not been delineated. In a recent study, Siskin and coworkers [34] showed that decarboxylation of naphthoic acid under hydrothermal conditions was attended by some binaphthyl; however, the coupling aspect was not elaborated in that study. We have examined the literature and conducted over 40 experiments with monomeric model compounds (including polycycylic) in organic media to see if crosslinking results directly from decarboxylation, and how crosslinking may be affected by ion exchange, the presence of a hydrothermal environment, and other conditions relevant to pretreatments we are testing in this project.

Decarboxylation Literature

Examination of the literature on decarboxylation [35,36,37,38], as well as earlier results obtained at SRI on decarboxylation under coal liquefaction conditions [39], allow us to make the generalization that coupling is not typically a widespread result of decarboxylation (except for the "dry" pyrolysis of alkaline earth salts [37,38]. Beyond this generalization, we will make only limited reference to this earlier work: little of it had the specific goal of assessing the associated coupling, and much of it was low-temperature studies of structures specifically activated towards decarboxylation. Nevertheless, from the observation that decarboxylation of many acids occurs without substantial coupling [35-39,40], we draw the preliminary conclusions first, that it is critical to choose appropriate structures and conditions for decarboxylation of coal relevant polymeric models, and second, that there is reasonable hope for finding coal liquefaction (or pretreatment) conditions that significantly decrease any coupling that results from decarboxylation. In the following subsections we first summarize the results of the decarboxylation experiments performed in this project, and then in summary present a somewhat broader discussion of decarboyxlation as it applies to coal liquefaction, drawn from these recent experiments as well as from earlier SRI work and data in the literature.

2. The Decarboxylation of Activated and Unactivated Benzoic Acids

The carboxylic acids shown in Table IV-2 have been subjected to "liquefaction" conditions and the products analyzed by gas chromatography to determine the extent of decarboxylation and coupling that resulted.

Table IV-2 – Decarboxylation of Activated and Unactivated Benzoic Acids.

Acid Structure	Solvent System	Concentration m%	Reaction Time Hrs	% Decarboxylation	% Coupling[1]
$PhCO_2H$ [2,3]	Tet/THQ[4] 75/20	5	1	4	<20
	Tet/THQ/H_2O 55/20/20	5	1	5	<20
	Tet/PipPy 75/20	5	0.5	77	<3
	Tet/THQ/$Zn(OAc)_2$[7] 5/20	5	1	75	<5
	Tet/1-Naphthol 80/10	10	1	3	<2[5]
$Ca(PhCO_2)_2$	Tet/1-Naphthol 80/10	10	1	3	<2
4-OH-$PhCO_2H$	Tet	10	1	>98	<10
1-OH-$PhCO_2H$	Tet	20	1	>99	<5
3-OH-$PhCO_2H$	Tet	10	1	2	-
2-OMe-$PhCO_2H$	Tet	10	1	>98	<3
	Tet	20	1	>99	<3
	Tet/Pyrene	10	1	>99	<3
3-OMe-4-OH-$PhCO_2H$	Tet	10	1	>99	<2
3-OMe-4-OMe-$PhCO_2H$	Tet	10	1	~75	<3

1. This figure should be considered an upper limit; it represents the sum of small unidentified high mass peaks that are potential coupling products, given as a percent of decarboxylation. Thus larger values listed for cases where there is limited decarboxylation do not generally reflect larger absolute amounts of possible coupling products.
2. The first four sets of data for benzoic acid itself are taken from previous work.
3. For economy of space, the symbol "Ph" is used here to represent a single phenyl ring, regardless of whether there are 3, 4 or 5 unsubstituted positions on the ring.
4. "THQ" represents 1,2,3,4-tetrahydroquinoline, "Tet" is tetralin, and "PipPy" is the strong organic base/nucleophile 4-Piperidinopyridine.
5. Does not include formation of naphthylbenzoate ester or rearranged product of this ester.

The data in this table demonstrate that the decarboxylation of benzoic acid itself is slow at 400 °C in tetralin (3-5% in 1 hr), unless a fairly strong base or other decarboxylation promoter is present. Surprisingly, the decarboxylation of calcium benzoate in tetralin is no faster than that of the free acid. With respect to coupling, we see that when decarboxylation is promoted by bases, there is little or no evidence for coupling, either with benzene, tetralin, naphthalene, or even the very good acceptor, pyrene. This absence of coupling, together with the slow decarboxylation of benzoic acid itself at 400°C, raises the question whether unactivated aromatic carboxylic acids actually represent the acid species that undergo facile decarboxylation between 250 and 350°C during the heating of low-rank coals.

Therefore, we performed additional experiments to examine the behavior of benzoic acid derivatives known [35,36] to be activated toward decarboxylation via electrophilic attack. Thus far, we have tested the ortho- and para- substituted acids listed in Table IV-2. For all of these, except for the meta hydroxy acid and veratric acid (3-OMe-4-OMe-$C_6H_3CO_2H$, last row in Table IV-2), decarboxylation in tetralin was complete in one hour at 400°C. Again however, there was no substantial level of coupling products. (In some cases there were small chromatographic peaks, as yet unidentified, at higher retention times. We cannot rule out the possibility that these result from some type of coupling associated with decarboxylation, but in any case they amount to less than 5% at most of the decarboxylated acid.) For the meta-hydroxy acid, there was, as expected, very little decarboxylation.

Perhaps the most interesting result with the activated acids is that obtained with veratric acid, the only one of the activated acids not possessing a free phenolic OH. This acid did not undergo complete decarboxylation, but was recovered in ca. 25% yield after 1 hour in tetralin at 400 °C, in contrast to the analog containing a free -OH in the same position, which underwent complete decarboxylation. Because p-OMe is generally just as activating toward electrophilic attack as p-OH, the above difference indicates that the rate determining step cannot simply involve attack on the starting material itself. That is, this result suggests that the principal mode of decarboxylation by electrophilic attack either involves reaction of the phenoxy anion or the keto form of the phenolic acid, which is accessible only through the free phenol. Alternatively, the keto form might simply undergo thermal unimolecular bond cleavage (homolysis) to yield a stabilized radical (phenoxy) and the radical CO_2H, even through the latter is not a particularly stable radical.

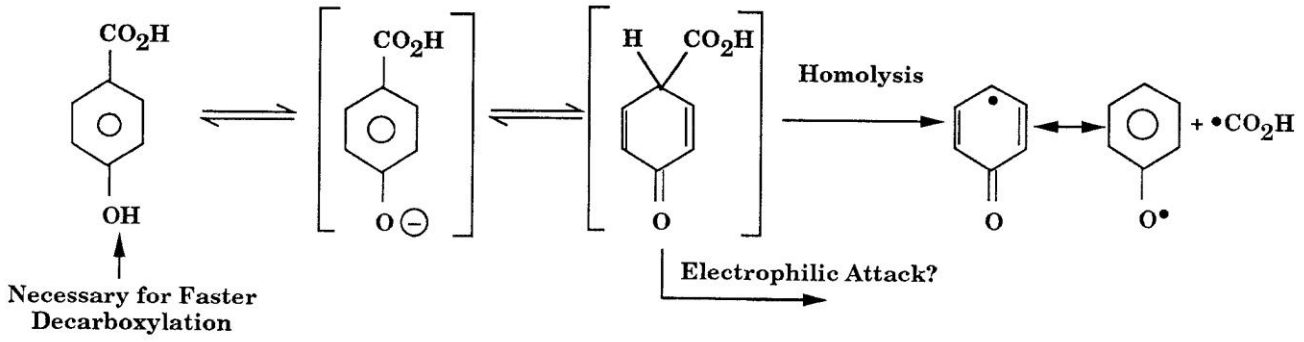

Assuming that a pre-equilibrium between the phenol and the keto-form is rapidly established and the homolysis of the keto-form would be the rate determining step, the net rate of decarboxylation can be readily estimated, since this case is exactly analogous to that described in the literature for benzyl phenols and phenoxy phenols [40]. This procedure leads to an estimated half-life at 400 ^{o}C of 1000 to 10,000 hours. Since the thermochemical estimates should be reasonably accurate here, and the assumption of a rapid pre-equilibrium leads to a lower limit on the half-life, we conclude that decarboxylation through homolysis of the keto-form can be ruled out as the reason for faster reaction of the acid containing a free -OH in the para position.
The remaining alternatives for reaction via the anion or keto-form do not appear particularly compelling, but we expect this issue will be clarified in the course of answering the ultimate question, "What are the conditions that enable decarboxylation to result in coupling?" In the meantime, the observation of very little coupling during the decarboxylations shown in Table IV-2 allows us to identify the following changes in substrate structure/reaction conditions that perhaps make the decarboxylation experiments more relevant to the conditions that actually prevail during liquefaction and also more likely to facilitate coupling, while yet remaining simple enough to provide chemical understanding.

Conditions likely to promote coupling in conjunction with decarboxylation:

1. Increased concentration and/or improved coupling partners for aryl radicals;

2. Decreased concentration of radical scavengers.

3. Electron-transfer agents that may convert carboxylate anions to radicals, which then decarboxylate to yield aryl radicals;

4. Conversion of the acids to their Ca or Mg salts, forms known in the coals themselves to increase char formation, and in alkane carboxylic acids [38] to yield ketone coupling products;

5. Addition of structures that may couple by forming electrophilic agents that attack the acids themselves, rather than merely react with aryl radicals produced in decomposition of the acids.

Item 1 has already been partially addressed with several of the experiments listed in Table IV-2, and did not result in significantly increased coupling. Items 2 and 3 are dealt with in considerable detail in the experiments described in the following subsection. Regarding Item 4, preliminary experiments with calcium benzoate (in solution, rather than neat) have not yielded additional coupling products, and Item 5 is also addressed below.

3. The Effect of Electron-Transfer Agents and the Acceptor/Scavenger Ratio

Because of the low levels of coupling products observed in the experiments described above, where we were attempting to grossly simulate the donor solvent environment of liquefaction by using tetralin or tetralin mixtures as the reaction medium, most of the remaining experiments were performed in

more oxidizing systems, i.e., without either hydro or alkylaromatic species in the mixture. In these experiments we used mixtures of benzoic acid/naphthalene as the basic system and then added various combinations of the reagents that were found from our previous studies to affect decarboxylation, particularly base (pyridine) and the potential electron transfer agents Fe_3O_4 and $Cu(OAc)_2$. In addition, we have performed a few experiments with phenylacetic acid to examine the behavior of a prototypical aliphatic acid.

In this portion of our decarboxylation studies, we have restricted the range of acids and broadened the range of reaction conditions under which these acids are being heated, in an attempt to bring about some coupling under conditions that perhaps approximate more closely those encountered in the thermal processing of low rank coals. In brief, we have tried various changes in reaction conditions that should make it more likely to form (from an un-activated acid) the carboxylate anion and oxidize it to the carboxyl radical, which should then readily decarboxylate to the phenyl radical. Under these conditions, literature data for the reactions of phenyl- and other aryl radicals [41,42] lead us to expect that any phenyl radicals formed will add very readily to essentially any aromatic system, displacing hydrogen to form biaryl linkages. We have allowed benzoic acid to react (at 400 °C) in the presence of varying amounts of naphthol, naphthalene, and methylnaphthalene, as well as tetralin, and have used the calcium salt of benzoic acid and pyridine as bases and Fe_3O_4 and $Cu(OAc)_2$ as electron-transfer agents. We performed a total of 21 experiments with cupric acetate or iron oxide, most of which we do not show in this report. The major differences between these two one-electron oxidants can be seen in the results shown in Table IV-3.

TABLE IV-3 – Effects of Different 1-Electron Oxidants on Coupling and Decarboxylation of Benzoic Acid During Reaction at 400°C for 1 Hour

	Reactants (mol%)[a]					Results				
Exp.	BA	Naphth.	Pyridine	Fe_3O_4	Cu Acet.	%Unr. Acid	% Ph-Naph[b]	% Py-Naph[b]	% Binaph.[b]	% Decarbox.[c]
1	11.3	68.8	9.8	10.1	—	19.5	3.2	2.93	2.66	57.3
2	10.4	70.4	8.9	—	10.3	< 0.1	0.28	0.65	2.03	83.4

[a] BA = benzoic acid; Naphth. = Naphthalene; Cu Acet.= Cupric Acetate monohydrate [$Cu(CH_3CO_2)_2 \cdot H_2O$].

[b] Ph-Naph = 1 and 2-phenyl naphthalene; Py-Naph = pyridinylnaphthalenes; Binaph. = binaphthalenes. Results are given as a mol% of the starting *benzoic acid*. It has thus been assumed that pyridinylnaphthalenes and binaphthalenes are coupling products that stem from decarboxylation after a shift of the radical center from the initial phenyl radical to either pyidine or naphthalene. This assumption is being checked and could be incorrect.

[c] Based on identified decarboxylated products including benzene and phenyl-containing coupling products.

Both agents markedly increase decarboxylation (from 3-5% as shown in Table IV-2 to at least ~60% as seen in Table IV-3). Decarboxylation rates are at least ten times faster with $Cu(OAc)_2$ than with Fe_3O_4, but the coupling is about ten times faster in the presence of Fe_3O_4. For present purposes, the results can be summarized as follows. The combination of pyridine and cupric acetate did enhance decarboxylation substantially, as the literature [35,36] indicates it should. However, we still see only very low levels of coupling products (other than ester formation from benzoic acid and naphthol, when

it is present). Furthermore, we see this lack of substantial coupling even when we have replaced most or all of the tetralin with naphthalene to provide more good acceptors for phenyl radicals and to decrease the scavenging ability of the system. Under these latter conditions, reported phenyl radical H-abstraction (from tetralin) and aryl radical addition rates [41,42,43] suggested that the addition should not be overwhelmed by scavenging of the phenyl radicals. Thus, from the data in Tables IV-2 and IV-3, it is still far from evident what chemical factors are here not allowing substantial coupling, but which may still allow such coupling during coal conversion.

After a few experiments with $Cu(OAc)_2$ and the mixed iron oxide Fe_3O_4, we switched to Fe_3O_4 because (1) coupling was greater with iron oxide and the parameters affecting it could be more readily explored, (2) iron is more coal-relevant than copper and (3) decomposition of the acetate led to unwanted buildup of non-condensable gases (presumably methane) and perhaps distorted chemistry because of the demand of methyl radicals for hydrogen. Iron sulfides and iron sulfates are of course also relevant, but we have, for the time being, confined our iron-promoted decarboxylation studies to Fe_3O_4 in order to focus on the impact of changing the organic structural parameters.

4. Coupling Product Distribution.

The nature and distribution of the coupling products themselves may provide an indication of the factors limiting coupling under the above reaction conditions. For the decarbozylation of benzoic acid in naphthalene, pyridine and Fe_3O_4, GC/MS analysis has allowed us to identify the coupling products 1- and 2-phenylnaphthalene, two isomers of pyridinylnaphthalene, and the 1,1', 1,2', and 2,2'-binaphthyls, as listed in Table IV-4.

Typically the 1-phenyl naphthalene is two to three times more abundant than the 2-phenylnaphthalene, in accord with the relative rates of radical addition and H-transfer to naphthalene that have been reported in the literature [44,45]. In the case of the binaphthyls, the ratio of 1,2'-, 1,1'-, and 2,2'-binaphthyl is typically 3:2:1. This product distribution is not in accord with the slightly higher thermodynamic stability of the 1-naphthyl radical, but is in accord with the known preference [42,43] for addition to the 1-position of the naphthalene ring. In any case it is the same product distribution as reported by Stein et al. [46] for radical induced binaphthyl formation. In the case of the pyridinyl naphthalenes, the point of connection of the pyridine to the naphthalene ring is inferred from the phenyl naphthalenes, but the connections to the pyridine ring are unknown. At this point we judge that the isomer distributuions are generally consistent with H-abstraction from either pyridine or naphthalene by the initially produced phenyl radical, followed by addition of the new aryl radical to naphthalene. However, the formation of similar amounts of pyridinyl naphthalenes and naphthylnaphthalenes is surprising in view of the fact that the reaction mixture contains seven times as much naphthalene as pyridine.

The decarboxylation products observed in more oxidizing systems (no donor solvent present, but with

TAB:E IV-4 – Effect of Fe_3O_4 and Pyridine on Decarboxylation and Coupling of Benzoic Acid During Reaction in Napthalene at 400 °C for 1 hour.

	Experiment							
	Condition 1		Condition 2		Condition 3		Condition 4	
Reactants	mmol	mol%	mmol	mol%	mmol	mol%	mmol	mol%
Benzoic Acid	0.1957	9.57	0.2031	10.00	0.2064	10.13	0.2260	11.26
Naphthalene	1.8499	90.43	1.6299	80.23	1.6205	79.49	1.3810	68.80
Pyridine	—	—	0.1985	9.77	—	—	0.1972	9.82
Fe_3O_4	—	—	—	—	0.2116	10.38	0.2030	10.11
Products								
Benzoic Acid	0.19999	102.19	0.18803	92.58	0.20587	99.74	0.0440	19.48
Naphthalene	1.84617	99.80	1.62816	99.89	1.5943	98.38	1.3269	96.08
Pyridine	—	—	0.15658	78.88	—	—	0.1726	87.54
Benzene	0.00833	4.26	0.03671	18.07	0.01336	6.47	0.1223	54.11
Naphthalene Impurities	0.01425	0.77	0.01243	0.76	0.01214	0.75	0.01051	0.76
Biphenyl[a]	< 0.00004	< 0.004	< 0.00004	< 0.004	< 0.00004	< 0.004	0.00031	0.14
1-Phenylnaphthalene[a]	0.00011	0.058	0.00048	0.23	0.00488	2.36	0.0050	2.20
2-Phenylnaphthalene[a]	0.00011	0.055	0.00041	0.20	0.0021	1.02	0.0022	0.99
1-Pyridinylnaphthalene[a]	—	—	< 0.00004	< 0.004	—	—	0.0048	2.45
2-Pyridinylnaphthalene[a]	—	—	< 0.00004	< 0.004	—	—	0.0018	0.90
1,1'-Binaphthalene[a]	< 0.00004	< 0.004	< 0.00004	< 0.004	0.00093	0.905	0.00089	0.79
1,2'-Binaphthalene[a]	< 0.00004	< 0.004	< 0.00004	< 0.004	0.00149	1.440	0.0016	1.44
2,2'-Binaphthalene[a]	< 0.00004	< 0.004	< 0.00004	< 0.004	0.00046	0.441	0.00049	0.43
% Decarboxylation[b]	4.4		18.5		9.9		57.6	
% (Coupling/Decarbox.)[b,c]	2.7		2.3		48.5		12.8	

[a] Mol percentages are based on the benzoic acid reactant. [b] Based on identified products. [c] It is assumed that pyridinylnaphthalenes and binaphthalenes are coupling products that stem from decarboxylation after a shift of the radical center from the initial phenyl radical to either pyridine or naphthalene (see text).

an added electron-transfer agent) tend to support the basic mechanism anticipated from the literature [35] and outlined below, whereby the benzoic acid is converted to benzoate by the base (1) and the benzoate anion to the radical by the electron transfer agent (2). The carboxyl radical then decomposes to CO_2 and phenyl radical (3). Phenylnaphthalenes result from net displacement of a naphthyl hydrogen by phenyl radical (4). If the phenyl radical were to abstract hydrogen from pyridine or naphthalene prior to successful addition, pyridinyl and naphthyl radicals would result. Attack of these secondary radicals on naphthalene could then explain the formation of pyridinylnaphthalenes and binaphthalenes, as briefly indicated above.

$$C_6H_5CO_2H + C_5H_5N \rightarrow C_6H_5CO_2^- + C_5H_5NH^+ \quad (1)$$

$$C_6H_5CO_2^- + Fe_3O_4 \rightarrow C_6H_5CO_2\bullet + Fe_3O_4^- \quad (2)$$

$$C_6H_5CO_2\bullet \rightarrow C_6H_5\bullet + CO_2 \quad (3)$$

$$C_6H_5\bullet + C_8H_{10} \rightarrow\rightarrow C_6H_5 - C_8H_{10} + H\bullet \quad (4)$$

It is interesting that a mechanism for the widely used copper/quinoline-promoted decarboxylation of aromatic acids was suggested as recently as 1970, and is still not entirely clear. There is very likely more than one mechanism for transition metal catalyzed decarboxylations operative for different substrates under different conditions.

The Effect of Iron Oxide and Base on Coupling

The four experiments in Table IV-4 also show the separate and combined impacts of iron oxide and pyridine on decarboxylation and coupling. All of the products discussed above are listed in this table, but the major points are contained in the first four rows, where the reactant identities and concentrations are listed, and the last two rows, where the percent decarboxylation and the percent of decarboxylation that leads to coupling are shown. It can be seen that the conditions strongly affect both the amount of decarboxylation and the degree of coupling. In naphthalene only (Condition 1), benzoic acid undergoes about 4.4% decarboxylation and only 2.7% of the decarboxylated material is found as the coupling product phenylnaphthalene. The addition of pyridine base (Condition 2) increases decarboxylation by a factor of four, but the fraction of decarboxylation that leads to coupling products is unaffected, remaining at 2.5 ± 0.2%. These results are consistent with a mechanism where decarboxylation involves primarily the carboxylate anion itself. To the extent that phenyl anion is the initial product of decarboxylation, its strong basicity is seems likely to have it abstract a proton rather than couple with another molecule. (FOOTNOTE— Note that in the "dry" or neat pyrolysis of alkaline earth salts of alkane carboxylic acids [38], where the products are ketones that apparently result from the attack of an alkyl carbanion on an adjacent metal carboxylate, all of the hydrogens except those alpha to the carboxyl group are many orders of magnitude weaker acids than a compound such as tetralin, which has benzylic hydrogens. Furthermore, in the pyrolysis of the neat salt, the chances that the carbanion will encounter another carboxylate group are clearly much enhanced. Just how relevant the pyrolysis of neat calicum alkanoates to coal conversion is not clear. It could be, for instance, that

preferential alignment of carboxylic acid groups at mineral matter interfaces during the coalification process results in an effective concentration of carboxylates that is much higher than their average concentration in the coal structure —END FOOTNOTE). The effect of base is then to increase the concentration of the benzoate anion and hence the rate of decarboxylation. The product is still phenyl anion, however, and the rate of coupling is therefore unaffected.

Substantial coupling is seen only in those systems where the 1-electron oxidant Fe_3O_4 has been added (Conditions 3 and 4). By itself, the addition of Fe_3O_4 leads to a factor of 2.5 increase in the rate of decarboxylation when compared with the naphthalene-only system. More significant, however, is the fact that now nearly one-half of the decarboxylated material is found as a coupling product. This result is consistent with the traditional organic chemistry picture of decarboxylation of aryl carboxylic acids outlined above, namely that the benzoate anion is oxidized to the carboxylate radical, which then loses CO_2 to give a phenyl radical. Phenyl then displaces a hydrogen from naphthalene to give phenylnaphthalene. Alternatively, phenyl can abstract a hydrogen from naphthalene to give naphthyl radical, which can then displace a hydrogen from naphthalene to give binaphthyl. At present, we are assuming that this is the source of essentially all the binaphthyl.

When both pyridine and Fe_3O_4 are added (Condition 4), the degree of decarboxylation increases to about 60%. However, the fraction of decarboxylated material that couples is only12.8%, a factor of 3.8 lower than with Fe_3O_4 only, but a factor of 5 greater than with no added Fe_3O_4. Apparently the base directly or indirectly facilitates the transfer of a hydrogen to phenyl radical before it can couple. Notice that this effect of added base in suppressing the fraction of decarboxylation that leads to coupling was not observed in the absence of Fe_3O_4 (compare the results for Conditions 1 and 2), consistent with the supposition that in the absence of Fe_3O_4 the bulk of the decarboxylation goes through a different species. Although these observations on the effect of the base are at present not fully understood, they obviously could have ramifications with regard to the design of a system which minimizes coupling reactions in coal liquefaction.

The Effect of Water

Because water has figured prominently in various coal pretreatment studies and because it has been shown to inhibit the coupling of phenolic structures, we added 10 mol% water to the system which has so far shown the greatest coupling (as a fraction of decarboxylation), namely the benzoic acid-naphthalene-Fe_3O_4 system. In the this case, however, there was no significant impact of water, either on decarboxylation or on coupling.

The Effect of H-Donors

Although as described above, we removed H-donors from the reaction mixtures in an attempt to produce enough coupling products so that the factors affecting their formation could be readily studied, we did not show above any single direct comparison of the impact of donors. Table IV-5 shows that the replacement of roughly half of the naphthalene with the H-donor tetralin decreased not only the fraction of the decarboxylation that eventually led to coupling, but also the extent of decarboxylation.

TABLE IV-5 – Effects of Solvent H-Donating Ability on Coupling and Decarboxylation of Benzoic Acid During Reaction of 400°C for 1 Hour in Presence of Base and the Electron Transfer Agent Cupric Acetate.

	Reactants (mol%)[a]						Results			
Exp.	BA	Naphth.	Tet / MN	Pyridine	Naphthol	Cu Acet.	%Unr. Acid	% Coupling[b]	% Decarbox.[c]	%(Coup/Decarb)
1	9.8	—	58.8	12.2	9.6	9.7	45.9	0.51[d]	46.5	1.1
2	10.4	70.4	—	8.9	—	10.3	<0.1	2.96	83.4	3.5

[a] BA = benzoic acid; Naphth. = Naphthalene; Tet/MN = 50:50 mol/mol mixture of tetralin and 1-methylnaphthalene; Naphthol = 1-naphthol; Cu Acet.= Cupric Acetate monohydrate [$Cu(CH_3CO_2)_2 \cdot H_2O$].

[b] Results are given as a mol% of the starting benzoic acid and refer to all peaks in the coupling region of the chromatogram.

[c] Based on identified decarboxylated products including benzene and phenyl-containing coupling products.

[d] This figure does not include 1% formation of naphthyl benzoate from benzoic acid and naphthol.

As discussed above, it was expected that the H-donor, functioning in its radical scavenger mode, would scavenge a larger fraction of the phenyl radicals before they could couple. However, we did not anticipate that the H-donor would also decrease the amount of decarboxylation, and we are not now able to rationalize this result. It would seem unlikely that that an initially produced carboxyl radical would have a sufficiently long lifetime before decarboxylation to allow any significant scavenging by tetralin.

5. Decarboxylation of Phenyl-Subsituted Alkane Carboxylic Acids

Since we do not know the distribution of carboxylic acid types in these coals, and since the oxidation of non-benzylic alcohol carbons in the original lignin structure is an alternative to oxidation of benzylic carbons to substituted benzoic acids, we have performed a few experiments on phenylacetic acid. This structure, having the carboxyl carbon β- to the aromatic ring, should be a reasonable prototype for all acids having the carboxyl carbon β- or further from the aromatic ring. Table IV-6 shows that the decarboxylation of this aliphatic acid, which in tetralin alone is about six times higher for phenylacetic acid than it is for benzoic acid in tetralin alone, is also markedly accelerated by electron-transfer agent and base.

TABLE IV-6 – Effects of Cupric Acetate and Pyridine on Decarboxylation and Coupling of Phenylacetic Acid During Reaction of 400°C for 1 Hour.

	Reactants (mol%)[a]					Results			
Exp.	Ph-AA	Tetralin	Naphth.	Pyridine	Cu Acet.	%Unr. Acid	% Coupling[b]	% Decarbox.[c]	%(Coup/Decarb)
1	10.3	87.7	—	—	—	64.4	2.8	21.7	12.7
2	9.5	—	71.3	9.3	9.9	< 0.01	15.7	85.9	18.3

[a] Ph-AA = phenylacetic acid; Naphth. = Naphthalene; Cu Acet.= Cupric Acetate monohydrate [$Cu(CH_3CO_2)_2 \cdot H_2O$].
[b] Not all peaks have yet been identified; results are based on sum of all peaks in the region of expected coupling products.
[c] Based on sum of identified decarboxylated products such as toluene and all coupling products which are assumed to have been decarboxylated.

However, it is curious that the extent of acceleration is actually less for this aliphatic acid than it is for benzoic acid. Although phenylacetic acid is inherently more reactive, the promoted decarboxylation is only about 85% in one hour, as compared to 98% or greater with benzoic acid in the presence of $Cu(OAc)_2$.

The extent of coupling that accompanies decarboxylation would seem (although some of the coupling products for phenylacetic acid have not yet been identified to the extent that they have for benzoic acid) to be somewhat higher than for benzoic acid under comparable conditions. This is somewhat surprising, since no species seem more thermodynamically equipped to couple than aryl radicals: no other radicals form nearly as strong a bond when they add to another aromatic ring. However, an a-priori prediction would have been difficult here, since the aryl radicals also form a comparable stronger bond to -H in the act of being scavenged.

The last category of decarboxylation experiments we have performed is that of alkylaromatic systems in which the carboxylic acid group is bonded to an aliphatic carbon. Since we do not know the distribution of carboxylic acid types in these coals, and since the oxidation of non-benzylic alcohol carbons in the original lignin structure is an alternative to oxidation of benzylic carbons to substituted benzoic acids, we have performed some experiments with phenylacetic acid, chosen as a reasonable prototype for all acids having the carboxyl carbon β- or further from the aromatic ring. Initial experiments with this category were described above (see Table IV-6). Those results will be briefly summarized here, followed by a description of the limited set of experiments performed since then, whose objective was to complete, to the extent possible, an outline of how aromatic and aliphatic carboxylic acids may contribute to retrograde reactions of low rank coals.

As discussed above, it was reported that decarboxylation of phenylacetic acid in tetralin proceeds with a rate about 6 times that of benzoic acid but slower than that of acids activated by e.g., an ortho or para hydroxy. Decarboxylation was found to have been accelerated by the combination of base and the electron-transfer agent cupric acetate, although surprisingly to a lesser degree than observed for benzoic acid. Finally, the gas chromatograms of the product mixture gave evidence for greater

coupling than with benzoic or the activated acids, but the products had not been identified at that time. A more complete study was done and summarized in Table IV-7 are the results of a series of experiments in which we have probed the effects of radical scavenger, base, and the 1-electron oxidant Fe_3O_4 on the conversion and coupling reactions of phenylacetic acid.

The electron transfer agent Fe_3O_4 was found to have a large effect on the reaction and so, in order to simplify the discussion, we will begin with a description of the results in experiments without this additive. In the absence of Fe_3O_4, toluene, the primary decarboxylation product, is formed in 27% yield after 1 hour in naphthalene at 400°C. As the naphthalene is replaced by the hydrogen donor tetralin, the yield of toluene gradually decreases until it is present in 20% yield when pure tetralin is used. Several coupling products were also identified, including 1,3-diphenylacetone (DPA), bibenzyl, t-stilbene, benzylnaphthalenes, and phenylnaphthalenes. The yield of the major coupling product, DPA, decreases from 5.6% yield in naphthalene to 1.3% in tetralin. By contrast, replacement of naphthalene by tetralin increases benzylnaphthalene formation from 0.05% to 0.5%. The net effect of the hydrogen donor remains favorable, however, decreasing the ratio of (% coupling/% reaction) from 13 to 5%.

Most of the above results are explainable by the general mechanistic picture of decarboxylation that was summarized above, i.e., that decarboxylation proceeds primarily through the carboxylate anion, at least for unactivated species in the absence of electron transfer agents. The 25% decrease in toluene formation as the solvent is changed from naphthalene to the radical scavenger tetralin could indicate that some portion of the reaction involves radical species, but it could also reflect slightly different abilities of the two compounds to solvate the anion intermediate. In any case, radicals do play some role, since bibenzyl and t-stilbene are apparently primary and secondary recombination products of the relatively stable benzyl radical, an intermediate whose presence is also consistent with the formation of benzylnaphthalenes. The above products are formed in small amounts only (< 0.5%), however, and it may well be that the benzyl radicals stem from toluene, rather than directly from the decarboxylation of phenylacetic acid.

The most difficult products to explain are phenylnaphthalene and 1,3-diphenylacetone (DPA). Although the former is only a trace product under the present conditions, it would seem to indicate the formation of some phenyl radicals in the system, which is not easy to understand. Further, as will be discussed below, this species becomes significantly more important in the presence of Fe_3O_4. The formation of 1,3-diphenylacetone is also not well understood at this time. For the present we note only that the analogous product from benzoic acid, benzophenone, was not observed. This suggests that the α-CH_2 of phenylacetic acid is involved in the formation of this product. Note also that DPA is the only coupling compound identified thus far where the carboxylate oxygen was partially retained in the retrograde product.

TABLE IV-7 – Effects of Radical Scavenger and 1-Electron Oxidant on Coupling and Decarboxylation of Phenylacetic Acid During Reaction at 400°C for 1 Hour.

	Reactants (mol%)[a]	Results (as a % of starting PAA[a])						
Exp		%Unr. Acid	Toluene	BB+SB[b,c]	DPA[b,c]	Bz-Naph[b]	Ph-Naph[b]	%Coup./ %Reaction[d]
1	PAA/Naph 10.9/89.1	57.1	27.2	0.41	5.6	0.047	0.065	13.3
2	PAA/Naph/Tet 11.1/77.9/11.0	65.0	27.3	<0.15	5.3	0.23	<0.05	15.8
3	PAA/Naph/Tet 9.9/20.5/69.6	72.3	21.1	<0.15	2.6	0.46	<0.05	11.0
4	PAA/Tet 10.3/89.7	67.2	19.7	<0.15	1.3	0.48	<0.05	5.4
5	PAA/Naph/Pyridine 9.8/79.0/11.2	61.3	31.6	0.39	5.1	0.052	<0.15	14.3
6	PAA/Naph/Fe_3O_4 9.8/79.9/10.3	34.7	35.7	7.2	5.5	3.3	2.4	28.2
7	PAA/Naph/Tet/Fe_3O_4 9.9/70.7/9.5/9.9	31.6	35.3	4.8	20.9	1.7	0.52	43.2
8	PAA/Naph/Tet/Fe_3O_4 9.9/44.5/35.6/10.0	35.2	32.7	2.5	23.8	1.1	0.17	42.5
9	PAA/Tet/Fe_3O_4 10.0/80.0/10.0	42.0	29.2	1.1	23.6	0.62	<0.05	43.7

[a]PAA = phenylacetic acid; Naph = Naphthalene; Tet = Tetralin
[b]BB = Bibenzyl; t-SB = trans-stilbene; Bz-Naph = 1 and 2-benzyl naphthalenes; Ph-Naph = 1 and 2-phenyl naphthalenes.
[c]These species stem from two units of phenylacetic acid; given percentages are *twice* the mol%.
[d]Based on identified coupling products and unreacted phenylacetic acid.

Effect of Added Base

A slight increase of 16 % in the rate of decarboxylation was effected by the addition of 11 m% of pyridine to the phenylacetic acid/naphthalene mixture (see Table IV-7, exps. 1 and 5). This is a much smaller increase than was observed with benzoic acid, where a 300% increase was observed (see Table IV-4). In the benzoic acid case, it was thought that the function of base was to increase the concentration of the carboxylate anion which was the species postulated to undergo decarboxylation. Why base would be much less effective in the case of phenylacetic acid is not presently understood. Rates of coupling reaction were essentially unaffected by the addition of the pyridine.

Effect of Added Fe_3O_4

Consistent with previous results on benzoic acid, addition of 10 m% of the electron transfer agent Fe_3O_4 to the phenylacetic acid/naphthalene mixture leads to more reaction and more coupling. The primary decarboxylation product toluene shows about a 30% increase in its rate of formation when compared to the naphthalene only case. The effects on coupling products are more dramatic, with the sum of bibenzyl and t-stilbene increasing by a factor of 18 and the products benzylnaphthalene and phenylnaphthalene by factors of 70 and 36, respectively. These results are consistent with our previous postulate that iron oxide leads to the generation of radicals in the system. We had suggested that the carboxylate anion was oxidized to the carboxyl radical, which then loses CO_2 to generate the corresponding radical. In the present instance, this would lead to benzyl radical, thus explaining the large increase in the expected products from this intermediate (bibenzyl, t-stilbene, and benzylnaphthalene). It is less clear how Fe_3O_4 induces the formation of phenyl radicals, which presumably are responsible for the formation of phenylnaphthalene. In any case, addition of the radical scavenger tetralin to the system has the expected effect on these products, reducing their rates of formation. Most severely affected are phenylnaphthalenes, which drop from a 2.4% yield in naphthalene solvent to < 0.05% in pure tetralin. This is suggestive of very efficient scavenging of C_6H_5 by tetralin, a not unexpected result given that the C-H bond in benzene is > 20 kcal/mol stronger than that in tetralin. Judging from the products from benzyl radical, tetralin is effective but somewhat less so in scavenging such resonance stabilized radicals with their more similar C-H bond strengths.

The most surprising result concerns the coupling product DPA. In pure naphthalene solvent, the addition of 10 m% of Fe_3O_4 to the mixture had no effect on DPA formation (Table IV-7, exps. 1 and 6), which remained constant at 5.5%. However, when 10 m% of the naphthalene was replaced by tetralin the DPA production increased four-fold, accounting for 21% of the starting acid. Further addition of tetralin then had only a small effect, with the yield of DPA remaining a constant 23-24%. This behavior is quite different from that observed in the absence of Fe_3O_4, where the shift from naphthalene to tetralin smoothly reduced DPA formation from 5.5 to 1.1%. The dramatic effect of the combination of tetralin/Fe_3O_4 on the formation of this product is presently not understood. One possibility is that the

tetryl radicals in the system are donating an electron to the Fe_3O_4 and it is the reduced form of Fe_3O_4 that is catalyzing the formation of DPA. It is not clear, however, why carboxylate anions or benzyl radicals, both of which are present even when pure naphthalene is the solvent, would not be just as effective in this regard.

In the absence of electron transfer agents, our previous results (see Tables IV-4 to IV-7) showed that coupling of activated acids was a very minor process under reductive coal liquefaction conditions. However, because of the large effect of Fe_3O_4 on the coupling products that were observed with benzoic and phenylacetic acid, we thought it important to examine the behavior of the activated acid o-anisic acid (2-methoxybenzoic acid) in the presence of this electron transfer agent. As shown in Table IV-8, we find an 6.9% yield of xanthenes from o-AA in naphthalene when 10 m% of iron oxide is added. The question is how does this product arise? Is it a direct product of decarboxylation or is it formed from some species that has already lost CO_2? Phenol and Cresol are major decarboxylation products that we suspected could form reactive intermediates. As shown by the latter two experiments in Table IV-8, it is in fact these species that are responsible for the formation of xanthenes. The data demonstrate that the self- coupling of o-cresol gives methylxanthene (Equation 7) while the cross-coupling of phenol with o-cresol gives the unmethylated parent. From a thermodynamic point of view, the net formation of water is very favorable and will help to drive the reaction

TABLE IV-8 – Fe_3O_4 Induced Coupling of Decarboxylation Products of Anisic Acid

Exp	Reactants (mol %)[a]	Results (as a % of starting material)					
		%Unr. Acid	Anisol	PhOH[4]	o-Cresol	Xanth[a,b]	Me-Xanth[a,b]
1	o-AA/Naph/Fe_3O_4 12.8/77.7/9.9	<0.1	19.8	46.3	12.5	6.9	1.7
2	Cresol/Naph/Fe_3O_4 9.7/80.3/10.0	- - -	- - -	6.3	67.8	0.36	4.2
3	Cresol/PhOH/Naph/Fe_3O_4 8.0/8.2/75.5/8.3	- - -	- - -	81.7	73.9	4.6[c]	2.1[c]

[a]o-AA = ortho-anisic acid (2-methoxybenzoic acid); Naph = Naphthalene; Cresol = ortho-Cresol, PhOH = phenol, Xanth = Xanthene; Me-Xanth = Methylxanthene (isomer undefined).
[b]These species stem from two units of phenylacetic acid; given percentages are *twice* the mol%.
[c]Given as a percentage of the *sum* of the starting phenols.

No product attributable to the self-coupling of phenol was found so it is apparent that the juxtaposed methyl and hydroxy groups are a structure that preferentially leads to coupling reactions under our conditions. With regard to coal liquefaction, it is apparent not only that such reactive structures may be generated during decarboxylation of activated acids, but also that they may pre-exist in the coal matrix and lead to retrograde reactions independent of decarboxylation reactions.

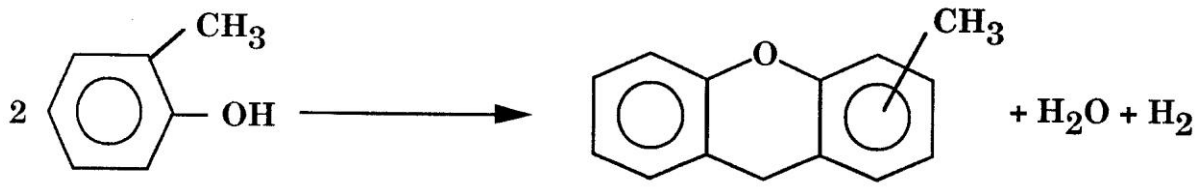

(7)

6. Additional Decarboxylation Studies

During this project, we completed a survey of the decarboxylation and coupling of some prototypical monomeric carboxylic acids under "liquefaction" conditions. The bulk of these results were discussed in Section 5 (above) and in the American Chemical Society Fuel Division preprint [47]. The additional experiments performed involved testing the effect of iron sulfide as another iron salt of potential importance in crosslinking during the heating of coals. We also tested the effect of water on the behavior of phenylacetic acid. We found that the addition of FeS to benzoic acid in naphthalene increased the decarboxylation (during 1 hr at 400°C) from 4.5% to 45.5%. However, the coupling (to phenylnaphthalene, expressed as a % of the decarboxylation that yielded coupling) increased only from 2.5% to 5.7%. The increase in decarboxylation is several times greater than that observed with Fe_3O_4, but the increase in coupling to about 6% is much less than the ~50% seen with Fe_3O_4. Thus the principal general conclusion to be drawn from the relative impact of FeS is that the lower iron sulfides, which have long been considered to have a net benefit on liquefaction, are not likely to be a cause of retrograde reaction during coal heating.

In the decarboxylation of phenylacetic acid, we found the addition of water substantially suppressed the formation of dibenzylketone from the decarboxylation of phenylacetic acid in naphthalene. We believe, for the following reasons, that this to be a true chemical effect rather than a simple dilution effect. First, a chemical effect is expected: if the ketone formation is the result of the formation of phenylketene via the acid anhydride, as we have speculated, then water would inhibit the formation of the anhydride and/or react with the ketene to regenerate the original acid. Second, the extent of the suppression is several times greater than would be expected from a decreased concentration of acid, assuming a coupling that has a net second-order dependence on acid and that the acid and water were completely miscible. It would probably be appropriate to prepare the calcium salt of phenylacetic acid to observe its decarboxylation behavior. Heating of the neat calcium salts of aliphatic acids is known to generate ketone coupling products [$Ca^{++}(RCO2_2^-)_2 \rightarrow R(C=O)R$], so behavior of calcium phenylacetate and calcium hydrocinnamate [$Ca^{++}(PhCH_2CH_2CO_2^-)_2$] may be as relevant to coupling during the heating of coals as the behavior of alkaline earth salts of aromatic acids.

We have prepared, purified, and tested the behavior of the calcium salts of benzoic acid and anisic acid [$Ca^+C_6H_4(o\text{-}OCH_3)CO_2^-$] when heated, both in a poor "liquefaction" medium and neat. In brief, the results are that the decomposition of the calcium salts does *not* substantially increase the tendency for

crosslinking to occur in association with decarboxylation. We have prepared but not yet purified the calcium salt of vanillic acid [$Ca^{+}C_6H_4$(o-OCH_3)(p-OH)CO_2^{-}], which is difficult to purify by crystallization from aqueous solution. The major remaining possibility we wish to test as a route to facile coupling of activated carboxylic acid species (such as anisic and vanillic acid- like structures) is route in which the presence of the acid in its salt form makes electrophilic displacement of the CO_2 group by a proton much less likely and allows instead for some other electrophile (such as $HOC_6H_4CH_2^{+}$) to perform the displacement, generating a new carbon-carbon linkage.

D. Summary and Conclusions

1. Model Polymer Synthesis

The preparation of polymer mixtures dominated by hexa(phenylene) showed that characterization and functionalization of moderate molecular weight polyphenylenes proves to be very difficult, owing to the insolubility even of these low molecular weight oligomers. On the other hand, the preparation of moderate molecular weight C-C-O polymers (n = 10 to 30) has proven to be easier than we had anticipated, after difficulties with unwanted side reactions were suitably minimized with a phase-transfer catalyst approach. Although these polymers have a labile backbone and do not therefore provide a refractory framework with which to study unencumbered the reactions of carboxylic acid groups we plan to attach to the polymers, these materials will constitute the most coal-related polymer models that have been studied to date. They will, therefore, provide very appropriate surrogates for addressing the retrograde reactions of phenolic and carboxylic acid functions.

The preparation of moderate molecular weight C-C-O polymers (n = 10 to 30) has been further optimized. The synthesis of the 4-hydroxyphenethyl halide needed for the phase-transfer-catalyzed polymerization has been shortened from three separated procedures to a sequence of three reactions carried out effectively in a single step. NMR, GPC, and pyrolysis-FIMS analyses of the polymer subsequently produced from this iodide show it to have a weight-average molecular weight of somewhat over 4000 (n = ~35), to have the desired phenyl-O-C-C- structure and to be contaminated with ≤5% of related olefins and n-butyl amine. Pyrolysis-FIMS analysis supports the purity of the polymer and reveals that coordinated cleavage or unzipping appears to be very facile at about 380°C. This coordinated cleavage does not result from any radical pathway we can identify at this time, but it is strikingly reminiscent of the cleavage reported for lignins themselves (and not understood in those systems either).

2. Decarboxylation and Coupling in Monomeric Systems

From the results described above, together with previous decarboxylation studies we have examined, we reach the following preliminary conclusions. First, simple benzoic acids (i.e., unsubstituted by anything except carbon) do not rapidly decarboxylate below 400 ^{o}C, except in the presence of strong base and or electron transfer agents, and second, upon decarboxylation, they tend to form rather smaller amounts of coupling products than might have been expected, either with themselves or with aromatics that are part of the solvent system. This is true even when the system contains no H-donor component that might be expected to scavenge aryl radical intermediates before they could couple. It is also true even when aromatics such as pyrene or naphthol, which are very good radical acceptors, have been added to the system. These low levels of coupling raise two important questions. First, is coupling associated with decarboxylation as important a part of retrograde reactions in low-rank coals as it has been assumed to be? Second, if decarboxylation is an important prelude to retrograde reactions with real coals, doesn't the rather low level of coupling observed with model carboxylic acids suggest that this doesn't have to be so?

The electron-transfer agent cupric acetate, as expected from the literature, was very effective in promoting decarboxylation, but the fraction of this added decarboxylation that resulted in coupling was low, typically less than 10%. The mixed iron oxide, Fe_3O_4, was somewhat less effective at promoting decarboxylation, but the fraction of the decarboxylation that results in coupling is 4 to 5 times higher. One very surprising observation was that pyridine, while promoting decarboxylation (as expected), decreased by a factor of four the fraction of decarboxylation that led to coupling. Perhaps the pyridine not only serves to "hold" the proton while the anion undergoes electron transfer and decarboxylation, but then "hands it back" to the decarboxylation intermediate (i.e., either the aryl radical or anion) before coupling can occur. We do not fully understand this chemistry yet, but it clearly could have profound implications for reducing decarboxylation-instigated coupling during coal liquefaction.

Decarboxylation of phenyl-substituted alkane carboxylic acids was examined using the model compound phenylacetic acid. Its behavior was examined under a variety of conditions to probe the effects of added radical scavenger, base, and the electron transfer agent Fe_3O_4. Both decarboxylation and coupling were faster than with benzoic acid. Consonant with the results with benzoic acids, added scavenger decreased the degree of coupling in the absence of Fe_3O_4. Surprisingly, however, the addition of scavenger in the presence of Fe_3O_4 led to a 4-5 fold increase in the formation of the coupling product 1,3-diphenylacetone. This product accounted for about 40% of the reacted acid when this combination of reagents was present. In addition, since the analogous product was not identified in the benzoic acid system, this product indicates that some of the major coupling pathways of phenylacetic acid, and perhaps all alkane carboxylic acids, are significantly different than those of benzoic acids.

The reaction of the activated acid o-Anisic acid (2-methoxybenzoic acid) in the presence of Fe_3O_4 was also examined. Xanthenes were formed in about 9% yield under some conditions. These products were demonstrated to stem from the reactions of cresol with either phenol or itself, rather than directly from o-Anisic acid (the phenols are decarboxylation products of o-Anisic acid). It is apparently the juxtaposition of the methyl and hydroxy groups that leads to the retrograde reactivity. These results suggest that phenolic groups could play a major, or even dominant role in the retrograde reactions that occur during coal liquefaction in the temperature regime associated with CO_2 loss. Since such structures may be present in the coal matrix even prior to decarboxylation, what remains unclear is exactly to what degree such reactions necessarily arise as a consequence of decarboxylation.

V. TASK 4 - DATA INTEGRATION AND REPORTING

A. Studies on Coals and Modified Coals

The key results for experiments with coals and modified coals were summarized in the ACS Denver paper, titled "The Effects of Moisture and Cations on liquefaction of Low Rank Coals [16]." The conclusions from this paper are as follows:

- The tar yields and liquefaction yields are reduced for all three cations tested (K^+, Ca^{++}, Ba^{++}) and are lower for the fully exchanged coals. The ability of cations to act as initial crosslinks is an important aspect of their role in retrogressive reactions.

- The previously observed correlation between pyrolysis tar and liquefaction yields for coals and modified coals appears to hold for the vacuum-dried cation-exchanged coals, but not always for the re-moisturized coals.

- The total evolution of CO_2 and CO from pyrolysis is changed significantly by cation-exchange. However, only in the case of CO does the evolution profile change significantly.

- After careful demineralization, a calcium form Zap or Wyodak coal can be prepared at pH= 8, which is similar to the raw coal with regard to pyrolysis and liquefaction behavior.

- At pH=8, cations are most likely to be coordinating multiple oxygen functionalities around themselves through electrostatic type interactions, which diminishes the importance of valency.

- Some of the moisture in a coal is associated with the cations. The moisture content has a larger role in liquefaction than in pyrolysis because it is present for a longer period of time.

B. Preparation and Study of Polymeric Models

We believe that —(Ph-O-CH_2CH_2)$_n$ — and related polymers contain a linkage that, to the best of our knowledge, is more representative of what is likely to be present in low-rank (and perhaps bituminous) coals than that of any other polymers that have yet been used for coal studies. Since more effort than we originally expected has been required to obtain this polymer with enough purity to draw meaningful mechanistic conclusions, we agreed that now that we have a good route to it, the first priority for future work would be to obtain 5-10 g of —(Ph-O-CH_2CH_2)$_n$—. This will enable us to perform multiple liquefaction tests as well as to run other "conversion" tests (i.e., TG-FTIR and Pyrolysis-FIMS). The result of these experiments should be a good indicator of the chemical changes these structures undergo during pretreatment and liquefaction. The second priority would be to extend this to the structure that is presumably even more relevant to low-rank coals, namely the —[C_6H_3(o-CH_3)-O-CH_2CH_2]$_n$ — polymer. Only when these polymers have been successfully prepared in

these amounts will we proceed to the task of third priority, namely further modification of one or both of the above structures to contain carboxylic acids. An additional reason for our suggestion of this prioritization is that results to date on the decarboxylation and coupling of aliphatic and aromatic carboxylic acids suggests, as summarized below, that coupling following decarboxylation may not be the major source of retrograde reactions during pretreatment and liquefaction.

C. Decarboxylation and Coupling of Aromatic and Aliphatic Acids

Our studies of decarboxylation under conditions relevant to coal conversion indicate at this point that (1) decarboxylation of unactivated acids is not responsible for the CO_2 evolution observed in the 300-350^{o}C range and (2) decarboxylation of activated acids does not readily provide enough coupling to account for substantial crosslinking of coal structures. However, to continue these studies we need to perform more experiments with the calcium salts of both unactivated and activated acids under conditions relevant to the coal studies where decarboxylation has been correlated with crosslinking. These experiments would include the salts of benzoic p-hydroxy benzoic acid and o-methoxy benzoic acid and would be both in solvents and neat. With these experiments, two hypotheses could be tested that may explain the lack of coupling we have observed thus far with presumably coal-like carboxylic acid structures.

First, we suggest that since decarboxylation of acids is activated by one or more electron-releasing groups such as -OH and -OMe and produces phenolic structures that we have already shown to be susceptible to coupling, the real crosslinking may not result directly from the decarboxylation but secondarily from the activated phenols that are thereby produced. Second, since the decarboxylation of activated acids apparently proceeds via electophilic attack of a proton on the aromatic carbon bearing the carboxylic acid group, decarboxylation with coupling *could* occur if attack were instead by a carbon-centered electrophile. In this scenario, the reason why preparation of calcium-exchanged coals yields more crosslinking could be that when the acids are present mainly in the calcium form, the ratio of protons to other electrophiles decreases and the ratio of clean decarboxylation to decarboxylation accompanied by coupling goes down. At present, this appears to be the best candidate explanation for reconciling the observed crosslinking and decarboxylation of coals with the surprising lack of crosslinking accompanying the decarboxylation of pure activated acids.

D. Publications from this Project

Three papers were prepared for the International Conference on Coal Science (Banff, Alberta, CANADA, September 12-17, 1993) based on the work done under this project. The first is titled "The Role of Cations in Retrogressive Reactions During Pyrolysis and Liquefaction," which summarized the work done on coals and modified coals. The second is titled "Application of a Spectral Deconvolution Technique to Coal FT-IR Spectra," which described the use of FT-IR methods for measurement of

carboxyl and hydroxyl functions. The third paper is titled "Pyrolysis Pathways and Kinetics of Polymeric Models for Low-Rank Coals" which focused on the thermal decomposition chemistry of the β-ether-linked lignin model polymers. In addition, two papers were prepared for the American Chemical Society (ACS) Division of Fuel Chemistry Meetings: 1) “Decarboxylation and Coupling Reactions of Coal Structures” (Washington, DC, 1992) [47]; and 2) “The Effect of Moisture and Cations on Liquefaction of Low Rank Coals” (Denver, 1993) [16].

REFERENCES

1 Bishop and Ward, Fuel, **37**, 191, (1958).
2 Schafer, H., Fuel, **49**, 197, (1970).
3 Hengel and Walker, Fuel, **63**, 1215 (1986).
4 Serio, M.A., Solomon, P.R., Kroo, E., Charpenay, S., and Bassilakis, R., "Fundamental Studies of Retrograde Reactions in Direct Liquefaction," Final Report for Contract No. DE-AC22-88PC88814 (Dec., 1991).
5 Schafer, H., Fuel, **51**, 4, (1972).
6 van Bodegom, B., van Veen, J.A., van Kessel, G.M.M., Sinnige-Nijssen, M.W.A., and Stuiver, H.C.M, Fuel 63, 346 (1984).
7 Wornat, M.J., and Nelson P.F., Energy and Fuel, 6 (2) (1992).
8 Jain, M.K., Burgdorf, D., and Narayan, R., Fuel, 70, 573 (1991).
9 Starsinic, M., Otake, Y., Walker, Jr., P.L., Painter, P.C., Fuel, 63, 1002 (1984).
10 Serio, M.A., Kroo, E., Teng, H., Charpenay, S., and Solomon, P.R., "Fundamental Studies of Water Pretreatment of Coal," Final Report under Contract No. DE-AC22-89PC89878 (1992).
11 Jackson, R.S., Griffiths, P.R., Anal. Chem., 63, 2557 (1991).
12 Pierce, J.A., Jackson, R.S., Van Every, K.W., Griffiths, P.R., Anal. Chem., 62, 447, (1990).
13 Friesen, W.I., Michaelin, K.H., Appl. Spec., 45, 50 (1991).
14 .Solomon, P.R., Hamblen, D.G., Carangelo, R.M., ACS Symposium Series, 205, 4, 77 (1982).
15 Solomon, P.R., Carangelo, R.M., Fuel, 61, 663, (1982) and Fuel, 67, 949, (1987).
16 Serio, M.A., Kroo, E., Teng., H., Solomon, P.R., "The Effects of Moisture and Cations on Liquefaction of Low Rank Coals," ACS Div. of Fuel Chem. Prepr. 38(2), 577 (1993).
17 Bamfield, P., Quam, P.M. Synthesis, 537, (1978).
18 Handbook of Chemistry and Physics, 57th Edition, Ed. Robert C. Weast, Chemical Rubber Publishing Co., Cleveland, Ohio, p. C0-480 (1976).
19 Handbook of Chemistry and Physics, 57th Edition, Ed. Robert C. Weast, Chemical Rubber Publishing Co., Cleveland, Ohio, p. C-172, (1976).
20 Poutsma, M.L., "A Review of Thermolysis Studies of Model Compounds Relevant to Processing of Coal," Oak Ridge national Laboratory Report ORNL/TM-10637 (1987).
21 Gilbert, K.E., Gajewski, J.J., J. Org. Chem., 47, 4899 (1982).
22 Klein, M.T., Virk, P.S., Ind. Eng. Chem., Fudam, 22, 35 (1992).
23 Britt, P., Buchanan, A.C., Energy and Fuels, 6, 110, (1992).
24 Surynam, M.M., Kafafi, S.A., Stein, S.E., J. Am. Chem. Soc., 11, 4594 (1989).
25 McMillen, D.F., Manion, J.A., Malhotra, R., Am. Chem. Soc. Div. Fuel Chem. Preprints, 37 (4), 1636 (1992).
26 Squire, D.R., Solomon, P.R., DiTaranto, M.B., "Synthesis and Study of Polymer Models Representative of Coal Structure – Phase II," Final Report, Gas Research Institute, August 1985.
27 Harrison, I.T., J. Chem. Soc. Chem. Commun., 616, (1969).
28 McCarthy, J.R., Moore, J.L., Cregge, R.J., Tet. Lett., 5186 (1978).
29 Carroll, J.F., Kulkowit, S., McKervey, M.A., J. Chem. Soc. Chem. Commun., 57 (1980).
30 Suuberg, E.M., Lee, D., Larsen, J.W., Fuel, 64, 1668 (1985).
31 Serio, M.A., Hamblen, D.A., Markham, J.R., Solomon, P.R., Energy Fuels, 1, 138, (1987).
32 Solomon, P.R., Serio, M.A., Deshpande, G.V., Kroo, E., Energy Fuels, 4, 42 (1980).
33 Serio, M.A., Solomon, P.R., Deshpande, G.V. Kroo, E., Bassilakis, R., Malhotra., R., McMillen, D.F., Am. Chem. Soc. Div Fuel Cherm. Prep., 35(1), 61 (1990).
34 Siskin, M., private communication, (1991).
35 March, J., Advanced Organic Chemistry, 3rd Edition, John Wiley and Sons, New York, p 507, 562, 653, 842, 928 (1985).
36 Cohen, T., Schambach, J. Am. Chem. Soc., 92, 4951 (1988).
37 Friedel, C. Justus Liebigs Ann. Che., 108, 122 (1958).

38 Hites, R.A., Biemann, K.J., Am. Chem. Soc., 94, 5772 (1972).
39 McMillen, D.F., unpublished work (1985).
40 McMillen D.F., Ogier, W.C., Ross, D.S., J. Org. Chem., 46, 3322 (1981).
41 Fahr, A., Stein, S.E., J. Phys. Chem., 92 4951 (1988).
42 Chen, R.H., Kafafi, S.A., Stein, S.E., Am. Chem. Soc., 111, 1418 (1989).
43 Fahr, A., Mallard, W.G., Stein, S.E., 21st Symposium International on Combustion: The Combustion Institute, 825, (1986).
44 Herndon, W.C., J. Org. Chem., 46, 2119 (1981).
45 McMillen, D.F., Malhotra, R., Chang, S.J., Fleming, R.H., Ogier, W.C., Nigenda, S.E., Fuel, 66, 1611 (1987).
46 Stein, S.E., Griffith, L.L., Billmers, R., Chen, R.H., J. Org. Chem., 52, 1582 (1987).
47 Manion, J.A., McMillen, D.F., and Malhotra, R., ACS Div. of Fuel Chem. Preprints, 37, (4), 1720 (1992).